

# **Nanoparticle Formulations for New Cytostatic Agents against Glioblastomas**

A Thesis  
Submitted to the  
Department of Pharmaceutical Technology  
at the  
Goethe University  
Frankfurt am Main, Germany  
by  
Telli Hekmatara

In Partial Fulfillment of the  
Requirements for the Degree  
of  
Doctor of Philosophy  
(Pharmaceutics)

Frankfurt am Main, 2008  
(D30)

Vom Fachbereich Biochemie, Chemie und Pharmazie  
der Goethe-Universität Frankfurt am Main als Dissertation angenommen.

Dekan: .....Prof. Dr. Harald Schwalbe

1. Gutachter: .....Prof. Dr. Jörg Kreuter

2. Gutachter: .....Prof. Dr. Jochen Klein

Datum der Disputation:.....

*To my parent Dr. M. H. Hekmatara and Manijeh Rabbani*



# Table of Contents

---

<b>Abbreviations .....</b>	<b>7</b>
<b>1 Zusammenfassung .....</b>	<b>10</b>
<b>2 Theory: Drug delivery to the brain by nanoparticles .....</b>	<b>16</b>
<b>2.1 Structure of the blood-brain barrier .....</b>	<b>16</b>
2.1.1 Physical barrier: Tight junctions .....	16
2.1.2 Neurovascular units/cells associated to the BBB.....	17
2.1.3 Metabolic barriers: Enzymes .....	18
<b>2.2 Transport across the blood-brain barrier .....</b>	<b>19</b>
2.2.1 Cell migration .....	19
2.2.2 Passive diffusion .....	19
2.2.3 Carrier-mediated efflux.....	20
2.2.4 Carrier-mediated influx.....	20
2.2.5 Vesicular transport .....	20
2.2.5.1 Absorptive-mediated transcytosis (AMT) .....	21
2.2.5.2 Receptor-mediated transcytosis (RMT).....	21
2.2.6 The role of tight junctions.....	21
<b>2.3 Drug delivery to the CNS .....</b>	<b>22</b>
2.3.1 Craniotomy-based drug delivery.....	23
2.3.2 Disruption of the BBB .....	23
2.3.3 Chemical modification of the drug .....	24
2.3.4 Inhibition of efflux mechanisms .....	24
<b>2.4 Nanocarriers for brain delivery .....</b>	<b>25</b>
2.4.1 Biodistribution of the nanoparticles to the normal brain .....	25
2.4.2 Distribution of the nanoparticles under the pathological condition of the brain ...	27
2.4.3 Brain delivery with PBCA nanoparticles coated with polysorbate 80 .....	28
<b>2.5 Pharmacological activity of the nanoparticle-bound drugs .....</b>	<b>29</b>
2.5.1 Neuroactive agents.....	29
2.5.2 Doxorubicin .....	31
2.5.3 Mechanisms of drug delivery to the brain by nanoparticles .....	33
<b>2.6 Toxicological aspects.....</b>	<b>43</b>

<b>3 Materials and Methods.....</b>	<b>46</b>
<b>3.1 Poly(butyl cyanoacrylate) nanoparticles.....</b>	<b>46</b>
3.1.1 Doxorubicin-loaded PBCA nanoparticles.....	47
3.1.2 Preparation of drug-loaded PBCA nanoparticles in the presence of organic solvents .....	48
3.1.3 Characterisation of nanoparticles.....	48
3.1.3.1 Determination of the particle size and the zeta potential.....	49
3.1.3.2 Analytical ultracentrifugation (ANUC) .....	50
3.1.3.3 Scanning Electron Microscopy (SEM) .....	51
3.1.3.4 Atomic Force Microscopy (AFM) .....	51
3.1.3.5 Evaluation of the loading capacity of the nanoparticles .....	52
3.1.3.5.1 Doxorubicin assay.....	53
3.1.3.5.2 Loperamide assay.....	54
3.1.3.5.3 Paclitaxel assay .....	55
3.1.3.6 Determination of polymer yield.....	55
3.1.3.7 Determination of residual organic solvents .....	57
3.1.4 Coating of the nanoparticles with surfactants.....	58
3.1.5 <i>In vivo</i> experiments .....	59
3.1.5.1 Tail-flick test.....	59
3.1.5.1.1 Loperamide-loaded PBCA nanoparticles for tail-flick test .....	60
3.1.5.2 Chemotherapy of 101/8 rat glioblastoma using doxorubicin formulations ....	60
3.1.5.2.1 Intracranial implantation of rat glioblastoma.....	60
3.1.5.2.2 Doxorubicin formulations and treatment regimen.....	61
3.1.5.2.3 Histological analysis .....	61
3.1.5.2.4 Immunohistochemical analysis.....	62
3.1.5.2.5 Measurement of tumour size.....	63
3.1.5.2.6 Analysis of proliferation .....	63
3.1.5.2.7 Analysis of vessel density .....	63
3.1.5.2.8 Analysis of necrosis .....	64
3.1.5.2.9 Analysis of GFAP expression of glioma cells .....	64
3.1.5.2.10 Analysis of microvascular proliferation.....	64

## Table of Contents

3.1.5.2.11 Analysis of VEGF expression of glioma cells.....	64
3.1.5.2.12 Statistical analysis.....	64
3.1.5.3 Chemotherapy of 101/8 rat glioblastoma using paclitaxel formulations .....	65
<b>3.2 Human serum albumin nanoparticles.....</b>	<b>66</b>
3.2.1 Nanoparticle preparation.....	67
3.2.1.1 Yield determination of the HSA nanoparticles.....	67
3.2.1.2 Preparation of sulfhydryl-reactive HSA nanoparticles.....	67
3.2.1.3 Purification of apolipoproteins A-I and B-100.....	68
3.2.1.4 Thiolation of apolipoproteins.....	68
3.2.1.5 Modification of the nanoparticles by thiolated apolipoproteins .....	68
3.2.1.5.1 Micro BCA protein assay.....	68
3.2.1.6 Loperamide loading in the apolipoprotein-modified nanoparticles.....	69
3.2.2 Apolipoprotein-modified HSA nanoparticles for tail-flick test.....	69
3.2.3 Loading of thalidomide in HSA nanoparticles .....	70
3.2.3.1 Determination of thalidomide loading.....	71
3.2.3.1.1 Thalidomide assay by HPLC .....	71
3.2.3.2 Thalidomide solubility in different solvents and surfactants.....	72
3.2.3.3 Chemotherapy of 101/8 rat glioblastoma using thalidomide formulations ....	73
<b>3.3 Diindolylmethane-loaded poly(lactide-co-glycolide) nanoparticles .....</b>	<b>74</b>
3.3.1 Preparation of DIM-loaded PLGA nanoparticles by nanoprecipitation .....	74
3.3.1.1 Characterisation of the DIM-loaded PLGA nanoparticles.....	75
3.3.2 Determination of DIM maximum solubility in aqueous media.....	75
3.3.3 Determination of DIM stability in organic media.....	76
3.3.3.1 DIM assay by HPLC.....	76
<b>4 Results .....</b>	<b>78</b>
<b>4.1 Poly(butyl cyanoacrylate) nanoparticles.....</b>	<b>78</b>
4.1.1 Characterisation of doxorubicin poly(butyl cyanoacrylate) nanoparticles .....	79
4.1.1.1 Size, polydispersity, and surface charge of the nanoparticles .....	79
4.1.1.2 Morphology of the nanoparticles .....	79
4.1.1.3 Drug loading .....	80

4.1.2 Histopathologic and immunocytochemical evaluation of the treatment with different formulations of doxorubicin.....	80
4.1.2.1 Tumour size .....	85
4.1.2.2 Proliferation .....	86
4.1.2.3 Vessel density .....	86
4.1.2.4 Expression of glial fibrillary acidic protein (GFAP), expression of vascular endothelial growth factor (VEGF), incidence and dimension of necrosis, and microvascular proliferation.....	87
4.1.3 Characterisation of drug-loaded PBCA nanoparticles prepared in the presence of organic solvents .....	88
4.1.3.1 Size, polydispersity and surface charge of the nanoparticles .....	89
4.1.3.2 Morphology of the nanoparticles .....	92
4.1.3.3 Particle yield .....	93
4.1.3.4 Drug loading .....	93
4.1.3.5 The content of residual organic solvents .....	93
4.1.3.6 Loperamide-loaded PBCA-based formulations for the tail-flick test.....	94
4.1.3.7 Treatment of rats bearing intracranial transplanted glioblastoma 101/8 using paclitaxel-loaded nanoparticle formulations.....	95
<b>4.2 Characterisation of human serum albumin nanoparticles .....</b>	<b>97</b>
4.2.1 Size, polydispersity and surface charge of the nanoparticles .....	98
4.2.2 Characterisation of the HSA nanoparticles modified by apolipoprotein A-I and B-100.....	98
4.2.2.1 Size, polydispersity and surface of the nanoparticles .....	100
4.2.2.2 Tail-flick test with apolipoprotein-modified HSA nanoparticle formulations .....	101
4.2.3 Thalidomide bound to human serum albumin nanoparticles.....	103
4.2.3.1 Size, polydispersity, and surface of the nanoparticles .....	103
4.2.3.2 Drug loading .....	104
4.2.3.3 Solubility of thalidomide .....	104
4.2.3.4 Treatment of rats bearing intracranial transplanted glioblastoma 101/8 using different thalidomide formulations .....	105



<b>4.3 Characterisation of poly(lactide-co-glycolide) nanoparticles .....</b>	<b>107</b>
4.3.1 Size, polydispersity, and surface charge of the nanoparticles .....	107
4.3.2 Morphology of the nanoparticles .....	108
4.3.3 Drug loading .....	108
4.3.4 Determination of maximum solubility in aqueous media.....	109
4.3.5 DIM stability in organic media .....	109
<b>5 Discussion.....</b>	<b>110</b>
<b>5.1 Doxorubicin-loaded poly(butyl cyanoacrylate) nanoparticles.....</b>	<b>110</b>
<b>5.2 Drug-loaded PBCA nanoparticles prepared in the presence of organic solvents</b>	
.....	<b>112</b>
5.2.1 Analgesic effect of loperamide-loaded in PBCA nanoparticles (tail-flick test) ..	113
5.2.2 Chemotherapy of 101/8 glioblastoma using paclitaxel-loaded PBCA nanoparticles	
.....	114
<b>5.3 Human serum albumin nanoparticles.....</b>	<b>115</b>
5.3.1 Covalent linkage of Apolipoprotein A-I and B-100 to human serum albumin	
nanoparticles .....	115
5.3.2 Thalidomide bound to HSA nanoparticles.....	116
<b>5.4 DIM loaded in PLGA nanoparticles .....</b>	<b>118</b>
<b>6 Conclusion .....</b>	<b>119</b>
<b>6.1 Antiangiogenic effects of doxorubicin-loaded poly(butyl cyanoacrylate)</b>	
<b>nanoparticles .....</b>	<b>119</b>
<b>6.2 Encapsulation of water-insoluble drugs in poly(butyl cyanoacrylate)</b>	
<b>nanoparticles .....</b>	<b>119</b>
<b>6.3 Covalent attachment of apolipoprotein A-I and apolipoprotein B-100 to albumin</b>	
<b>nanoparticles enables drug transport into the brain.....</b>	<b>120</b>
<b>6.4 Thalidomide bound to human serum albumin nanoparticles .....</b>	<b>120</b>
<b>6.5 Encapsulation of diindolylmethane in poly(lactide-co-glycolide) nanoparticles.</b>	<b>120</b>
<b>7 Summary.....</b>	<b>121</b>

<b>8 References.....</b>	<b>127</b>
<b>9 Curriculum Vitae.....</b>	<b>145</b>
<b>10 Patent and Publications.....</b>	<b>147</b>
<b>Acknowledgments .....</b>	<b>148</b>

## Abbreviations

ABC	ATP-binding cassette
AFM	Atomic Force Microscopy
AJ	Adherent junctions
AMT	Absorptive-mediated transcytosis
ANUC	Analytical ultracentrifugation
Apo	Apolipoprotein
AUC	Area under the curve
BBB	Blood-brain barrier
BCA	n-butyl-2-cyanoacrylate
BCRP	Breast cancer resistance protein
BEC	Brain endothelial cells
BISF	Brain interstitial fluid
BSA	Bovine serum albumin
CH <sub>2</sub> Cl <sub>2</sub>	Dichloromethane
CNS	Central nervous system
CSF	Cerebrospinal fluid
DAB	Diaminobenzidine
Dal	Dalargin
DIM	3,3'-diindolylmethane
DMBA	$\alpha$ -dimethylbenzanthracene
DMSO	Dimethylsulfoxide
Dox	Doxorubicin
Dox-NP	Doxorubicin bound to poly(butyl cyanoacrylate) nanoparticles
Dox-NP + PS 80	Doxorubicin bound to poly(butyl cyanoacrylate) nanoparticles coated with polysorbate 80
Dox-sol	Doxorubicin solution
EM	Electron microscopy
EPR effect	Enhanced permeability and retention effect
EtOAc	Ethylacetate

## Abbreviations

EtOH	Ethanol
F68	Poloxamer 188; Pluronic <sup>®</sup> F68
FITC	Fluoresceine isothiocyanate
GC	Gas chromatograph
GFAP	Glial fibrillary acidic protein
H&E	Hematoxylin and eosin
HPLC	High performance liquid chromatography
HSA-NP	Human serum albumin nanoparticles
i-PrOH	Iso-propanol
JAM	Junctional adhesion molecule
LDC	Lipid drug conjugate
LDH	Lactate dehydrogenase
LDL-R	Low density lipoprotein receptor
LRP	Low-density lipoprotein receptor-related protein
MeOH	Methanol
MOAT	Multi-specific organic anion transporter
MPS	Mononuclear phagocyte system
MRP	Multi-drug resistance associated protein
NMDA	N-methyl-D-aspartate
NP	Nanoparticles
ODN	Antisense oligonucleotides
PBCA-NP	Poly(butyl cyanoacrylate) nanoparticles
PBS	Phosphate buffered saline
PCS	Photon correlation spectroscopy
PEG	Poly(ethylene glycol)
PEG-PE	1,2-Dioleoyl-sn-Glycer-3Phosphoethanolamine-N-Methoxy(Polyethylene glycol)-5000][sodium salt]
Pgp	P-glycoprotein
PHDCA-NP	Poly(hexadecyl cyanoacrylate) nanoparticles
PLGA-NP	Poly(lactide-co-glycolide) nanoparticles
PMMA-NP	Poly(methyl methacrylate) nanoparticles

## Abbreviations

PEG	Poly(ethylene glycol)
PS 80	Polysorbate 80; Tween <sup>®</sup> 80
PVA	Polyvinylalcohol
PXL	Paclitaxel
PXL-NP	Paclitaxel bound to poly(butyl cyanoacrylate) nanoparticles
PXL-NP + PS 80	Paclitaxel bound to poly(butyl cyanoacrylate) nanoparticles coated with polysorbate 80
RMT	Receptor-mediated transcytosis
SEM	Scanning Electron Microscopy
SLN	Solid lipid nanoparticles
SR-BI	Scavenger receptor class B type I
TFA	Trifluoroacetic acid
Thal-HSA-NP	Thalidomide-loaded HSA nanoparticles
TJ	Tight junctions
ZO	Zonula occludens
$\gamma$ -GTP	$\gamma$ -glutamyl transpeptidase

# 1 Zusammenfassung

Viele hochaktive Zytostatika sind zurzeit für die systematische chemotherapeutische Anwendung nicht einsetzbar, weil ihr Eintritt ins Gehirn durch die Blut-Hirn-Schranke (BHS) blockiert wird. Die Entwicklung einer Möglichkeit zum Transport dieser Stoffe über diese Schranke würde das Potenzial einer systemischen Chemotherapie bedeutend erhöhen.

## **Chemotherapie von Glioblastomen mit Doxorubicin beladenen Nanopartikeln**

In früheren Studien wurde gezeigt, dass die Überlebenszeiten von Ratten mit ins Gehirn transplantierten 101/8 Glioblastomen durch mit Polysorbat 80 überzogenen Doxorubicin-Nanopartikel signifikant verlängert werden können. Ziel der vorliegenden Studie war es, die Effizienz dieser Doxorubicin-beladenen Nanopartikel mit morphometrischen, histologischen und immunohistologischen Methoden zu untersuchen, um so die Tiere weniger zu belasten als das in Letalitätsstudien erfolgt. Das 101/8 Glioblastom wurde dazu intrakranial männlichen Wistar-Ratten implantiert. Die Ratten wurden randomisiert in drei Gruppen geteilt: die erste Gruppe erhielt keine Behandlung (Kontrolle, n = 20), die zweite Gruppe wurde mit Doxorubicin-Lösung (Dox-sol, n = 18) und die dritte Gruppe mit Polysorbat 80-überzogenen Doxorubicin-Nanopartikeln (Dox-NP + PS 80, n = 18) behandelt.

Die Versuchstiere erhielten die Doxorubicin-haltige Zubereitung an den Tagen 2, 5 und 8 nach Tumorimplantation als Injektion in die Schwanzvene. Die Dosierung wurde an das Körpergewicht der Tiere angepasst und betrug  $3 \times 1,5$  mg/kg Doxorubicin.

Die Tiere der Kontrollgruppe wurden an den Tagen 6, 8, 10, 12, und 14 nach der Tumorimplantation getötet und ihre Gehirne entnommen. Die Gehirne der Ratten, die die Doxorubicin-Zubereitungen erhielten, wurden an den Tagen 10, 14, und 18 nach der Implantation entnommen. Die Rattenhirne wurden histologisch auf folgende Merkmale hin untersucht: Tumorgroße, Zellproliferation, Gefäßdichte, Expression des sauren Gliafaserproteins (GFAP, Glial Fibrillary Acidic Protein), Expression des vaskulären endothelialen Wachstumsfaktors (VEGF, Vascular Endothelia Growth Factor), Häufigkeit und Ausmaß des nekrotischen Areal und mikrovaskuläre Proliferation.

Die Tumore zeigten die Zeichen von Malignität wie z.B. Invasion in das Gehirngewebe und rasche mitotische Aktivität. Die Tumorproliferation blieb auf hohem Niveau stabil.

Insgesamt war der Tumor durch ein reproduzierbares Wachstumsmuster gekennzeichnet und in seiner Entwicklung einem menschlichen Glioblastom vergleichbar und durch eine diffuse Infiltration des Gehirns charakterisiert. Das umliegende Gehirngewebe wies an den Grenzen des soliden Tumors keine Zeichen von Verkapselung auf. Somit erfüllt das 101/8 Glioblastom dementsprechend Kriterien für ein zuverlässiges, menschliches Tumoren adäquates Glioblastom-Modell.

Dox-NP + PS 80 zeigten im Vergleich zu Dox-sol und der Kontrollgruppe eine deutliche Antitumoraktivität, wie eine verkleinerte Tumorgroße, niedrige Proliferationsraten und kleine nekrotische Flächen. Diese Ergebnisse korrelierten mit einer vorherigen Letalitätsstudie ([Steiniger 2004](#)) bei der im gleichen Glioblastom-Modell mehr als 20% der Tiere, die mit diesen Nanopartikeln behandelt wurden, eine Langzeitremission zeigten. Der Behandlungseffekt mit den Nanopartikeln im Vergleich zur Behandlung mit Doxorubicin-Lösung oder der unbehandelten Kontrollgruppe wurde durch verminderte Gefäßdichte, Abnahme der VEGF-Expression und durch das Fehlen von mikrovaskulärer Proliferation aufgezeigt. Die drastische Wirkung von Dox-NP + PS 80 auf die Vaskularisierung ist vermutlich auf die zytotoxische und darüber hinaus auf eine anti-angiogenetische oder Wirkung von Doxorubicin zurückzuführen.

### **Verkapselung von schlecht wasserlöslichen Arzneistoffen in Poly(butylcyanoacrylat)-Nanopartikel (PBCA-NP)**

Die Entwicklung von parenteralen Zubereitungen mit schlecht wasserlöslichen Arzneistoffen stellt eine große Herausforderung dar. In diesen Präparaten wurden die Arzneistoffe bisher meist in nichtwässrigen, organischen Lösungsmitteln gelöst. Diese Lösungen wurden meist, aber nicht immer, unmittelbar vor der Anwendung mit wässrigen Medien verdünnt ([Strickley 2004](#)). Die meisten dieser Vehikel sind nicht inert und können während der Therapie eine Vielzahl von Nebenwirkungen oder Arzneistoffwechselwirkungen hervorrufen.

Die Nanopartikeltechnologie stellt eine vielversprechende Methode dar, den Arzneistoffgehalt in einem wässrigen Medium zu erhöhen und damit die in-vivo-Effizienz zu optimieren. Dementsprechend wurde in diesem Teil der vorliegenden Studie die Effizienz dieser Methode unter Verwendung von Poly(butylcyanoacrylat)-Nanopartikeln und den beiden hydrophoben Arzneistoffen Loperamid und Paclitaxel untersucht. Für diesen Zweck

## Zusammenfassung

wurde das Standardprotokoll für die Herstellung von Nanopartikeln so modifiziert, dass Arzneistoff-beladene Nanopartikel in einem Gemisch aus wässrigem Medium und 10% (v/v) organischem Lösungsmittel durch anionische Emulsionspolymerisation von Butylcyanoacrylat (BCA) hergestellt und das Lösungsmittel später entfernt werden konnte. Das Lösungsmittel wurde je nach Arzneistofflöslichkeit ausgewählt. Die Nanopartikel wurden mit Dextran 70.000, Poloxamer 188 oder 1,2-dioleoyl-sn-glycero-3-phosphoethanolamin-N-[methoxy(polyethylene glycol)-5000]-Natrium-Salz (PEG-PE) stabilisiert. Das Polymerisationsmedium bestand aus einer Stabilisator-Tensid-Mischung in 0,01 N HCl und einem geeigneten organischen Lösungsmittel im Verhältnis 1:9. Die Anwesenheit von organischen Lösungsmitteln im Polymerisationsmedium beeinflusste die physikochemischen Eigenschaften von unbeladenen Nanopartikeln nicht. Es konnte gezeigt werden, dass sich in Anwesenheit von Dichlormethan, Methanol oder Ethanol die Effizienz der Einbettung von Loperamid in Nanopartikel bis zu 80% erhöhte. Die Loperamid-beladenen Nanopartikel wurden zusätzlich mit 1% Polysorbat 80 überzogen.

Wie in den Veröffentlichungen von Alyautdin *et al.* ([Alyautdin 1997](#)) beschrieben, wurde diese Zubereitung mit und ohne Coating Mäusen injiziert und der analgetische Effekt mittels des Tail-Flick-Tests bestimmt. Als Kontrolle wurde eine Loperamidlösung verwendet. Der Arzneistoff Loperamid gehört zur Klasse der Opioide, besitzt aber wegen der Effluxaktivität der Pgp-Pumpe keine Gehirngängigkeit und keine zentral-analgetischen Effekt. Wie erwartet wies die Loperamidlösung deshalb dementsprechend keinen derartigen Effekt auf. Im Gegensatz dazu erzeugten die Polysorbat 80-überzogenen Loperamid-Nanopartikel und auch die nicht-überzogenen Loperamid-Nanopartikel einen deutlichen analgetischen Effekt. Unsere Ergebnisse zeigten darüber hinaus, dass auch Poloxamer 188 einen Transport von Arzneistoffen über die BHS ermöglicht.

Die Beladung von PBCA-NP mit Paclitaxel war auch in Anwesenheit eines Stabilisatorgemisches aus Dextran und Poloxamer 188 relativ niedrig (~ 25%). Der Höchstwert der Beladung wurde in Anwesenheit von PEG-PE (~ 45%) erreicht, und die Effizienz der Verkapselung konnte bis auf 55 µg/mg PBCA-NP gesteigert werden. Dieses Ergebnis korreliert mit den Ergebnissen von Mitra and Lin *et al.* ([Mitra and Lin 2003](#)). Es wurde vermutet, dass dies auf die bessere Löslichkeit von Paclitaxel durch Einschluss in PEG-PE-Mizellen und/oder die Affinität dieser Mizellen zur Nanopartikelmatrix



zurückzuführen ist. Paclitaxel ist ein Pgp-Substrat, weswegen die Penetration ins ZNS nach einer systemischen Applikation für die Therapie nicht ausreichend ist. Das Ziel war es zu untersuchen, ob mit Polysorbat 80- oder Poloxamer 188 (F68)-überzogene Nanopartikel es ermöglichen, Paclitaxel über die BHS zu transportieren. Deshalb wurde die Antitumoreffizienz von drei Paclitaxel-Zubereitungen ebenfalls in den 101/8 Gehirntumor-tragenden Ratten untersucht. Die verwendeten Formulierungen waren Paclitaxel-beladene PBCA-Nanopartikel (PXL-NP), mit Polysorbat 80 überzogene PXL-NP (PXL-NP + PS 80) und mit Poloxamer 188 überzogene PXL-NP (PXL-NP + F68). Unbehandelte Ratten und Ratten, die mit der Paclitaxel-Lösung behandelt worden waren, wurden als Kontrolle eingesetzt.

Wegen der niedrigen Paclitaxel-Beladung der Nanopartikel konnte die empfohlene Dosierung von Paclitaxel (17,80 mg/kg (Fetell 1997, FDA)) nicht eingehalten werden. Deshalb wurden diese Paclitaxel-Zubereitungen in der gleichen Dosierung wie Doxorubicin appliziert ( $3 \times 1,5$  mg/kg an den Tagen 2, 5 und 8 nach Tumorimplantation). Keine der Paclitaxel-Zubereitungen konnte die Überlebenszeit im Vergleich mit der Kontrolle verbessern, was an der niedrigen Dosierung und der kurzen Behandlungsdauer liegen könnte.

### **Apolipoprotein A-I- und B-100-modifizierte Albumin-Nanopartikel zur Überwindung der Blut-Hirn-Schranke**

Apolipoprotein A-I und B-100 wurden kovalent durch den NHS-PEG-Mal 3400-Linker an HSA Nanopartikel (HSA-NP) gebunden. Loperamid wurde als Model-Arzneistoff an die Nanopartikel adsorbiert und Mäusen injiziert und der analgetische Effekt mittels des Tail-Flick-Tests bestimmt. Nach 15 Minuten wiesen beide Nanopartikel-Zubereitungen, an die Apolipoprotein A-I oder B-100 gebunden worden war, starke analgetische Wirkungen auf, die bis zu einer Stunde dauerten. Die MPE-Werte („maximal possible effect“-Wert) der Zubereitungen betragen ca. 65% beziehungsweise 50% und waren statistisch unterschiedlich verglichen mit den beiden Kontrollen (unmodifizierte, Loperamid-beladene Nanopartikel und Loperamidlösung). Letztere hatten keine Wirkung. Das Ergebnis zeigte auch, dass mehr als ein Mechanismus der Interaktion der Nanopartikel mit den Endothelzellen des Gehirns existiert, welcher im Folgenden dann einen Transport der Arzneistoffe ins ZNS ermöglicht. Apolipoprotein B-100 kann über Lipoprotein-Rezeptoren durch die BHS

transportiert werden, Apolipoprotein A-I ermöglicht dies über SR-BI (Scavenger-Rezeptor), der auch in der BHS lokalisiert ist.

### **Thalidomid-beladene Human-Serumalbumin-Nanopartikel (Thal-HSA-NP)**

Thalidomid ist ein antiangiogenetischer Arzneistoff mit schlechter Wasserlöslichkeit, der meistens oral verabreicht wird. Dennoch wäre die parenterale Anwendung in besonderen klinischen Situationen zu bevorzugen, wie z.B. bei schwacher Darmabsorption oder bei durch Chemotherapie verursachter Übelkeit.

Das Ziel dieses Teils der Arbeit war es, eine injizierbare Zubereitung auf Human-Serumalbumin-Nanopartikel-Basis zu entwickeln. Wie bereits früher berichtet wurde, ist die Thalidomidlöslichkeit in Wasser und in 5% Glukoselösung nur 52 µg/ml beziehungsweise 70 µg/ml (Eriksson 2000). Es konnte nun in der vorliegenden Arbeit gezeigt werden, dass die Thalidomidmenge in einer Zubereitung durch Bindung an die Nanopartikel verachtfacht werden konnte und die Thalidomidkonzentration in der Nanopartikelsuspension bis zu 400 µg/ml betrug. In dieser Studie wurde zum Vergleich zusätzlich der Einfluss von Hilfsstoffen auf die Thalidomidlöslichkeit untersucht. Die Lösungen beinhalteten: 5% Glukose, 10% Polysorbat 80, 10% Poloxamer 188 oder Cremophor<sup>®</sup> EL-Ethanol (51:49). Thalidomid wurde als Racemat eingesetzt. In keiner dieser Lösungen war jedoch die Thalidomidlöslichkeit höher als in der Nanopartikelzubereitung.

Die Antitumoraktivität von unmodifizierten Thalidomid-beladenen HSA-NP (Thal-HSA-NP) und von mit Polysorbat 80-überzogenen Thal-HSA-NP (Thal-HSA-NP + PS 80) wurden sodann in 101/8 Gehirntumor-tragenden Ratten ermittelt. Die Wirkungen dieser Zubereitungen wurden mit einer oralen Zubereitung verglichen. Unbehandelte Tiere dienten als Kontrollgruppe. Die Nanopartikel wurden intravenös appliziert. Im Vergleich zu den Kontrollgruppen hat jedoch keine dieser Zubereitungen eine Wirkung auf die Verlängerung der Rattenüberlebenszeit gezeigt. Dieses Ergebnis lag vermutlich an der niedrigen Dosierung und dem unadäquaten Dosierungsplan.

### **Verkapselung von Diindolylmethan in Polymilchsäure-Nanopartikel**

3,3'-Diindolylmethane (DIM) gehört zu den Indolalkaloiden von Kreuzblütlern und besitzt eine Wirksamkeit gegen Krebs, besonders bei Estrogen-abhängigen Tumoren (Chen 1998).

## Zusammenfassung

Der Nachteil von DIM ist seine schlechte Wasserlöslichkeit. Zudem ist DIM lichtempfindlich und produziert farbige Abbauprodukte. Allerdings behalten diese Produkte trotz ihres farbigen Aussehens ihre Wirkung. Das Ziel in diesem Arbeitsteil war es zu untersuchen, ob sich die Wasserlöslichkeit von DIM und die Lichtstabilität durch die (Poly[Lactid-co-Glycolid]-Nanopartikel (PLGA-NP)) verbessert. Die Verkapselung von DIM in PLGA-NP ergab eine wesentlich verbesserte Zubereitung: DIM-Gehalt wurde 600-fach erhöht und DIM konnte gegen die Farbveränderungen geschützt werden.

## **2 Theory: Drug delivery to the brain by nanoparticles**

The brain is one of the least accessible organs for the delivery of drugs due to the presence of the blood-brain barrier (BBB) formed by the cerebral capillary endothelial cells. The BBB provides the neuroprotective function against harmful substances in the blood stream, while supplying the brain with the required nutrients for a proper function (Begley 2000).

The existence of such a barrier was first noticed by Paul Ehrlich in the late 19th century. In 1900, Lewandowsky suggested a presence of the mechanical membrane which separates the blood from the brain and, therefore, limits the central nervous system (CNS) action of some intravenously administered drugs (Zlokovic 2008). This theory was further expanded by Goldmann (1909, 1913) who administered a dye, trypan blue, to stain the brain and spinal cord tissue. It was suggested that such a barrier did not exist between the cerebrospinal fluid (CSF) and the brain. Electron microscopy (EM) studies with ferritin and horseradish peroxidase have shown that the BBB is localised at the level of tight junctions (TJ) between adjacent brain endothelial cells (BEC) (Reese and Karnovsky, 1967; Brightman and Reese, 1969). Later, the definition of the BBB has changed from being an impermeable barrier to a highly specialised and diverse transport system for chemically well-defined substrates (Zlokovic 2008).

### ***2.1 Structure of the blood-brain barrier***

The BBB limits transport into the brain through both, physical (tight junctions) and metabolic (enzymatic) barriers (Zlokovic 2008, Begley 2003a).

#### **2.1.1 Physical barrier: Tight junctions**

At the physical level, the BBB is composed of a tightly sealed monolayer of the BEC closely joined to each other by tight junctions, thus forming a continuous cellular membrane which restricts the transport of molecules from the blood to the brain interstitial fluid (BISF) and vice versa (Zlokovic 2008).

The tight junction consists of the three integral membrane proteins, claudin, occludin, and junctional adhesion molecule (JAM) which together with several peripheral proteins constitute the junctional complex (Figure 1).

A number of peripheral proteins, regarded as scaffolding or linkers for the integral molecules of the tight junction in endothelia and epithelia, form a cytoplasmic plaque adjacent to the junctional cell membrane. The plaque proteins are a part of the tight junction complex and include the guanylate kinases such as ZO-1 (220 kDa), ZO-2 (160 kDa) and ZO-3 (130 kDa). Another plaque protein is cingulin (140 kDa), which is myosin-like and binds to the ZO complex and to F-actin of the cytoskeleton (Begley 2003b).

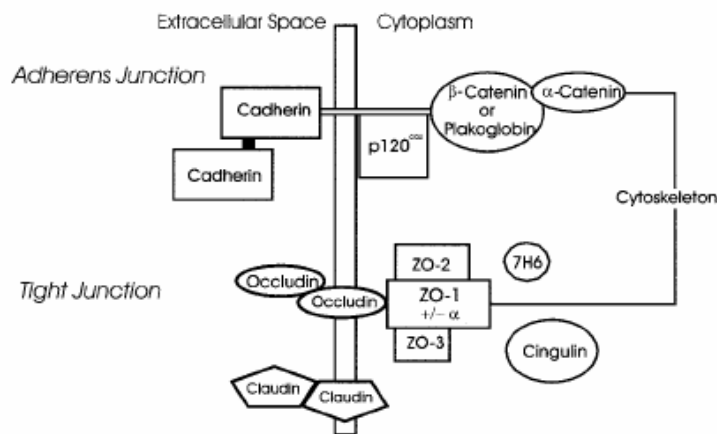


**Figure 1.** Simplified illustration of the molecular composition of the tight junctions (TJ) and adherent junction (AJ); The TJ proteins are occludin, claudins, zonula occludens (ZO)-1, ZO-2, ZO-3, cingulin, 7H6. The AJ are composed of cadherins, catenins, and p120 (Kniesel 2000).

### 2.1.2 Neurovascular units/cells associated to the BBB

Pericytes are distributed discontinuously along the length of the capillaries and partially surround the endothelium. The cerebral endothelial cells and the pericytes are surrounded by the same extracellular matrix (basement membrane). Foot processes from astrocytes form a network fully covering the capillaries. Axons from neurons also abut closely against the endothelial cells and contain vasoactive neurotransmitters and peptides. Microglia (perivascular macrophages) are the resident immunocompetent cells of the brain and they are derived from systemic circulating monocytes and macrophages (Begley 2004) (Figure 2).

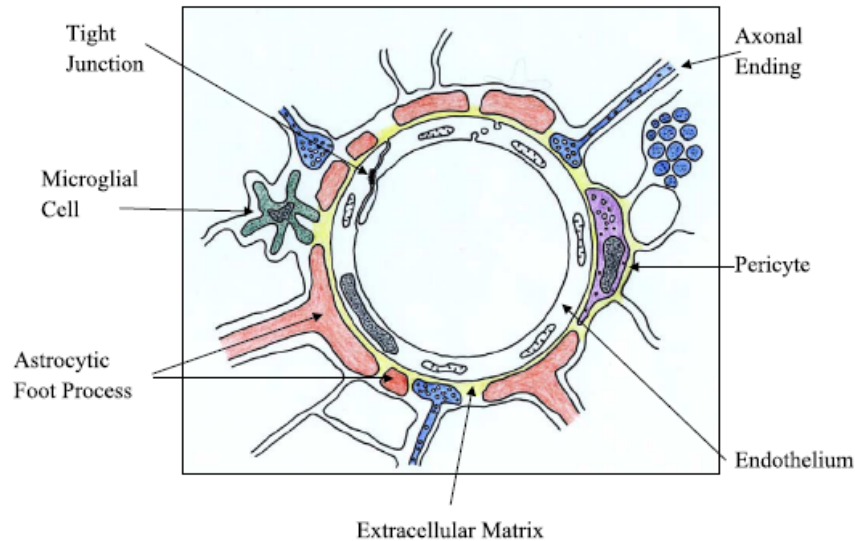


**Figure 2.** Schematic diagram of the neurovascular unit/cell association forming the BBB; Tight junctions and pericytes are surrounded by extracellular matrix. Foot processes from astrocytes and axons are closely against the endothelial cells. Microglia are the resident immunocompetent cells of the brain (Begley 2004).

The cell membrane of the endothelial cell has a uniform thickness, with very few pinocytotic vesicles (hollowed out portion of the cell membrane filled with fluid, forming a vacuole which allows for nutrient transport), and it also lacks fenestrations (i.e. openings). Therefore, the transit across the BBB involves translocation through the capillary endothelium, the internal cytoplasmic domain, and then through the abluminal membrane and pericyte and / or basal lamina (Cucullo 2005).

The cerebral capillary endothelial cell possesses a higher number and volume of mitochondria than the general body capillary cells suggesting that the enhanced cerebral capillary work capacity may be related to the energy-dependent transcapillary transport (Oldendorf 1977).

### 2.1.3 Metabolic barriers: Enzymes

The enzymatic barriers at the cerebral endothelia are capable of metabolising many drugs and solutes as they pass through the BBB.

The barriers contain active phase 1 (cytochromes P450, flavin-dependent oxygenases, monoamine oxidases, reductases, hydrolases) and phase 2 enzymes (conjugating enzymes, sulphotransferases, GSH-transferases, UDP-glucuronosyltransferases) (Begley 2003b).

There are a number of enzymes specific for the brain capillaries. Enzymes such as  $\gamma$ -glutamyl transpeptidase ( $\gamma$ -GTP), alkaline phosphatase, and aromatic acid decarboxylase are present in the cerebral microvessels in elevated concentrations; yet in the non-neuronal capillaries the concentrations of these enzymes are either low or absent. The presence of  $\gamma$ -GTP and alkaline phosphatase enzymes at the luminal side of endothelium and functioning of the  $\text{Na}^+$ - $\text{K}^+$ -ATPase and the sodium dependent (A-system) neutral amino acid transporter at the abluminal portion of the endothelium give the membrane surface of the endothelium a polarity feature.

Structural, pharmacological, and biochemical evidence for luminal and abluminal polarization of receptors, enzymes, and channels at the cerebral endothelia (Vorbrot 1993) establish the BBB to be a working non-stagnant membrane unequivocally evolved to maintain brain homeostasis.

## ***2.2 Transport across the blood-brain barrier***

### **2.2.1 Cell migration**

Under normal physiological condition, lymphocyte traffic into the CNS is very low and tightly controlled by the BBB. In contrast, under inflammatory conditions of the CNS, such as multiple sclerosis, circulating lymphocytes and monocytes/macrophages readily cross the BBB and gain access to the CNS leading to edema, inflammation and demyelination. Passage across endothelium must be preceded by temporary adhesion of the lymphocytes to the endothelium by way of cell adhesion molecules expressed on both, immunocytes and endothelium (Figure 3a). Immunocytes migrate across CNS endothelium both, paracellularly and transcellularly (Begley 2003b).

### **2.2.2 Passive diffusion**

The passive diffusion proceeds from low to high concentrations. Simple diffusion is a spontaneous process depending on random movement of the solutes (Figure 3b). Some of the lipophilic substances (alcohol, narcotics, and anticonvulsants) can diffuse passively through the endothelial cell membrane and enter the CNS (Begley 2003b).

### **2.2.3 Carrier-mediated efflux**

Active efflux pumps such as the ATP-binding cassette (ABC) transporters, P-glycoprotein (Pgp), multidrug resistance associated protein (MRP), multi-specific organic anion transporter (MOAT), and breast cancer resistance protein (BCRP) represent the principle efflux mechanisms which transport a wide range of compounds out of the CNS. The ABC transporters are able to hydrolyse ATP which provides the energy for moving the substrates against a concentration gradient and opposing their natural tendency to partition into the lipid of the cell membrane. Pgp is the most important ABC transporter expressed at the apical surface of the choroid plexus. Pgp is involved in extruding many of the drug molecules from the brain. These drugs are mainly large planar molecules such as steroids and glucuronides ([Cordon-Cardo 1989](#)) (Figure 3c).

### **2.2.4 Carrier-mediated influx**

Carrier-mediated transport at the BBB contributes to the transport of many necessary polar metabolites and nutrients which they can carry into the CNS by transporters. Some polar substances such as monocarboxylates, hexoses, amino acids, nucleoside, glutathione, and small peptides are transported in this way. Carrier-mediated influx can be passive or secondarily active. Some of these transporters are expressed in both, the luminal and abluminal membranes of the cerebral endothelial cells (Figure 3d).

### **2.2.5 Vesicular transport**

Viruses and some solutes such as peptides and proteins are transported across the cells by vesicular transcytosis. Transcytosis begins as a microinvagination of the cell membrane to form a caveola (pit) which later would pinch off and migrate to the opposite side of the cell membrane. The free vesicle then would fuse and release its contents into the periendothelial basal lamina ([Begely 2003b](#)).



### 2.2.5.1 Absorptive-mediated transcytosis (AMT)

Absorptive-mediated transcytosis is a nonselective, slow process by which endothelial cells endocytose macromolecules nonspecifically bound to the luminal surface, with subsequent discharge to the perivascular space. Substances using this pathway include positively charged proteins that interact with negative electric charges of the endothelial membrane and accumulate on the membrane surface of the endothelial cells ([Abbott 1996](#)) (Figure 3f).

### 2.2.5.2 Receptor-mediated transcytosis (RMT)

The receptor at the apical plasma membrane of the endothelial cell binds to a circulating ligand (Figure 3e). Once the receptor binds to the ligand, the process of endocytosis is initiated as the receptor–ligand complexes cluster and then the membrane invaginates. This leads to the formation of intracellular transport vesicles. Brain influx of nutrients such as iron, insulin, and leptin occurs by a transcellular receptor-mediated transport mechanism known as transcytosis ([Brown 1991](#)).

### 2.2.6 The role of tight junctions

The tight junctions between the BBB endothelial cells have a higher endothelial electrical resistance, in the range of 1500 - 2000  $\Omega \times \text{cm}^2$  (pial vessels), as compared to 3 - 33  $\Omega \times \text{cm}^2$  in the other tissues. The net result of this elevated resistance is a low paracellular pathway. The tight junction effectively blocks an aqueous route of free diffusion for polar solutes from the blood and prevents these solutes from free access to the brain interstitial (extracellular) fluid.

As assessed *in vitro* by the passive flux or extracellular probes such as albumin or inulin, the phosphorylation of the proteins constituting the tight junctions enhances their permeability. Moreover, extracellular signals can influence the permeability of the tight junctions by the cytoskeleton ([Begley 2003b](#)) (Figure 3g).

Potential routes for transport across the BBB are schematically presented in Figure 3.

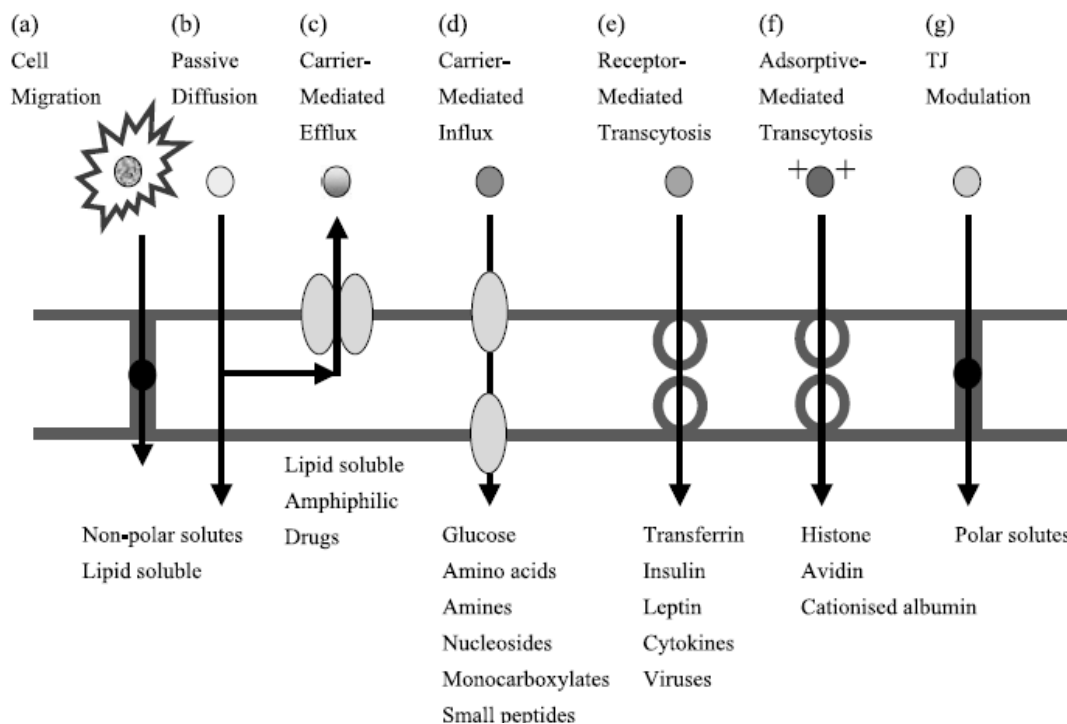


**Figure 3.** Potential routes for transport across the BBB. (a) Leukocytes may cross the BBB adjacent to, or by modifying, the tight junctions. (b) Solutes, especially those with lipophilic properties may passively diffuse through the cell membrane and cross the endothelium. (c) Active efflux carriers may intercept some of these passively penetrating solutes and pump them out of the endothelial cell. (d) Carrier-mediated influx, which may be passive or secondarily active, can transport many essential polar molecules such as glucose, amino acids, and nucleosides into the CNS. (e) RMT can transport macromolecules such as peptides and proteins across the cerebral endothelium. (f) AMT appears to be induced nonspecifically by charged macromolecules can also result in transport across the BBB. (g) Tight junction modulation may occur, which relaxes the junctions and wholly or partially opens the paracellular aqueous diffusional pathway (taken from Begley 2003a).

### 2.3 Drug delivery to the CNS

Many potentially active drugs are not able to enter the CNS in sufficient quantity to be effective. In general, diffusion across the BBB is only feasible for lipophilic molecules (<500 Da) with fewer than five hydrogen bonds *via* lipid-mediated diffusion. However, accumulation of these molecules in the brain is often restricted due to the ABC efflux transporters, such as Pgp or MRP (section 2.2.3).

A route for drugs delivery into the CNS *via* the olfactory epithelium is another possibility for some type of drugs. However, a significant fraction of this fluid appears to re-circulate back into the subarachnoid CSF and may carry the drug applied to the olfactory mucosa back into the subarachnoid space of the CNS (Begley 2003b).

The strategies employed to facilitate the drug transport to the CNS are described below.

### **2.3.1 Craniotomy-based drug delivery**

Several strategies employ craniotomy-based drug delivery, including either intraventricular drug diffusion or local intracerebral implants (Begely 2004).

Although these procedures can significantly increase drug levels in the brain, all of them are highly invasive. In addition, the craniotomy-based drug delivery relies on diffusion from the local depot sites; since diffusion decreases with the square of the diffusion distance, the effective treatment volume is often limited (Pardridge 1999). Indeed, the diffusional distance that can be reached in the brain using such systems does not exceed 5 mm whereas tumour areas beyond this distance remain unattainable (Roullin 2002).

### **2.3.2 Disruption of the BBB**

The rate of extravasation of the systemically administered drugs into the brain parenchyma can be enhanced by an osmotic opening of the BBB (Misra 2003).

The osmotic opening was developed initially for the patients with rapidly growing high grade gliomas. Intracarotid injection of an inert hypertonic solution such as mannitol or arabinose or vasoactive agents such as bradykinin (Bonstelle 1983, Nomura 1994) has been employed to initiate endothelial cells shrinkage and opening of the BBB tight junctions for a period of a few hours (Misra 2003).

The above approaches are most suited to short-term treatments, where a single or infrequent exposure to a drug is required. The determination of the therapeutic drug levels after disrupting of the BBB showed that the drug accumulated in the tumour core, but it was absent at its growing margins. Accordingly, the therapeutic drug levels could be found in necrotic tumour areas, while in peritumoural regions the drug levels were markedly lower or non-detectable (Donelli 1992).

### 2.3.3 Chemical modification of the drug

The CNS penetration is feasible for substances characterised by low molecular weight, lack of ionisation at physiological pH, and lipophilicity. Synthesising a hydrophobic analogue of small hydrophilic drugs is a strategy. This strategy has been frequently employed, but the results have often been disappointing due to an unexpected toxic effect of the new hydrophobic analogue (Misra 2003). Additionally, the new lipophilic compounds are often potential substrates for the ABC efflux transporters.

Another approach for the delivery to the CNS is the use of a prodrug, which involves the administration of the drug in a form that is inactive, or weakly active, but it is readily able to penetrate the BBB. In many cases, however, a suitable prodrug cannot be synthesised or the resulting molecule is too large.

The conjugation of the drug with the BBB specific transport vector is another strategy. This method takes advantage of the normal endogenous transport pathways within the brain capillary endothelium; the disadvantage is a low carrying capacity of the vector molecules that is generally limited by 1:1 stoichiometry of a carrier to a drug (Pardridge 1999).

### 2.3.4 Inhibition of efflux mechanisms

Several inhibitors, both competitive and noncompetitive, have been developed to modulate the activity of the major ABC transporters Pgp, MRP, and BCRP such as verapamil (Bart 2000) or Pluronic<sup>®</sup> L-61 (Venne 1996). One recent example for inhibiting the activity of Pgp efflux pump is the co-administration of valspodar with paclitaxel which produced an increasing paclitaxel level in the brain. The results showed an improvement of the therapeutic effect which assessed as the tumour growth inhibition in mice (Fellner 2002).

Although the use of the inhibitors of the ABC transporters can markedly enhance the BBB uptake of the drugs, the down-modulation of the efflux transport activity may, however, allow other toxic substrates to enter the brain more freely. Thus, the long-term treatment may not be possible due to enhanced adverse effects (Begley 2004).

## ***2.4 Nanocarriers for brain delivery***

Employment of the nanocarriers is a new strategy to enhance the drug delivery across the BBB.

*Nanoparticles* (NP) for purposes of drug delivery, are defined as submicron (<1  $\mu\text{m}$ ) colloidal particles. This definition includes solid nanoparticles (nanospheres) in which the active ingredient (drug or bioactive agent) is adsorbed, dissolved, or dispersed throughout the matrix and nanocapsules in which the active ingredient is confined to an aqueous or oily core surrounded by a polymeric wall. Alternatively, the drug can be covalently attached to the surface or into the matrix (Kreuter eds. 1994).

The nanoparticles are generally made from biocompatible and biodegradable materials, such as polymers, either natural (e.g. gelatin, albumin) or synthetic (e.g. polylactides, poly(alkyl cyanoacrylates)) or solid lipids. In the body, the drug loaded in nanoparticles will be released from the polymer matrix. The release mechanism is usually diffusion assisted by matrix swelling, erosion, or degradation.

In the early 1980s, Prof Speiser at the ETH (Swiss Federal Institute of Technology) in Zurich suggested that nanoparticles could be used for the drug delivery across the BBB. He was also the first to systematically develop nanoparticles for drug delivery purposes (Kreuter 2004).

### **2.4.1 Biodistribution of the nanoparticles to the normal brain**

The pharmacokinetic rule states that the mass of drug delivered to the brain is equally proportional to the BBB permeability coefficient and the area under the curve (AUC; plasma drug concentration-time curve) (Pardridge 1999).

The general approach to increase drug circulation time is the application of the long-circulating nanoparticles that avoid their rapid clearance by the tissues of the mononuclear phagocyte system (MPS). The particle uptake by macrophages could be decreased by interference with their opsonisation, which prevents complement activation and recognition of the particles (steric stabilisation of the particles or the so-called “stealth” effect).

Generally, steric stabilisation of nanocarriers in the blood stream can be achieved by physical adsorption of non-ionic surfactants or amphiphilic block copolymers, such as poloxamers or

poloxamines (block copolymers of poly(oxyethylene) and poly(oxypropylene)) or by their incorporation during the production of NP. Alternatively, particles can be formed from an amphiphilic copolymer, in which the hydrophobic block is able to form a solid phase, whereas the hydrophilic part provides the protection of the surface. All of these technological approaches have proved to be successful for the extension of the circulation time of NP and, in accordance with the pharmacokinetic rule. These approaches also afforded an enhancement of the brain delivery of NP and bound drugs (Moghimi 2001 and 2003).

Hydrophilic poly(ethylene glycol) (PEG) conformation at the surface of nanoparticles is another important factor for repelling of the opsonin and reducing the nanoparticle uptake by neutrophilic granulocytes *in vivo*. The PEG blocks have a brush-like (elongated coil, high density) or a mushroom-like (random coil, low density) conformation (Figure 4). The brush-like and intermediate configurations of the PEG-blocks at the nanoparticle surface reduced phagocytosis and complement activation, whereas the mushroom-like configuration of these blocks activated the complement and favoured phagocytosis. Gref *et al.* (Gref 2000) showed the maximum anti-opsonin effect with PEG of 5000 Da and above.

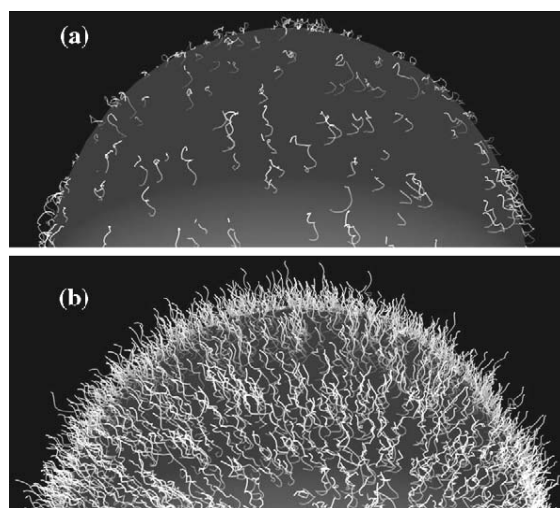


**Figure 4.** Schematic diagrams of PEG configurations on the upper hemisphere of a polymeric nanoparticle. (a) the low density “mushroom” configuration where most of the chains are located closer to the particles surface, (b) the high density of the PEG chains leads to the “brush” configuration where most of the chains are extended away from the surface (Owens 2006).

This approach proved to be efficient for brain delivery. As an example, doxorubicin (Dox) was delivered to the brain with the stealth (PEGylated) solid lipid nanoparticles (Zara 2002,

[Fundaro 2000](#)). The pharmacokinetic study of Dox bound to solid lipid nanoparticles (SLN) administered intravenously in rabbits demonstrated that the circulation time of the nanoparticle-bound drug was considerably increased as well as the drug concentration in the brain. The concentration of solid lipid nanoparticle was decreased in other organs (liver, heart, lungs, spleen, and kidney) compared to the drug in the solution. It is noteworthy that a decrease of Dox accumulation in the heart will reduce the cardiotoxicity of this drug. The integral pharmacokinetic parameter, the AUC of SLN-bound doxorubicin increased with the increasing content of a stealth agent (stearic acid - PEG 2000) present on the particles ([Zara 2002](#)). Compared to the non-stealth SLN, the SLN containing 0.45% of the stealth agent produced a 9-fold increase of Dox concentration in the brain.

#### **2.4.2 Distribution of the nanoparticles under the pathological condition of the brain**

The BBB function can be considerably compromised by tumour growth. As shown by tomography and magnetic resonance imaging, microvascular permeability correlates with the tumour histological grade. While the vasculature of low grade gliomas (brain tumours which arise from glial cells) is close to normal, high-grade gliomas are characterised by both, neovascularisation and vascular hyperpermeability, which is similar to other solid tumours, although less pronounced ([Hobbs 1998](#), [Roberts 2001](#), [Pluen 2001](#), [Vajkoczy 2004](#)).

In contrast to normal cerebral capillaries, vessels in gliomas are tortuous and sinusoidal; they are characterised by open interendothelial and transendothelial gaps, fenestrations, and increased microvascular diameter (3 - 40  $\mu\text{m}$  versus  $\sim 3 - 5 \mu\text{m}$  for cortical capillaries) and vessel wall thickness (0.5  $\mu\text{m}$  versus 0.26  $\mu\text{m}$ ) ([Schlageter 1999](#)). These abnormalities contribute to an increase in non-selective transendothelial transport and microvascular permeability and, consequently, impairment of the BBB functions at the tumour site. The intravenously injected nanoparticles and macromolecules (with a molecular weight of above 45 kDa) are able to extravasate across the leaky endothelium and then they accumulate in the tumour. This phenomenon is known as ‘the enhanced permeability and retention effect’ (the EPR effect) (Figure 5).

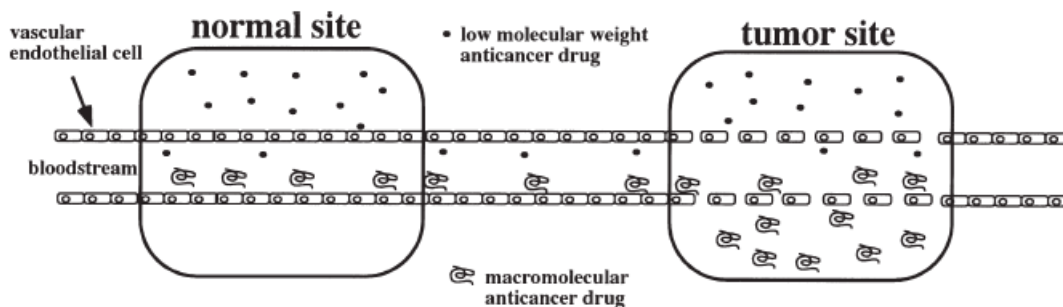


**Figure 5.** Enhanced permeability and retention (EPR) effect (Yokoyama 2005).

The lack of lymphatic drainage in tumours also contributes to the accumulation of the nanoparticles in certain solid tumours.

However, in order to take good advantage of these features, the particles have to stay long enough in the circulation to reach the tumour, which can be achieved by PEGylation or by coating with certain surfactants (Kreuter 2004).

A comparative biodistribution study was done for PEGylated poly(hexadecyl cyanoacrylate) nanoparticles (PEG-PHDCA-NP) and non-stealth PHDCA NP in rats bearing intracranial 9L glioblastoma (Brigger 2002). As expected, accumulation in tumour was about 3 times higher for the long-circulating PEG-PHDCA-NP than for PHDCA-NP; the latter had a very short circulation time due to a rapid and massive uptake by the MPS tissues. Nevertheless, both carriers were able to extravasate across the BBB at the tumour site and to accumulate preferentially in the tumour rather than in the peritumoural brain or the healthy contralateral hemisphere. In addition, a 4- to 8-fold higher accumulation of the PEGylated NP was observed also in parts of the brain protected by the normal BBB, as compared to PHDCA-NP.

### 2.4.3 Brain delivery with PBCA nanoparticles coated with polysorbate 80

One of the pioneer studies demonstrated the role of polysorbate 80 (Tween<sup>®</sup> 80; PS 80) coating of the nanoparticles for brain delivery, was performed *in vitro*, for bovine brain microvessel endothelial cells (Borchard 1994). The <sup>14</sup>C-labelled poly(methyl methacrylate) nanoparticle uptake into these cells was most effectively enhanced when they were coated with PS 80. These results were later substantiated by Ramge *et al.* (Ramge 2000). This



group investigated the uptake of rhodamine 6G-labelled poly(butyl cyanoacrylate) nanoparticles (PBCA-NP) into human as well as bovine primary brain capillary endothelial cells. The uptake was evidenced by fluorescence measurements as well as by laser confocal scanning microscopy. The PS 80-coated particles were taken up much more rapidly and in significant amounts, i. e. 20-fold, higher amounts than uncoated particles. These studies indicated that the uptake apparently occurs by endocytosis. Similar results were obtained with RBE4 cells (Alyautdin 2001).

The efficacy of PS 80-coating for brain targeting *in vivo* was most clearly demonstrated by Gulyaev *et al.* (Gulyaev 1999). PS 80-coated PBCA nanoparticles delivered doxorubicin in very considerable amounts to the rat brain (up to 6 µg/g), whereas a free drug could not penetrate across the BBB in detectable concentrations. It is noteworthy that PS 80 coating only moderately increased the plasma AUC of the nanoparticle-bound Dox (by ~70%) which suggests that the mechanism of brain delivery could be specific (discussed below, section 2.5.2).

## ***2.5 Pharmacological activity of the nanoparticle-bound drugs***

### **2.5.1 Neuroactive agents**

The PBCA-NP coated with PS 80 enabled transport of a number of drugs across the BBB, following intravenous injection. These drugs include hexapeptide endorphin dalargin (Kreuter 1995, Alyautdin 1995), dipeptide kytorphin (Schroeder 1998), loperamide (Alyautdin 1997), tubocurarine (Alyautdin 1998), and N-methyl-D-aspartate (NMDA) receptor antagonists MRZ 2/576 and MRZ 2/596 (Friese 2000a, b).

The brain delivery of these substances using nanoparticles was supported by using pharmacological tests. The nociceptive threshold of the nanoparticle formulations of dalargin, kytorphin, and loperamide was determined by the tail-flick test (Alyautdin 1995, Kreuter 1995) or by the hot-plate test (Schroeder 1996, Ramge 1999). In contrast to the drugs bound to PS 80-coated NP, the drug solutions or uncoated nanoparticulate formulations did not exhibit any significant effects (Figure 6). The antinociceptive effect of dalargin bound to PS 80-coated NP was accompanied by a pronounced Straub effect (tail

erection) and was totally blocked by a prior injection of naloxone ( $\mu$ -opiate receptor antagonist) demonstrating the involvement of the opioid receptors. These CNS effects provided additional evidence that dalargin was transported across the BBB in a dose-dependent manner. The antinociceptive effects of dalargin were obtained also when the NP were coated with polysorbates 20, 40, 60, or 80, whereas other surfactants, such as poloxamers 184, 188, 338, 407, poloxamine 908, Brij<sup>®</sup>35, Cremophor<sup>®</sup>EZ, or Cremophor<sup>®</sup>RH 40 were ineffective (Schroeder 1998, Kreuter 1997).

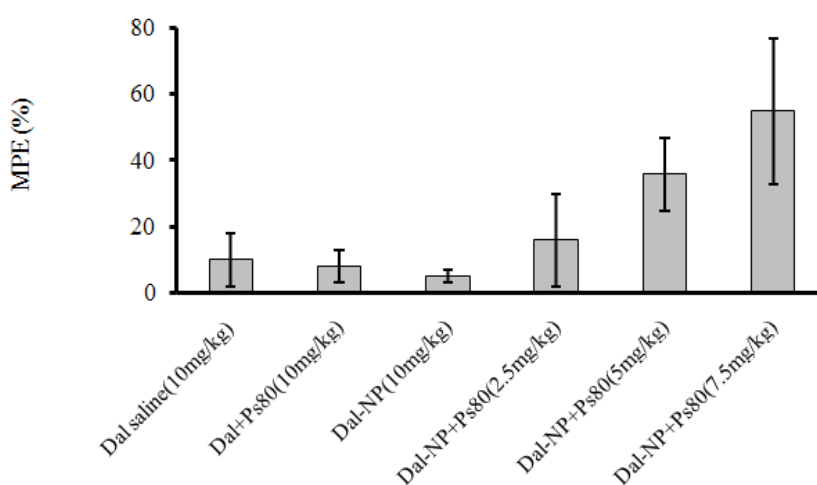


**Figure 6.** Antinociceptive effect after intravenous injection of different dalargin (Dal) formulation into ICR mice. Percentage of maximal possible effect (MPE%) determined by tail flick test 45 min after *i.v.* injection of dalargin in solutions and bound to non-coated and polysorbate 80-coated PBCA-NP (n = 5); NP = nanoparticles; PS 80 = polysorbate 80. Values are mean  $\pm$  SD. Adapted from Kreuter *et al.* (Kreuter 1995).

The same series of experiments were repeated with loperamide-bound PBCA-NP coated with PS 80. Loperamide ( $\mu$ -opiate receptor agonist) is a Pgp substrate; therefore it lacks the central pharmacological effect. Again, a strong dose-dependent analgesic effect and a typical Straub effect were observed with loperamide after binding to nanoparticles and overcoating with PS 80. There were no effects without this coating.

Transport of tubocurarine across the BBB was demonstrated using an *in situ* perfused rat brain technique together with a simultaneous recording of the electroencephalogram (Alyautdin 1998). Tubocurarine (a quaternary ammonium salt) does not penetrate into the brain across the normal BBB. However, a direct intraventricular injection of tubocurarine provokes the development of epileptiform spikes that can be recorded by the encephalogram.

Neither tubocurarine solution nor tubocurarine-loaded NP without PS 80-coating or a mixture of PS 80 and tubocurarine was able to influence the encephalogram. However, the addition of tubocurarine-loaded NP coated with PS 80 caused frequent severe spikes.

A novel non-competitive NMDA receptor antagonist MRZ 2/576 is a potent but rather short-acting anticonvulsant. The short effect of this drug (5 - 15 min) is most probably due to its rapid elimination from the CNS by efflux transporters that can be blocked by probenecid. Administration of the drug-bound PBCA-NP coated with PS 80 prolonged the duration of the anticonvulsive activity in mice up to 210 min and after probenecid pre-treatment up to 270 min compared to 150 min with probenecid and MRZ 2/576 alone (Friese 2000b). The results of this study demonstrate that PS 80-coated PBCA-NP not only enhances the brain delivery of drugs that are not able to freely penetrate the BBB, but they can also prolong the CNS availability of the drugs that have a short duration of action.

### 2.5.2 Doxorubicin

Doxorubicin (Dox) is an anthracycline antibiotic with a broad spectrum of the anticancer activity. Dox is a DNA intercalator and inhibits also the progression of the enzyme topoisomerase II. However, due to delivery problems, Dox is so far not applied for the systemic treatment of gliomas: the drug is a substrate of the ABC transporter and does not penetrate into the brain in therapeutic concentrations (von Holst 1990). However, Dox exhibits a cytotoxic effect against glioma cells *in vitro* and prolongs the survival time in patients with glioma upon intra-tumoural administration (Stan 1999, Walter 1995).

The cytotoxicity of Dox-loaded PBCA-NP coated with different surfactants was investigated in the rat glioma cell lines GS-9L, F-98, and RG-2 employing the tetrazolium (MTT) and the lactate dehydrogenase (LDH) assays (Sanchez de Juan 2006). The MTT assay based on the mitochondrial activity and LDH assay based on the LDH, released from the cytosol of damaged cellular membrane, are both demonstrating the cells viability after the exposure to the drug. The results confirmed the high efficacy of Dox against glioblastoma cells in tissue cultures as suggested earlier by Stan *et al.* (Stan 1999).

The therapeutic potential of brain targeting using surfactant-coated Dox-loaded PBCA-NP was clearly demonstrated by the experiments concerning the chemotherapy of intracranial glioblastoma (Gulyaev 1999, Steiniger 2004, Ambruosi 2006a, Petri 2007).

In the study of Steiniger *et al.* (Steiniger 2004) the glioblastoma-bearing rats (total  $n = 151$ ) were subjected to  $3 \times 1.5$  mg/kg or  $3 \times 2.5$  mg/kg of Dox in different formulations injected intravenously on days 2, 5, and 8 after tumour implantation. The most prominent result was achieved in the group treated with  $3 \times 1.5$  mg/kg of Dox-bound to PS 80-coated NP: a significant increase in survival time was obtained and more than 20% animals showed a long-term remission (Figure 7).

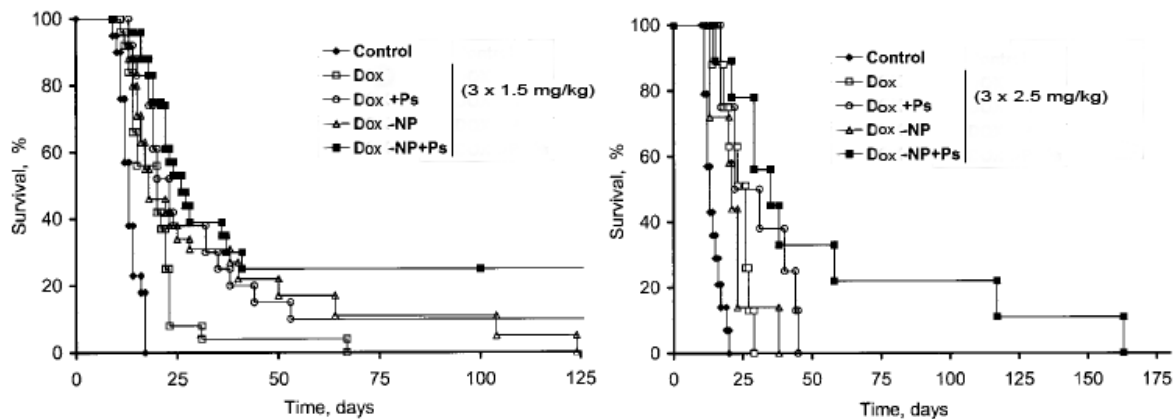


**Figure 7.** Percentage of survival (Kaplan-Meier plot) of rats with intracranially transplanted glioblastoma 101/8 after intravenous injection of doxorubicin formulations: (left) doxorubicin dosage 1.5 mg/kg; (right) doxorubicin dosage 2.5 mg/kg, both administered on days 2, 5 and 8 using one of the following formulations; Dox, doxorubicin in saline; Dox+PS, doxorubicin in saline plus polysorbate 80; Dox-NP, doxorubicin bound to poly(butyl cyanoacrylate) nanoparticles; Dox-NP+PS, doxorubicin bound to poly(butyl cyanoacrylate) nanoparticles coated with polysorbate 80 (Steiniger 2004).

These animals were sacrificed after 6 months, and no histological evidence of tumour was observed. Preliminary histology confirmed lower tumour sizes and lower values for proliferation and apoptosis in this group. The mean survival time was even more prolonged in the group treated with  $3 \times 2.5$  mg/kg of Dox, indicating a dose dependence of the antitumour effect. However, long-surviving animals in this group died before day 180 most probably due to the high toxicity of this regimen. Interestingly, the survival time was also increased in the groups treated with Dox solution in 1% PS 80 and Dox bound to non-coated PBCA-NP. This phenomenon could most probably be explained by the EPR effect

associated with a higher permeability of the BBB at the tumour site that allowed entry of other formulations into the brain (Vajkoczy 2004).

The higher efficacy of the PS 80 coated nanoparticles may be explained by the ability of these carriers to deliver the drug across the BBB at an early stage of tumour development due to a receptor-mediated mechanism. In this way doxorubicin is able to reach those parts of the brain which are still protected by an intact BBB.

It is noteworthy that clinical signs of neurotoxicity were absent throughout the study. Moreover, the histological study of the animals treated with the dose of  $3 \times 2.5$  mg/kg and sacrificed on day 12 did not reveal any signs of neurotoxicity.

Ambruosi *et al.* (Ambruosi 2006) have extensively studied the role of passive doxorubicin transport across the leaky BBB to the brain tumour using PBCA-NP coated with two surfactants, poloxamer 188 and poloxamine 908. The long-term remission of 20% (4/20) of both formulations was achieved and attributed to EPR effect. Although poloxamer 188 and poloxamine 908 could not provide any drug transport across the intact BBB of healthy animals (Kreuter 1997, Calvo 2001), these surfactants could facilitate the particle extravasation across the BBB at the tumour site.

### 2.5.3 Mechanisms of drug delivery to the brain by nanoparticles

A number of possibilities could explain the mechanisms of drug delivery across the BBB by means of NP:

1. *Opening of the BBB due to surfactant coating or particle interaction with the brain endothelium:* A mechanism of general toxicity characterised by an increase in the permeability of endothelial cell membranes and/or an opening of the tight junctions between the endothelial cells.
2. *Adhesion of NP to the capillary wall:* Increased retention of NP in the brain blood capillaries could create a higher concentration gradient that would enhance the transport to the brain.

3. *Endocytosis of the NP by brain endothelial cells*: Uptake followed by the drug entering to the residual brain and diffusion after its release by desorption or biodegradation from the nanoparticle system (Begley 2000).
4. *Transcytosis of the NP*: Translocation of the NP through the endothelial cell layer with bound drugs.
5. *Influence on the cell membrane permeability*: The nanoparticle could induce changes in the endothelial cell membrane viscosity/fluidity thus enhancing drug penetration into these cells.
6. *Inactivation of the Pgp efflux pump*: Certain surfactants, including PS 80, were shown to inhibit this efflux system and to reverse MDR (Woodcock 1990 and 1992, Zordan-Nudo 1993, Nerurkar 1996).

The mechanism of the delivery of the drugs across the BBB by NP is not still fully elucidated. However, it is reasonable to assume that more than one mechanism could enable the significant drug transport by NP into the brain.

The theory of the non-specific permeabilisation and then opening of the BBB, *mechanism 1*, is unlikely to contribute to the nanoparticle-mediated drug delivery to the brain. The necessity of drug binding to the PBCA-NP and lack of efficacy of a drug in a surfactant solution is suggesting more specific mechanism for drug transport across the BBB (Alyautdin 1995, Gulyaev 1999, Kreuter 1995, Steiniger 2004, Kreuter 2003).

Moreover, the integrity of the BBB in rats was evaluated by the measurement of the inulin spaces (Alyautdin 2001): After administration of PS 80-coated PBCA-NP, the space volumes increased only slightly without significantly disrupting the BBB. In another study, with an *in vitro* BBB model consisted of a co-culture of bovine brain capillary endothelial cells and rat astrocytes, the permeability was evaluated by measuring the flux of the extracellular markers [<sup>14</sup>C]-sucrose and [<sup>3</sup>H]-inulin across a cell monolayer. After co-incubation of these cells with PS 80-coated or uncoated PBCA-NP, no significant changes in permeability were observed (Kreuter 2003). By contrast, in a similar study with the same BBB model, the result showed over 10-fold increase in the sucrose and inulin fluxes. However, in this case, serum

was not added to the cell medium, which could impair the integrity of the cell layer (Olivier 1999).

Steiniger *et al.* (Steiniger 2000) demonstrated that slight changes in the *in vitro* models of the BBB can lead to considerable discrepancies in the results. In this study, a BBB model was made from a cultivated bovine brain capillary endothelial cells which was originating from the grey matter and no astrocytes were co-cultured. After incubation with 10 µg/ml of the NP preparation, the [<sup>14</sup>C]-sucrose flux increased 2-fold with uncoated and 6.5-fold with PS 80-coated PBCA-NP.

In several studies, the opinion that toxicity is not the mechanism for the nanoparticle-mediated drug transport across the BBB with other types of NP was substantiated (Calvo 2001, Koziara 2003 and Lockman 2003).

The evaluation of the modification of the BBB permeability due to PHDCA-NP or surfactants using [<sup>14</sup>C]-sucrose was performed Calvo *et al.* (Calvo 2001). None of the nanoparticulate preparations modified the low passage of sucrose, which indicates that the penetration of the NP was not associated with the increase of the BBB permeability. However, 1% solution of PS 80 noticeably increased the concentration of sucrose in all the brain structures.

Two types of SLN with a size of about 100 nm, consisting of emulsifying Wax / Brij<sup>®</sup> 78 or Brij<sup>®</sup> 72 / PS 80, were made by Koziara *et al.* (Koziara 2003) and Lockman *et al.* (Lockman 2003). These NP were labeled with entrapped [<sup>3</sup>H]-cetyl alcohol and the permeability of the BBB was investigated by an *in situ* brain perfusion measuring the cerebral perfusion flow of the [<sup>14</sup>C]-sucrose. For both SLN types significant brain uptake was measured. The transfer rate of the SLN stabilised by PS 80 (Brij<sup>®</sup> 72/PS 80) NP from perfusion fluid into the brain was significantly higher than that of the NP stabilised by Brij<sup>®</sup> 78 (E. wax/Brij<sup>®</sup> 78). At the same time, these NP did not induce statistically significant changes in the BBB integrity, permeability, or choline transport. In addition, it was shown that the particles had a minimal effect on the BBB integrity. The Western blot analysis confirmed that the incubation of these NP with bovine brain microvessel endothelial cells did not alter the expression of the BBB junctional proteins, such as occludin and claudin-1. The above data suggest that the

brain uptake of these NP was not associated with paracellular transport or opening of the tight junctions.

Although an increased concentration of the nanoparticles on the walls of the blood capillaries of the brain would enhance the transport across the endothelial cell layer and delivery to the brain, **mechanism 2**, the drug would still be subjected to very effective efflux pumps located in the luminal membrane of the endothelial cells such as Pgp. The efficient efflux of known substrates for Pgp loperamide, doxorubicin, and tubocurarine showed that this mechanism is largely insignificant (Begley 1996).

The fundamental study of Tröster *et al.* (Tröster 1990) with <sup>14</sup>C-labelled poly(methyl methacrylate) nanoparticles (PMMA-NP) in rats investigated the influence of different surfactants on the biodistribution and the brain uptake. The preparations were administered intravenously after incubation of the NP in 1% surfactant solutions. Poloxamine 908 was the most effective among other surfactants for increasing the plasma concentration of the NP (100-fold increase 30 min after injection), whereas PS 80 produced only a 5-fold increase, yet showed a similar brain uptake. The author suggested that the PMMA-NP were not engulfed by the endothelial cells lining the vasculature but rather adhered to these cells.

This mechanism was also suggested by Zara *et al.* (Zara 2002), among other possibilities, for doxorubicin-loaded stealth solid lipid nanoparticles (SLN). Doxorubicin was bound to these particles using hexadecylphosphate as counterion. The enhanced uptake of doxorubicin in the brain was associated with the increase in the concentration of stealth agent in the SLN. Although the higher stealth agent concentration led to a parallel increase in the surface hydrophilicity of the carriers, it did not hinder the NP interaction with the cell membrane and the passage through the BBB. This observation implies the involvement of an additional mechanism in the doxorubicin transport to the brain with the stealth SLN.

Endocytosis of the NP by brain microvessel endothelial cells and release of the drug in these cells, **mechanism 3**, is the most likely mechanism which has been demonstrated for the drugs loaded in the PBCA-NP *in vitro* and *in vivo* (Kreuter 2001 and 2002a).

In the study of Ambruosi *et al.* (Ambruosi 2005) the brain uptake of empty <sup>14</sup>C-PBCA nanoparticles overcoated with PS 80 and doxorubicin-loaded <sup>14</sup>C-PBCA nanoparticles



overcoated with PS 80 was investigated. An about one hour delay in the increase in the brain concentrations with two polysorbate-coated nanoparticle preparations was observed. This delay is attributed to delivery mediated by PS 80-coating (Alyautdin 1995 and 2001, Kreuter 1995, Alyautdin 1997, Gulayev 1999) and might reflect the time-consuming process of endocytosis.

In addition, the uptake of fluorescent PBCA-NP labelled with rhodamine 6G was observed in cultured human, bovine, and murine brain microvessel endothelial cells (Ramge 2000). Uptake of the surfactant-coated NP was far more pronounced compared to the uncoated particles, even though in the bovine cells a slight increase in uptake of the uncoated particles was observed with the increasing time of incubation. Using image analysis software, a 20-fold increase in uptake of coated with respect to uncoated nanoparticles was observed in 2 h. The human cells also exhibited the enhanced uptake of the coated NP.

The uptake of fluorescent PBCA-NP by rat brain endothelial cells of the RBE4 cell line was also demonstrated by Alyautdin *et al.* (Alyautdin 2001). The PBCA nanoparticles were labeled with fluorescein isothiocyanate (FITC) dextran 70,000. After addition of PS 80-coated NP, the cells showed a punctate appearance of fluorescence concentrated within the cells. In contrast, after treatment with the uncoated nanoparticles no fluorescence was observable within the cells, even after the addition of a 10-fold higher concentration of nanoparticles, while a strong fluorescence was apparent in the surrounding medium. In none of the above experiments addition of PS 80-coated or uncoated NP appeared to damage the RBE4 cells.

There are indications that PS 80-coated PBCA-NP bind to a lipoprotein receptor, like low density lipoprotein receptor (LDL-R) or low-density lipoprotein receptor-related protein (LRP). The polysorbate coating led to the adsorption of apolipoprotein E (Apo E) and apolipoprotein B (Apo B) from the blood after the *i.v.* injection. The NP thus could mimic lipoprotein particles, which would then interact with the lipoprotein receptors located on the brain capillary endothelial cells. A subsequent endocytosis of the NP together with the bound drugs would then occur (Kreuter 2004).

Additionally, it was shown that coating of PBCA-NP with Apo E and B in the absence of surfactant was also sufficient for drug transport to the brain (Kreuter 2002). PBCA-NP loaded with dalargin or loperamide were coated with the Apo AII, B, CII, E, or J without

coating or after precoating with PS 80. After *i.v.* injection to mice the antinociceptive threshold was measured by the tail flick test. An antinociceptive effect was achieved only after the treatment with dalargin- or loperamide-loaded PBCA-NP coated with PS 80 and/or with Apo B or E. The effect was higher when the NP were first coated with PS 80 and then overcoated with apolipoprotein E. Furthermore, the antinociceptive threshold of PS 80-coated dalargin-loaded PBCA-NP was determined in Apo E-deficient and normal mice. In the apolipoprotein E-deficient mice, the antinociceptive effect was considerably reduced in comparison to the normal mice. Similar antinociceptive effects were also achieved after coating of dalargin-loaded particles with apolipoprotein B.

Consistent results were reported in the study of Michaelis *et al.* (Michaelis 2006). The human serum albumin nanoparticles (HSA-NP) were modified by covalent linkage to Apo E, and loperamide was absorbed on the surface of these NP. The ability of these particles to transport loperamide across the BBB was tested *via* the tail-flick test. Loperamide solution and unmodified HSA-NP loaded with loperamide were used as controls. The Apo E-coupled HSA-NP revealed strong antinociceptive effects whereas the control formulations including non-modified HSA-NP were unable to transport loperamide across the BBB. This result has corroborated the earlier findings which showed that association of Apo E to the nanoparticles can mediate the drug transport to the brain. Bound drugs then may further be transported into the brain by diffusion after release within the endothelial cells or, alternatively, by transcytosis, as observed for LDL by Dehouck *et al.* (Dehouck 1997).

Furthermore, Petri *et al.* (Petri 2007) observed the involvement of apolipoprotein A-I (Apo A-I) in the brain delivery of Dox loaded in the surfactant-coated PBCA-NP in glioblastoma-bearing rats. In this study, Dox loaded-PBCA-NP were produced using two different stabilisers, dextran and poloxamer 188 (Pluronic<sup>®</sup> F68; F68). Then the NP were overcoated with either F68 or PS 80. The treatment regimen used in this study was  $3 \times 1.5$  mg/kg on days 2, 5, and 8 after the tumour implantation. This regimen had previously proved to be efficient against glioblastoma (Steiniger 2004). All formulations produced extended survival times when compared to untreated animals. It was also shown that the presence of Dox and the NP as formulation parameters increased the therapeutic efficacy, whereas the effect of

the stabilisers/surfactants used (i.e. polysorbate 80, poloxamer 188, and dextran) could not be differentiated from each other.

Both formulations of Dox containing poloxamer 188 as a coating material or as a stabiliser produced a long-term remission in 20% of the animals (4/20 and 2/10, respectively). The effect of these formulations was comparable to that of doxorubicin bound to PBCA-NP stabilised with dextran and coated with PS 80, which produced 22% (5/23) of long-term survivors. The study further investigated the plasma protein adsorption patterns of Dox-loaded PBCA-NP stabilised with dextran and coated with poloxamer 188 or PS 80. Both formulations adsorbed high amounts of Apo A-I and J. Furthermore, the adsorbed amounts of albumin, IgG  $\gamma$ , Apo C-III, and thiostatin were comparable. Differences could be observed, for example, in the adsorption of antitrypsin for the nanoparticles coated with poloxamer 188 and transferrin for the nanoparticles coated with PS 80 (Figure 8).

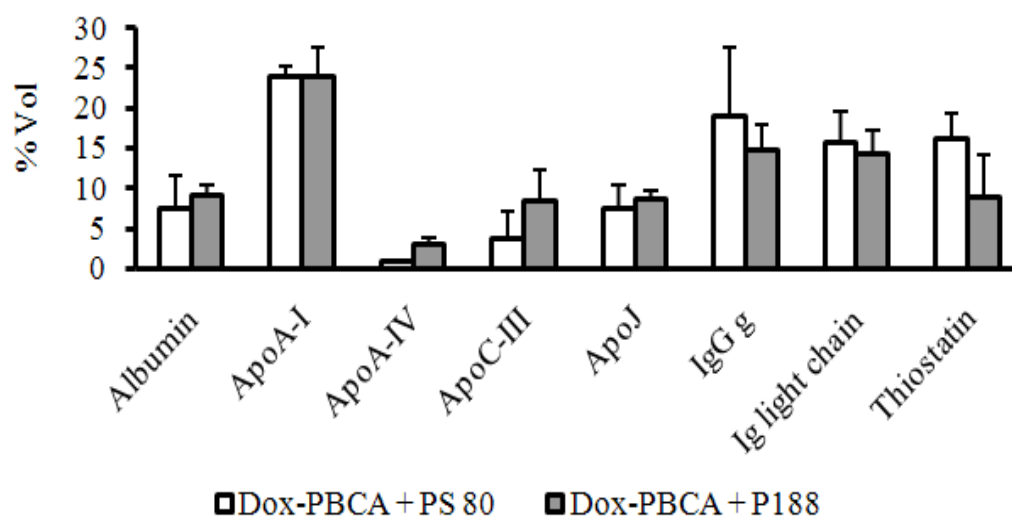


**Figure 8.** Similarity of plasma proteins pattern adsorbed by Dox-loaded PBCA nanoparticles coated with polysorbate 80 (Dox-NP/Dex+PS 80) or poloxamer 188 (Dox-NP/Dex+F68) in rat plasma (taken from Petri 2007).

The protein patterns of the uncoated nanoparticles differed considerably from the adsorption pattern of the surfactant-coated nanoparticles. The amount of albumin adsorbed on the surface of uncoated particles exceeded 50% of the total amounts of adsorbed proteins.

The role of PS 80-coating of the nanoparticles that facilitated their interaction with the brain microvessel endothelial cells has been also demonstrated for other types of NP. Lipid drug conjugate (LDC) nanoparticles were composed of stearic acid and diminazene. PS 80 was used as an emulsifier (Gessner 2001). Confocal laser scanning microscopy of the murine brain tissue showed Nile Red-labelled LDC particles adhering to the endothelium of the brain vessels and dye diffusing into the brain tissue. After incubation of the nanoparticles in murine plasma, the plasma protein adsorption pattern was investigated by two-dimensional electrophoresis. The result revealed a strong adsorption of apolipoproteins A-I and A-IV onto LDC the nanoparticles surfaces. However, apolipoprotein E could not be identified. The authors suggested that the ability of the PS 80-coated nanoparticles to deliver drugs to the brain is not only mediated by adsorption of apolipoprotein B and E but it probably involves a “team-work” of other apolipoproteins that prevent the hepatic uptake of the nanoparticles, thus facilitating brain delivery.

Petri *et al.* (Petri 2007) suggested another hypothesis. It was hypothesized that ApoA-I adsorbed on the surface of Dox-loaded NP could bind to the scavenger receptor class B type I (SR-BI). This receptor is expressed on the membranes of the endothelial cells of brain capillaries (Panzenboeck 2002, Balazs 2004, Krieger 1999). The uptake of Dox into the cells could be assisted by circumvention of the transmembrane efflux pump Pgp, which is expressed by the blood-brain vessel endothelial cells and represents an important constituent of the BBB. This circumvention could be enabled by simultaneous release of Dox and the degradation product of PBCA (= polycyanoacrylic acid) at the cell membrane. An ion-pair previously formed by polycyanoacrylic acid and Dox could enable the crossing of the cell membrane without being recognised by Pgp (Verdiere 1997). Retention of the particles by the SR-BI receptor on the cell walls combined with a slow degradation would augment this process.

The adsorptive endocytosis is a likely mechanism of the enhanced transport of antisense oligonucleotides (ODN) across the BBB with the positively charged Nanogel™ particles (Vinogradov 2002 and 2004). The main obstacle to effective therapy with ODN compounds is their anionic characteristic and relatively large molecular structure, which hampers their access to the target sites localised in the cell cytoplasm and/or nucleus. On the other hand,

the positively charged NP are believed to interact electrostatically with the negatively charged cell membrane, which is followed by the internalisation of these particles within these cells *via* the adsorptive endocytosis. Indeed, positively charged Nanogel formulation allowed more effective ODN transfer across the monolayers of brain microvessel endothelial cells, as compared to the electroneutral formulation. This result is in concert with the *in vivo* data demonstrating the substantial brain/plasma ratio of the ODN achieved after injection of ODN-loaded Nanogel particles. The cationic nature of this carrier system may also influence intracellular trafficking of ODN. Thus, delivery with Nanogel particles afforded effective release of ODN and its accumulation within the nucleus, whereas free ODN molecules are mainly localised within endosomal and lysosomal compartments and their access to the nucleus is usually achieved only after the addition of chloroquine. It is possible that following the internalisation, the cationic nanoparticles interact with the negatively charged endosomal membrane, which may cause destabilisation of the membrane and facilitate the release of ODN and its access to the nucleus.

Presently, little is known about transcytosis of the nanoparticles with bound drugs, ***mechanism 4***. It is possible that after their endocytotic uptake the particles can be transcytosed through the brain blood vessel endothelial cells.

*In vitro* transcytosis of LDL across the blood-brain barrier was observed in the Cecchelli-Model by Dehouck *et al.* (Dehouck 1997). Furthermore, cholesterol depletion was upregulated the expression of the LDL receptor in this model.

Transcytosis of cationic polysaccharide nanoparticles coated with a lipid bilayer across the *in vitro* BBB model was observed by Fenart *et al.* (Fenart 1999). The BBB model consisted of a co-culture of bovine brain capillary endothelial cells and rat astrocytes. Neutral, anionic, and cationic 60-nm NP were prepared from cross-linked maltodextrin derivatised or not (neutral) with anionic (phosphates) or cationic (quaternary ammonium) ligands. The particles were labelled with fluorescein and coated (or not) with a lipid bilayer. Cationic lipid-coated NP were found to be the best for permeating across the BBB, whereas coating of the neutral particles did not significantly alter their permeation characteristics. No modification of the paracellular permeability was observed during the incubation of cells with the NP, so this increase was not due to a breakdown of the barrier. The distribution of

these particles throughout the cytoplasm was characteristic for transcytosis. In contrast, the perinuclear localisation of non-coated polysaccharide nanoparticles showed an intracellular accumulation of these NP in a degradation compartment.

The observations of Kreuter *et al.* (Kreuter 2003) did not support the theory of the fluidisation of the endothelium by surfactants, **mechanism 5**. Experiments with some surfactants using the tail-flick test and dalargin showed that polysorbate 20, 40, 60 were able to transport dalargin into the brain and to produce an antinociceptive effect, although this effect was somewhat lower than with polysorbate 80. However other polysorbates such as PS 83 and PS 85 did not induce a significant CNS effect. This indicates that the transport of dalargin and the other drugs across the BBB cannot be due to a simple surfactant effect on the endothelial cells or on the tight junctions, since some of the surfactants were inactive. It might be argued that polysorbates would interact much more strongly with the NP than other surfactants (Kreuter 1997).

It was also reported that the treatment which caused membrane fluidisation can lead to inhibition of Pgp. Pluronics with intermediate lipophilic properties, such as Pluronic<sup>®</sup> P85, showed the strongest fluidisation effect on the cell membranes along with the most efficient reduction of intracellular ATP synthesis. The changes in the cell membrane viscosity/fluidity inhibited the efflux system, such as Pgp, and facilitated the brain uptake of Pgp-dependent drugs (Batrakova 2001 and 2003).

The enhanced drug delivery to the brain with PS 80-coated PBCA nanoparticles may be associated with the inhibition of the transmembrane efflux pumps, such as MRP and Pgp, **mechanism 6**. Indeed, all drugs delivered to the brain with PS 80-coated NP, such as loperamide, dalargin, doxorubicin, and MRZ 2/576, are the Pgp and/or MRP substrates.

The ability of PACA-NP to overcome MDR mediated by Pgp was described extensively (Vauthier 2003a, Hu 1996, Verdiere 1997). Poly(isobutyl cyanoacrylate) NP could reverse the Pgp-dependent MDR to Dox and produced considerable cytotoxic effects in P388/ADR cells resistant to Dox (Hu 1996, Verdiere 1997, Vauthier 2003b).

Accordingly GS-9L cells exhibiting the highest Pgp expression were the most resistant toward both, free and nanoparticle-bound Dox. Among the surfactants used, only PS 80-coating significantly enhanced the cytotoxicity of the nanoparticle-bound doxorubicin in all cell lines, including the Pgp-expressing GS-9L cells, whereas the other surfactants, poloxamer 188, and poloxamine 908 (Tetronic<sup>®</sup> 908), had negligible influence (Sanchez de Juan 2006).

Possible mechanisms of Dox transport across the BBB with PACA-NP are summarised in Figure 9.

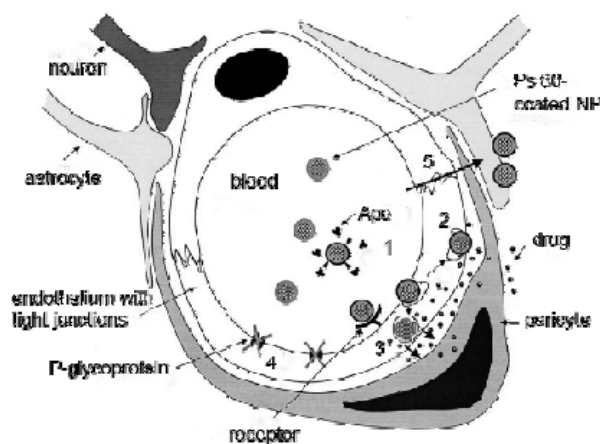


**Figure 9.** Hypothetical mechanism of drug delivery to the brain by means of polisorbate 80-coated poly(alkyl cyanoacrylate) nanoparticles. (1) adsorption of apolipoprotein(s) onto the nanoparticles; (2) transcytosis of the nanoparticles; (3) endocytosis followed by intracellular degradation of the nanoparticles, resulting in release of the drug and diffusion towards the interior of the brain; (4) inhibition of P-glycoprotein; (5) modulation of tight junction opening (taken and modified from Vauthier 2003b).

## 2.6 Toxicological aspects

As mentioned above, NP are able to reduce drug toxicity largely due to their altered body distribution and/or the absence of the peak concentration of the drug. In addition, the use of nanoparticles has been shown to improve lifespan and inhibit tumour growth *via* an increased distribution in tumour.

The acute toxicity after intravenous injection of doxorubicin bound to PBCA nanoparticles was investigated in healthy and glioma 101/8-bearing rats (Gelperina 2002). No significant

difference in the parameters of acute toxicity were found between the four Dox formulations: Dox solution in saline, Dox solution in saline containing 1% PS 80, Dox bound to uncoated NP, and Dox bound to PBCA-NP coated with PS 80. Moreover, the results of this study indicated that the toxicity of doxorubicin bound to NP is similar to or even lower than that of the free doxorubicin.

It is known that Dox displays a pronounced cardiotoxicity that is associated with the peak cardiac concentration. The results of a recent study by Pereverzeva *et al.* (Pereverzeva 2007) demonstrated that the hematological, cardiac, and testicular toxicity of doxorubicin could be reduced by binding the drug to PBCA-NP and even more considerably by binding the drug to HSA-NP. The intravenously injected dose of Dox was 1.5 mg/kg. It was administered three times with 72-h intervals (days 2, 5, and 8 after tumour transplantation). Coating of PBCA-NP with PS 80 contributed to the reduction of the toxicity. The lower toxicity of the nanoparticle formulations most probably can be explained by the altered biodistribution of the drug mediated by the NP.

In another comparative toxicological study, Dox was injected at a higher dose of 6 mg/kg either as a single injection or in form of four weekly injections (Pereverzeva 2008). The animals received for 4 and 40 days a single injection or for 25 and 61 days multiple injections. The dynamics of body weight, haematological parameters, blood biochemical parameters, and urinalysis were determined. The pathomorphological evaluation included macroscopic evaluation and weight measurement of the internal organs. The heart, lung, spleen, testes, and liver were also subjected to a histological evaluation. The overall result of this study suggested that the surfactant-coated nanoparticles formulation of Dox possesses a very favorable toxicological profile. Specifically, this study revealed again a major advantage of these NP - a considerably reduced cardio- and testicular toxicity, as compared to a free drug, thus corroborating previous observations (Couvreur 1982 and 1986, Pereverzeva 2007).

Similar toxicological observations were made in the above mentioned chemotherapy study of Steiniger *et al.* (Steiniger 2004). A limited dose-dependent systemic toxicity was found in the group treated with Dox in saline. The autopsy of the whole body in healthy animals in this study revealed an empty gastrointestinal tract only in animals treated with Dox solution.



## | Theory

Healthy animals treated with Dox solution also showed slight signs of lung edema, which was confirmed by histology. These changes were not observed in animals treated with Dox bound to the NP.

Importantly, an indication of short-term neurotoxicity (increased apoptosis in areas distant from the tumour, increased the expression of glial fibrillary acidic protein (GFAP) or ezrin on distant astrocytes or degenerative morphological changes of neurons) were entirely absent in the animals sacrificed on the day 12 post-implantation. The neurotoxicity indication were also absent in long-term survivors with no sign of chronic glial activation in areas distant from the tumour site. Moreover, long-term survivors did not exhibit any obvious neurological symptoms ([Steiniger 2004](#)).

In conclusion, the injectable NP carriers have the ability to revolutionize the treatment of the CNS diseases. In particular, they have a potential for the systemic chemotherapy of glioblastomas.

## 3 Materials and Methods

### 3.1 *Poly(butyl cyanoacrylate) nanoparticles*

Three drugs, doxorubicin hydrochloride, loperamide hydrochloride, and paclitaxel, were loaded to PBCA nanoparticles. The nanoparticles were prepared by anionic polymerisation of n-butyl-2-cyanoacrylate (BCA) in the presence of the drug.

#### Chemicals

0.01 N Hydrochloric acid

1 N Sodium hydroxide

1,2-Dioleoyl-sn-Glycer-3

Phosphoethanolamine-N-  
[Methoxy(Polyethylene glycol)-5000]  
sodium salt (PEG-PE)

Dextran 70,000

D-mannitol

Doxorubicin hydrochloride

Loperamide hydrochloride

Milli-Q<sup>®</sup> water

n-Butyl-(2)-cyanoacrylate (Sicomet<sup>®</sup> 6000)

Paclitaxel

Poloxamer 188 (Pluronic<sup>®</sup> F68)

Solvents: dichloromethane, ethanol,  
ethylacetate, isopropanol

Polysorbate 80 (Tween<sup>®</sup> 80)

#### Manufacturer/supplier

Merck, Darmstadt

Merck, Darmstadt

Avanti Polar Lipids, Alabaster

Sigma, Steinheim

Merck, Darmstadt

Sicor, Milan

Sigma, Steinheim

Millipore, Eschborn

Sichel-Werke, Hannover

Yick-Vic Pharm-Chem. LTD, Hong-Kong

Sigma, Steinheim

Sigma, Steinheim

Fluka, Seelze

#### Instruments

Analytical balance Sartorius CP 224S

Eppendorf Centrifuge 5415D

Knick pH-Meter 766

#### Manufacturer/supplier

Sartorius, Göttingen

Eppendorf AG, Hamburg

Knick, Berlin

## Materials and Methods

Lyovac GT 2 Freeze-dryer	Leybold AG, Köln
Magnetic Stirrer RCT basic	IKA Labortechnik, Staufen
Magnetic Variomag <sup>®</sup> Multipoint HP15	Dr.Hoiss & Partner, München
Safety Cabinet Herasafe HS 12	Heraeus, Hanau
Sintered glass filter (G2)	Schott, Mainz
Ultrasonicator Sonorex RK 31	Bandeline, Berlin

### Working parameters

Freeze-drying	24 h at $2 \times 10^{-3}$ mbar
Stirring rate	550 rpm
Temperature	25 °C

### 3.1.1 Doxorubicin-loaded PBCA nanoparticles

Doxorubicin-loaded PBCA nanoparticles (Dox-PBCA-NP) were prepared by anionic polymerisation, as described by Steiniger *et al.* (Steiniger 2004). 1% (w/v) of BCA was added to a 1% (w/v) dextran 70,000 solution in 0.01 N HCl (pH 2) under constant stirring. After 40 minutes, doxorubicin hydrochloride was added into the polymerisation medium to obtain a final doxorubicin concentration of 0.25%. The polymerisation process was carried out for 2.5 h and then was completed by neutralisation with 0.1 N NaOH to pH value of  $6.5 \pm 0.5$ . The nanosuspension was filtered through a sintered glass filter G2 (pore size of 40 - 100  $\mu\text{m}$ ) to remove agglomerates that could occur during particle formation. Then the nanoparticles were freeze-dried in the presence of mannitol (3% w/v) that was used as cryoprotector. The samples were stored in a cool (4 °C) and dry place and protected from light.

After reconstitution with water, the freeze-dried nanoparticles yielded a homogeneous colloidal suspension stable for at least 24 h.

In some cases, for better reconstitution, vortexing (mechanical shaking) or ultrasonication were applied for 1 - 2 min.

Empty PBCA-NPs were prepared as described above in the absence of the drug.

### 3.1.2 Preparation of drug-loaded PBCA nanoparticles in the presence of organic solvents

The drug-loaded PBCA nanoparticles were prepared by anionic polymerisation of n-butyl-2-cyanoacrylate in the presence of a drug. 1% n-butyl-2-cyanoacrylate was added to a solution of dextran 70,000 (1% w/v) and poloxamer 188 (0.2% w/v) in 0.01 N HCl (pH 2.0) under stirring. In the case of paclitaxel, 1% PEG-PE also was used as an alternative stabiliser instead of dextran and poloxamer 188. After 30 minutes, the drug was added as a 1% solution in an organic solvent as follows: loperamide was dissolved in dichloromethane ( $\text{CH}_2\text{Cl}_2$ ), methanol (MeOH) or ethanol (EtOH); paclitaxel was dissolved in dichloromethane, methanol, iso-propanol (i-PrOH), or ethylacetate (EtOAc). The final drug concentration in the reaction media was 0.1% (w/v). The drug-to-polymer ratio was 1:10. The ratio organic phase – aqueous phase was always 1:10 (v/v). After 2.5 h the polymerisation was completed by neutralisation with 0.1 N NaOH. Stirring was continued for another 1.5 h at room temperature to achieve evaporation of the organic solvent; then the suspension was filtered through a G2 sintered glass filter to remove the agglomerates, and the final volume was adjusted to the initial quantity by water. The suspension was freeze-dried after addition of 3% w/v mannitol as a cryoprotector.

Empty PBCA-NPs were prepared, as described above, in the absence of the drug. Organic solvents were added into the polymerisation medium 30, 40, or 60 min after the monomer.

### 3.1.3 Characterisation of nanoparticles

The PBCA nanoparticles were tested *in vitro* for their size, size distribution, morphology, surface charge, drug loading, and drug content. Additionally, the particles prepared in the presence of organic solvents were tested for residual amount of these solvents.

### 3.1.3.1 Determination of the particle size and the zeta potential

<b>Chemicals</b>	<b>Manufacturer/supplier</b>
Milli-Q <sup>®</sup> water	Millipore, Eschborn

<b>Instruments</b>	<b>Manufacturer/supplier</b>
Dipcell	Malvern, Worcestershire
Malvern Zetasizer 3000 HSA	Malvern, Worcestershire
PCS-Cuvets (10 x 10 x 48 mm)	Sarstedt, Nürnberg

#### **Working parameters**

Refractive index	1.333
Scattering angle	90 °C
Temperature	25 °C
Viscosity	0.01 poise

Particle size and polydispersity of the nanoparticles were measured by photon correlation spectroscopy (PCS). The samples were diluted 1:400 with purified water (Milli-Q<sup>®</sup> water). Milli-Q<sup>®</sup> water refers to ultra-pure laboratory grade water that has been filtered and purified by reverse osmosis.

The zeta-potential ( $\xi$ -Potential) of the nanoparticles was measured by microelectrophoresis using the Dip Cell and the same equipment. Since the charge measurement depends on the ionic strength and the pH of the medium, all samples were prepared in purified water.

### 3.1.3.2 Analytical ultracentrifugation (ANUC)

<b>Chemicals</b>	<b>Manufacturer/supplier</b>
Milli-Q <sup>®</sup> water	Millipore, Eschborn
Sodium Chloride	Merck, Darmstadt
<b>Instruments</b>	<b>Manufacturer/supplier</b>
An-50Ti Rotor	Beckman Coulter, Fullerton
Beckman Optima XL-A Ultracentrifuge	Beckman Coulter, Fullerton
<b>Working parameters</b>	
Optical turbidity	Between 0.6 and 0.7 at 420 nm
Optical path length of Cuvette	1 cm
Optical path length of double-sector	12 mm
Rotor speed	3000 or 4000 rpm
Temperature	20 °C

Additionally, the particle size of empty and loperamide-loaded nanoparticles was evaluated by analytical ultracentrifugation on the basis of sedimentation velocity analysis, as described in Vogel *et al.* (Vogel 2002), Langer *et al.* (Langer 2003), and Bootz *et al.* (Bootz 2004). After redispersion the freeze-dried samples in water, they were further diluted 20-fold with a 0.9% NaCl solution in distilled water. Optical turbidity was between 0.6 and 0.7 at 420 nm in a 1 cm cuvette. The sedimentation velocity experiments were carried out using a Beckman Optima XL-A ultracentrifuge with an An-50Ti rotor, and double-sector charcoal-filled Epon centerpieces of 12 mm optical path length. Apparent absorbance (turbidity) versus radius data  $A(r,t)$  were collected at 420 nm, using a radial step size of 0.03 mm. The sedimentation velocity data were modeled as a distribution of non-diffusing particles using the l-s  $g^*(s)$  variant of the Sedfit program. The apparent sedimentation coefficients  $s_{20}$  were transformed to standard conditions and given as  $s_{20,w}$  modeled as l-s  $g^*(s)$  distribution of non-interactive species used in the Sedfit program by Schuck *et al.* (Schuck 2000). For transformation of the  $g^*(s)$  data into diameter distribution  $g^*(d)$  based on a solid sphere model, the partial specific volume of the particles as 0.871 was used (Bootz 2004).

### 3.1.3.3 Scanning Electron Microscopy (SEM)

#### Chemicals

Milli-Q<sup>®</sup> water

Sodium Chloride

#### Manufacturer/supplier

Millipore, Eschborn

Merck, Darmstadt

#### Instruments

Aluminum sample plate

EM Hitachi S-45000

Paint Shop Pro 5

#### Manufacturer/supplier

Work Studio, Frankfurt University

Hitachi, Tokyo

Jasc, Fremont

#### Working parameters

Detector

Upper detector

Duration of gold spraying

40 s

Electron emission

15-25 kv

A freeze-dried nanoparticle sample was redispersed in water to its initial volume and further diluted with water (1:10). The nanoparticles were applied to an aluminum sample plate and dried at room temperature for 2 h. In order to create electrical conductivity, the nanoparticles were placed onto an agar sputter coater and sprayed with gold for 40 s under argon gas. Then the sample was analysed with a field emission electron microscope at 15 - 25 kV with an upper detector. The pictures were taken using a digital system and the Paint Electronic software.

### 3.1.3.4 Atomic Force Microscopy (AFM)

#### Chemicals

Milli-Q<sup>®</sup> water

#### Manufacturer/supplier

Millipore, Eschborn

#### Instruments

Nanoscope IIIa AFM

with commercial Si<sub>3</sub>N<sub>4</sub> tip

Silicon plates

#### Manufacturer/supplier

Veeco, Santa Barbara

VWR, Darmstadt

**Working parameters**

Temperature 25°C

The samples were prepared by simply drying a small amount of the nanoparticle dispersion on the silicon plates. The measurement was done by an atomic force microscope in tapping mode. After the measurement, the images were flattened and no other filtering was done.

**3.1.3.5 Evaluation of the loading capacity of the nanoparticles**

**Chemicals**

Acetonitrile  
Milli-Q® water

**Manufacturer/supplier**

Merck, Darmstadt  
Millipore, Eschborn

**Instruments**

HPLC UV/VIS system  
Interface: D-7000  
Pump: D-7120  
Autosampler: D-7200  
Detector: D-7420, UV/VIS  
Centrifuge filter devices  
(Ultrafree MC, 100,000 NMWL)

**Manufacturer/supplier**

Merck Hitachi, Darmstadt  
Millipore, Eschborn

**Working parameters**

Duration and speed of centrifugation 15 min at 16000 x g

The drug content was measured after dissolution of the freeze-dried formulation in acetonitrile. The insoluble material was separated by centrifugation. The samples were then diluted with acetonitrile, and the drug concentrations were analysed by high performance liquid chromatograph (HPLC), as described below.

The amounts of free drug that are associated with the nanoparticles were calculated after separation by ultrafiltration: 400 µl of the nanoparticle suspension were centrifuged in



centrifuge filter devices. 100 µl of the filtrate were diluted with 900 µl water, and the concentration of the free drug was assessed by HPLC.

The percentage of the nanoparticle-bound drug was calculated by subtracting the free drug in the supernatant from the total amount in the vials.

The loading capacity of the nanoparticles (µg/mg) was calculated as the ratio of the drug content to the polymer amount, as assessed by the determination of the yield of PBCA (section 3.1.3.6).

For poorly water soluble drugs that had a negligible detectable free-drug in supernatant, the term encapsulation efficiency was used. The encapsulation efficiency (%) was calculated as the ratio of the drug content to the initial drug amount added.

### 3.1.3.5.1 Doxorubicin assay

#### Chemicals

Acetonitrile

Milli-Q<sup>®</sup> water

Trifluoroacetic acid (TFA)

#### Manufacturer/supplier

Merck, Darmstadt

Millipore, Eschborn

Fluka, Seelze

#### Instruments

HPLC column:

Lichrospher<sup>®</sup>-100 HPLC RP-18

#### Manufacturer/supplier

Merck, Darmstadt

#### HPLC parameters

Detection wavelength

$\lambda = 250 \text{ nm}$

Flow rate

0.8 ml/min

#### Mobile phase

water:acetonitrile:TFA

70:30:0.1

Volume of injection

20 µl

The assay of doxorubicin was performed by HPLC as described by Ambruosi *et al.* (Ambruosi 2006a). Accurately weighed amounts of doxorubicin were dissolved in 5 ml of

## Materials and Methods

acetonitrile-water. This solution was further diluted to obtain solutions with known concentrations in the range of 25 - 250 µg/ml. The chromatograms of these solutions were registered, and the peak areas were measured. The retention time was about 12 min.

### 3.1.3.5.2 Loperamide assay

#### Chemicals

Acetonitrile

Ethanol

Milli-Q<sup>®</sup> water

Sodium phosphate ( $\text{NaH}_2\text{PO}_4 \times 2 \text{H}_2\text{O}$ )

buffer: (3.12 g/l)

#### Manufacturer/supplier

Merck, Darmstadt

Merck, Darmstadt

Millipore, Eschborn

Merck, Darmstadt

#### Instruments

HPLC column:

Luna<sup>®</sup> 250 × 4.6 mm 5 µm particle C18

#### Manufacturer/supplier

Phenomenex, Torrance

#### HPLC parameters

Detection wavelength

$\lambda = 195\text{nm}$

Flow rate

1 ml/min

#### Mobile phase

Acetonitrile:Sodium phosphate buffer

40:60

Volume of injection

20 µl

The assay of loperamide was carried out as described by Chen *et al.* (Chen 2000). Loperamide stock solution (10 mg/ml) was prepared in 70% ethanol. This solution was further diluted to obtain solutions with known concentrations in the range of 10 - 100 µg/ml. The chromatograms of these solutions were registered and the peak areas were measured. The retention time of loperamide was 22 min.

### 3.1.3.5.3 Paclitaxel assay

#### Chemicals

Acetonitrile  
Milli-Q<sup>®</sup> water

#### Manufacturer/supplier

Merck, Darmstadt  
Millipore, Eschborn

#### Instruments

HPLC column:  
Lichrospher<sup>®</sup>-100 HPLC RP-18

#### Manufacturer/supplier

Merck, Darmstadt

#### HPLC parameters

Detection wavelength  $\lambda = 227\text{nm}$   
Flow rate 1 ml/min

#### Mobile phase

Acetonitrile:Water 6:40  
Volume of injection 20  $\mu\text{l}$

The assay of paclitaxel was performed as described in [\(Krishnadas 2003\)](#). A stock solution of paclitaxel in acetonitrile (1 mg/ml) was prepared. This solution was further diluted to obtain solutions with known concentrations in the range of 10 - 100  $\mu\text{g/ml}$ . The chromatograms of these solutions were registered, and the peak areas were measured. The retention time of paclitaxel was 5 min.

### 3.1.3.6 Determination of polymer yield

#### Chemicals

1 N NaOH  
Dichlormethane  
Milli-Q<sup>®</sup> water  
n-Butanol  
n-Pentanol  
Sodium sulfate, water-free

#### Manufacturer/supplier

Merck, Darmstadt  
Merck, Darmstadt  
Millipore, Eschborn  
Merck, Darmstadt  
Fluka, Seelze  
Merck, Darmstadt

## Materials and Methods

### Instruments

Gas Chromatograph: 5890 Series II  
Integrator: HP3396 A  
Fused Silica Capillary Column:  
(25 m × 0.25 mm ID)

### Manufacturer/supplier

Hewlett-Packard, Bad Homburg  
Macherey-Nagel, Düren

### GC parameters

Injector split / splitless HP 19251 – 60540, 250 °C  
Detector FID, 250 °C  
Oven temperature Gradient: 45 °C (3 min) → 10 °C (1 min)  
→ 130 °C (4 min)

### Stationary phase

Polyethylene glycol-2-nitroterephthalic acid 0.1 µm film thickness  
Gas Auxillary gas Helium, Hydrogen and Air  
Column flow 1.0 ml/min  
Split flow 10.0 ml/min  
Septum flow 1.1 ml/min  
Column + Aux 35 ml/min  
Column + Aux + Air 430 ml/min  
Column + Hydrogen + Aux 65 ml/min  
Column head pressure 94 kPa

The yield of PBCA was evaluated by the amount of butanol formed after hydrolysis of PBCA by sodium hydroxide, as described by Langer *et al.* (Langer 1994).

0.5 ml of the nanoparticle suspension were mixed with 0.5ml of 2 N NaOH and shaken overnight at room temperature to hydrolyze the ester groups of the polymer. 50 µl of this solution were mixed with 50 µl of internal standard (pentanol 0.5% solution) and diluted with 900 µl of water. 500 µl of this dilution were extracted with 1000 µl of dichloromethane, which then was dried with water-free sodium sulfate. 1 µl of the sample was injected into the gas chromatograph (GC) and analysed for the amount of butanol.

### 3.1.3.7 Determination of residual organic solvents

<b>Chemicals</b>	<b>Manufacturer/supplier</b>
Benzene	Sigma, Moscow
Dimethylsulfoxide (DMSO)	Sigma, Moscow
Solvents: ethanol, iso-propanol, dichloromethane, ethylacetate	Sigma, Moscow

<b>Instruments</b>	<b>Manufacturer/supplier</b>
Gas chromatograph: Crystall 2000	Chromatech, San Diego
Quartz capillary column: Zebron ZB-1 (methylpolysiloxane, 30 m × 0.53 mm × 0.3 μm)	Phenomenex, Torrance

#### **GC parameters**

Carrier gas	Nitrogen
Carrier gas velocity	30 cm/s
Column temperature	90 °C
Gas flow regulation	1:7
Injection volume	1 μl
Temperature of detector and injector	200 °C

Empty PBCA nanoparticles prepared in the presence of organic solvents were tested for residual amount of these solvents. The sample of PBCA nanoparticles prepared according to the standard technique in the absence of the organic solvents was used as control. The residual amount of the organic solvents in the nanoparticles was measured by GC. The samples of freeze-dried nanoparticles (0.20 - 0.30 g) were dissolved in 3 ml of DMSO. This solution was mixed with 1 ml of internal standard (0.01% benzene). 1 μl of this mixture was injected into the GC system, and the concentration of the organic solvent was measured. As shown by the background measurements, the detection limits for the solvents were as follows: ≥ 30 ppm for ethanol and dichloromethane, ≥ 20 ppm for iso-propanol, and ≥ 5 - 10 ppm for ethylacetate.

Preparation of the solutions:

*Internal standard:* 0.2 ml of benzene was transferred into a 25 ml vessel and diluted with DMSO to 25ml. 1 ml of this solution was transferred into a 10 ml vessel and diluted with DMSO to 10 ml.

*Standard solution:* 0.10 g of ethanol, iso-propanol, dichloromethane, and ethylacetate were transferred to 25 ml vessels and diluted to 25 ml with DMSO. 1 ml of each solution and 2.5 ml the internal standard solution were transferred to 10 ml vessels and diluted to 10 ml with DMSO.

*Sample solution:* approximately 0.20 - 0.30 g of the sample were transferred in to a vial, 3ml of DMSO and 1 ml of the internal standard solution was added. The clear solution was injected into a chromatograph.

The content of organic solvents was calculated as:

$$X = \frac{S_i^r \times S_{cm}^o \times m_i^o \times 4}{S_{cm}^r \times S_i^o \times m_x \times 25 \times 10} \times 100$$

$$X = \frac{S_i^r \times S_{cm}^o \times m_i^o \times 4}{S_{cm}^r \times S_i^o \times m_x \times 2,5}$$

Where:

$S_i^r$  · and ·  $S_i^o$  - peak area of an i-residual solvent in the chromatogram of the sample and standard solution, respectively.

$S_{cm}^r$  · and ·  $S_{cm}^o$  - peak area of benzene (internal standard) in the chromatogram of the sample and standard solution, respectively.

$m_i^o$  - weight of an i-residual solvent in the chromatogram of the standard solution

$m_x$  - weight of a sample

### 3.1.4 Coating of the nanoparticles with surfactants

The surface-modified nanoparticles were used in the *in vivo* experiments. For the surface modification, the freeze-dried nanoparticles were reconstituted with 1% (w/v) polysorbate 80 or poloxamer 188 (Table 1) and incubated for 30 minutes.

**Table 1.** Characteristics of surfactants used for coating of the nanoparticles.

Surfactant	MW (Da)	CMC, μM	CMC% (w/v)	HLB	Reference
Polysorbate 80	1310	12	0.0016	15	Merck index
Poloxamer 188	8400 – 8800	1140	1	29	Sigma Aldrich

CMC = critical micellar concentration, HLB = hydrophilic lipophilic balance

### 3.1.5 *In vivo* experiments

#### 3.1.5.1 Tail-flick test

##### Animals

Female ICR (CD1) mice 23 - 28 g

##### Supplier

Halan Winkelmann, Borchon

##### Instruments

Tail-Flick Analgesia meter

##### Manufacturer/supplier

Ugo Basile

The analgesic effect of the different nanoparticles preparation was measured using the tail-flick test. The tail-flick test measures the nociceptive threshold of the animals (mice) as they respond to the application of a hot light ray from a quartz projection bulb to a small area of their tails, so that the time for tail withdrawal is recorded. To prevent injuries the test was automatically truncated after 10 s (cut-off time). The response time for each animal was measured before (= pre-drug latency) and 15, 30, 45, 60, 90, 120, and 180 min after dosing (= post-drug latency). The maximal possible effect (MPE%) was calculated using the following equation:

$$\% \text{ MPE} = \frac{\text{Post-drug latency} - \text{pre-drug latency}}{\text{Cut-off time} - \text{pre-drug latency}} \times 100\%$$

The loperamide formulations were administered in the dose of 7 mg/kg into the tail vein.

### ***3.1.5.1.1 Loperamide-loaded PBCA nanoparticles for tail-flick test***

The animals were divided randomly into 3 groups (n = 10) and the following formulations were used:

- Solution of loperamide in 2.6% aqueous ethanol
- Loperamide bound to non-coated PBCA nanoparticles stabilised with dextran (1%) and poloxamer 188 (0.2%)
- Loperamide bound to PBCA nanoparticles stabilised with dextran (1%) and poloxamer 188 (0.2%) coated with PS 80.

The concentration of loperamide in the injection solutions was 0.7 mg/ml.

### **3.1.5.2 Chemotherapy of 101/8 rat glioblastoma using doxorubicin formulations**

The animal experiments were performed in accordance to the German Guidelines for Animal Experiments and authorized by the German Tierschutzgesetz and the Allgemeine Verwaltungsvorschrift zur Durchführung des Tierschutzgesetzes and were authorized by the Regierungspräsident Darmstadt (V54 - 19 c 20/15 - F116/15).

#### ***3.1.5.2.1 Intracranial implantation of rat glioblastoma***

##### **Animals**

Male Wistar rats (200 - 250 g)

##### **Supplier**

Harlan Winkelmann GmbH, Borcheln

##### **Instruments**

Glue (Turbo 2000 Kleber Universal)

Stereotactic device

Tuberculine syringe

##### **Manufacturer/supplier**

Boldt & Co, Wermelskirchen

Leitz, Wetzlar

B. Braun, Melsungen

The rat 101/8 glioblastoma was initially generated by injection of  $\alpha$ -dimethylbenzanthracene into the brain of Wistar rats (Yablonovskaya 1970). The transplantation of 101/8 glioblastoma in the present study was performed using fresh tumour tissue. Tumour tissue



from frozen stocks was transplanted into adult male Wistar rats which were caged in groups of 5 and acclimatized for 1 week and fed *ad libitum* with standard laboratory food and water. For tumour implantation, animals were deeply anesthetized by intraperitoneal injections of ketamin (80 mg/kg). Through a midline sagittal incision, a burr hole of 1.5 mm in diameter was made with a dental drill at a point 2 mm posterior to the right coronal suture and 2 mm lateral to the sagittal midline. Tumour cells were introduced into a tuberculin syringe linked to a 21 gauge needle. The tip was placed 4 mm below the bone surface and the tumour tissue was injected into the bottom of the right lateral ventricle. The scalp incision was closed with surgical glue. On day 14 after transplantation, the animals were sacrificed by carbon dioxide asphyxiation, and then decapitated. The tumour was excised, chopped with a scalpel, and triturated. Fresh tumour tissue ( $\sim 10^6$  tumour cells) was inoculated into the brain of the animals in the experimental groups, as described above.

### ***3.1.5.2.2 Doxorubicin formulations and treatment regimen***

The animals with implanted tumours were randomly divided into 3 groups;

- Untreated animals (control, n = 20)
- Animals treated with doxorubicin in solution (Dox-sol, n = 18)
- Animals treated with doxorubicin bound to PBCA nanoparticles coated with PS 80 (Dox-NP + PS 80, n = 18).

The treatment regimen was  $3 \times 1.5$  mg/kg on days 2, 5, and 8 after tumour implantation. The formulations were injected *i.v.* into the tail vein. The animals were sacrificed by carbon dioxide asphyxiation on days 10, 14, or 18 post-tumour implantation (n = 6/time point). Untreated animals (Control, n = 20) were sacrificed on days 6, 8, 10, 12, or 14 post-tumour implantation (n = 4/time point).

### ***3.1.5.2.3 Histological analysis***

#### **Chemicals**

Zinc formalin solution

#### **Manufacturer/supplier**

Thermo Shandon, Pittsburgh

## Materials and Methods

For histological analysis, brains were removed and fixed in zinc formalin solution at least 48 h and embedded in paraffin followed by routine hematoxylin and eosin (H&E) staining on 5 µm thick sections using routine protocols (Schoch 2006). One slide was prepared and analyzed for each animal.

### 3.1.5.2.4 Immunohistochemical analysis

<b>Chemicals</b>	<b>Manufacturer/supplier</b>
Biotinylated Isolectin B4	B-1205, 1:20, Vector Labs, Burlingame
Bovine serum albumin (BSA)	Sigma-Aldrich, Deisenhofen
Diaminobenzidine (DAB)	Sigma-Aldrich, Deisenhofen
Histofine universal immuno-peroxidase polymer	Nichirei Biosciences Inc., Tokyo
Mouse monoclonal antibody against GFAP	DakoCytomation, Glostrup
Rabbit monoclonal antibody against ki67	Neomarkers, Lab Visions Products, Fremont
Triton X-100	Zytomed, Berlin

Five µm thick deparaffinated sections were used for staining procedures. All slides were counterstained with alum-hematoxylin. Blocking of endogenous peroxidase activity was performed with 0.3% H<sub>2</sub>O<sub>2</sub> for 15 min. For antigen retrieval, the slides were boiled for 1 h in 10 mM citrate buffer (pH 6.0) for staining with antibodies against glial fibrillary acidic protein (GFAP) and Ki67. Then mouse monoclonal antibody against GFAP (M0761, 1:100) or rabbit monoclonal antibody against ki67 (RM-9106-S, 1:50) in blocking buffer (5% goat serum / 45% Tris buffered saline pH 7.6 (TBS) / 0.1% Triton X-100 in antibody diluent solution were applied over night. Histofine universal immuno-peroxidase polymer or anti-mouse or anti-rabbit were applied after washing with TBS. For staining with Isolectin B4, the slides were treated in a microwave oven (640 W) for 20 min in 1 mM EDTA (pH 8.0). Then, biotinylated Isolectin B4 (B-1205, 1:20) was applied for 30 min at room temperature in 100 µg/ml bovine serum albumin (BSA) in blocking buffer without goat serum. StreptABComplex HRP duet solution (K0492, DakoCytomation) was applied after washing

with PBS. The peroxidase reaction was detected using diaminobenzidine (DAB) as chromogen. As negative control, alternating sections were incubated without primary antibody or Isolectin B4.

### ***3.1.5.2.5 Measurement of tumour size***

<b>Instruments</b>	<b>Manufacturer/supplier</b>
Axioskop microscope	CarlZeiss Microimaging, Göttingen
NeuroLucida software-controlled computer system	MicroBrightField Europe, Magdeburg

An Axioskop microscope and a NeuroLucida software-controlled computer system were used for quantitative analysis of the area occupied by the tumour on H&E stained tissue sections to determine tumour size in each animal.

### ***3.1.5.2.6 Analysis of proliferation***

To analyse proliferation, immunohistochemical staining with antibodies against Ki67 were performed on tissue sections in each animal. The percentage of positively stained nuclei of all counterstained nuclei was determined in three visual fields (total area examined was 0.36 mm<sup>2</sup>).

### ***3.1.5.2.7 Analysis of vessel density***

<b>Instruments</b>	<b>Manufacturer/supplier</b>
Axioskop microscope	CarlZeiss Microimaging, Göttingen
Axiovision software	MicroBrightField Europe, Magdeburg

To analyse vessel density, tissue sections were stained with Isolectin B4 and analysed with Axiovision software. The software quantified the percentage of the area occupied by Isolectin B4<sup>+</sup> vessels in visual fields with a size of 0.412 mm<sup>2</sup>.

#### ***3.1.5.2.8 Analysis of necrosis***

For the analysis of necrosis, the following scoring system was applied to hematoxylin and eosin stained sections (only the tumour was assessed): 0 – no necrosis, 1 – solitary necroses, 2 – less than 50% of tumour area occupied by necroses, 3 – more than 50% of the tumour area occupied by necroses.

#### ***3.1.5.2.9 Analysis of GFAP expression of glioma cells***

For the analysis of GFAP expression, a score was assigned to tissue sections immunohistochemically stained with an antibody against GFAP only considering the area occupied by the tumour: 0 – no positive cells, 1 – less than 10% positive cells, 2 – more than 10% positive cells but less than 50% of cells, 3 – more than 50% of tumour cells positive for GFAP.

#### ***3.1.5.2.10 Analysis of microvascular proliferation***

For the analysis of microvascular proliferation, the following scoring system was applied to hematoxylin and eosin stained sections (only the tumour was assessed): 0 – no microvascular proliferation, 1 – solitary nodules of microvascular proliferation, 2 – more than five nodules of microvascular proliferation.

#### ***3.1.5.2.11 Analysis of VEGF expression of glioma cells***

For the analysis of VEGF expression, the following score was assigned to tissue sections immunohistochemically stained with an antibody against VEGF only considering the area occupied by the tumour: 0 – no positive cells, 1 – weak staining intensity, 2 – moderate staining intensity, 3 – strong staining intensity.

#### ***3.1.5.2.12 Statistical analysis***

All experiments were performed in a blinded manner. In case of comparison of two independent groups at a certain time point, the pairwise Student's t-test was used for the

statistical evaluation. In case of simultaneous comparison of all three groups at a certain time point, non-parametric, Kruskal-Wallis with post-hoc tests were used.

### 3.1.5.3 Chemotherapy of 101/8 rat glioblastoma using paclitaxel formulations

#### Animals

Male Wistar rats (200 - 250 g)

#### Supplier

Harlan Winkelmann GmbH, Borchon

Paclitaxel formulations were used for chemotherapy of 101/8 glioblastoma in rats. Paclitaxel formulations were injected *i.v.* into the tail caudal vein with the rate of 1 ml/min. The animals were implanted intracranially with the orthotopic tumour model 101/8 glioblastoma (sections 3.1.5.2.1 - 3).

The treatment regimen was  $3 \times 1.5$  mg/kg as drug (total dose 4.5 mg/kg) on days 2, 5, and 8 post-tumour implantation.

The animals were divided randomly into 4 groups ( $n = 10$ ) and the following formulations were used:

- Paclitaxel-loaded PBCA nanoparticles (PXL-NP)
- Paclitaxel-loaded PBCA nanoparticles + polysorbate 80 (PXL-NP + PS 80)
- Paclitaxel-loaded PBCA nanoparticles + poloxamer 188 (PXL-NP + F68 )
- Paclitaxel in organic solution (PXL)

The organic solvent contained 51% chremophor and 49% ethanol. 1 mg paclitaxel was dissolved in this solvent which prior to the administration was diluted with 5% glucose solution to obtained the desired dosage. The untreated animals were used as control.

The antitumour efficacy of these formulations was estimated by Kaplan-Meier plots which estimate the survival function from life-time data. The results also are presented as numeric values in the form of median and mean survival times. Median survival times are defined as the time from treatment at which half of the populations with tumour were found to be still alive. The mean survival time is estimated as the area under the survival curve, which it is the average time that animals remained alive.

### 3.2 Human serum albumin nanoparticles

<b>Chemicals</b>	<b>Manufacturer/supplier</b>
2, 4, 6-trinitrobenzenesulfonic acid (TNBS)	Sigma, Steinheim
2-iminothiolane-HCl (Traut's reagent)	Sigma, Steinheim
Apolipoprotein A-I (Apo A-I)	Calbiochem, Darmstadt
Apolipoprotein B-100	Calbiochem, Darmstadt
Ethanol	Merck, Darmstadt
Glutaraldehyde 25%	Sigma, Steinheim
Human serum albumin (Fraction V) (purity 96 - 99%), 65,000 Da	Sigma, Steinheim
Milli-Q <sup>®</sup> water	Millipore, Eschborn
NHS-PEG-Mal 3400	Nektar, Huntsville
<b>Instruments</b>	<b>Manufacturer/supplier</b>
Aluminum boats	Lüdi, Flawil
Centrifuge filter devices (Ultrafree MC 30,000 NMWL)	Millipore, Eschborn
D-Salt <sup>™</sup> Dextran desalting columns	Pierce, Rockford
Eppendorf Centrifuge 5417	Eppendorf AG, Engelsdorf
Eppendorf thermomixer 5436	Eppendorf AG, Engelsdorf
Filtration unit	Schleicher und Schüll, Dassel
Magnetic Variomag <sup>®</sup> Multipoint HP15	Dr. Hoiss & Partner, München
Micro BCA protein assay kit	Pierce, Rockford
Peristaltic pump	Ismatec IPN, Glattbrugg
Spectrophotometer Hitachi U3000	Berkshire, UK
Supermicro Balance	Sartorius, Goettingen
<b>Working parameters</b>	
Duration and speed of centrifugation	8 min at 16000 x g
Rate of pumping	1 ml/min

Rate of stirring	500 rpm
Temperature	25 °C

### 3.2.1 Nanoparticle preparation

Empty HSA nanoparticles were prepared by an established desolvation technique (Weber 2000a, Langer 2003). Briefly, 200 mg of HSA were dissolved in 2.0 ml of a 10 mM NaCl solution. The solution of HSA was filtered through 0.22 µm pore size Teflon syringe filters to remove dimmers and trimers. After the adjustment of the pH to 8.5, the desolvation of the HSA was performed by drop-wise addition of 8.0 ml ethanol under constant stirring. 100% cross-linked nanoparticles were obtained by adding 0.588 µl of 8% glutaraldehyde per mg of HSA. After 24 h of constant stirring, the resulting nanoparticles were purified by 3 cycles of centrifugation. After yield determination (section 3.2.1.1) of the nanoparticles, the samples were redispersed to the desired concentration (10 mg/ml) in water. Each redispersion step was performed in an ultrasonic bath.

#### 3.2.1.1 Yield determination of the HSA nanoparticles

In order to adjust the concentration of the nanoparticle, the content was determined by gravimetry (Dreis 2007). A 50.0 µl aliquot of the nanoparticle suspension was transferred to aluminum boats and dried for 2 h at 80 °C; the mass of the particle residue was determined using a Supermicro Balance.

#### 3.2.1.2 Preparation of sulfhydryl-reactive HSA nanoparticles

The nanoparticles were centrifuged and redispersed in phosphate buffered saline (PBS), pH of 8.0. A 10-fold molar excess of the NHS-PEG-Mal 3400 linker was added to the medium and for enhancing the reaction, the suspension was shaken for 1 h at room temperature. Afterward, the activated nanoparticles were purified by centrifugation and redispersion as described in section 3.2.1.

### **3.2.1.3 Purification of apolipoproteins A-I and B-100**

The purification of the apolipoproteins was performed as described by Michaelis *et al.* (Michaelis 2006). A D-salt™ Dextran Desalting column, equilibrated with PBS and saturated with a 1% albumin solution, was used according to the instruction sheet. The apolipoprotein solutions were added to the column, and fractions were collected stepwise by photometrical detection of the proteins at 280 nm in order to separate the apolipoproteins from disturbing salts.

### **3.2.1.4 Thiolation of apolipoproteins**

In order to attach the apolipoproteins to the activated HSA nanoparticles, sulfhydryl groups had to be introduced into the apolipoproteins. The apolipoproteins were dissolved in a PBS solution, pH 8.0, and a 50-fold molar excess of 2-iminothiolane (Traut's reagent) was added. The mixture was incubated for 12 h at 22 °C. The purification of the proteins was performed by size exclusion chromatography as described above (section 3.2.1.3).

### **3.2.1.5 Modification of the nanoparticles by thiolated apolipoproteins**

For the conjugation, 2 ml of thiolated lipoprotein solutions were added to 2 ml of activated nanoparticles and the mixture was stirred for 12 h at room temperature. The apolipoprotein-conjugated nanoparticles were purified by three steps of centrifugation and redispersed in water. Supernatants were collected to determine the amount of unbound apolipoproteins by standard micro BCA protein assay.

#### ***3.2.1.5.1 Micro BCA protein assay***

500 µl of micro BCA working reagent was added to 500 µl of the supernatant; then the mixture was incubated for 1h at 37 °C. The samples were analysed spectrophotometrically at 562 nm. The protein content of the samples was calculated relative to reference samples, which contained different concentrations of protein (HSA standards).



### 3.2.1.6 Loperamide loading in the apolipoprotein-modified nanoparticles

10 mg of the apolipoprotein-modified nanoparticles were incubated with 400 µl of loperamide solution (10 mg/ml in 42% (v/v) aqueous ethanol) under shaking for 2 h at room temperature. Then the mixture was centrifuged, and the concentration of unbound loperamide was determined in supernatant by HPLC. The nanoparticles were washed with water by centrifugation (16000 g, 8 min) and then redispersed in water for injection. The final concentration of the nanoparticles in the resulting suspension was 10 mg/ml.

Unbound loperamide in the supernatant was detected by HPLC according see section 3.1.3.5.2.

The size, polydispersity and the surface charge of the nanoparticles were measured as described in section 3.1.3.1.

### 3.2.2 Apolipoprotein-modified HSA nanoparticles for tail-flick test

#### Animals

#### Supplier

Female ICR (CD1) mice 23 - 28 g

Halan Winkelmann, Borcheln

The tail-flick test was performed as described above (see 3.1.5.1).

The animals were divided randomly into 4 groups (n = 10) and the following loperamide formulations were used.

- Loperamide-loaded in HSA nanoparticles with covalently attached apolipoprotein A-I
- Loperamide-loaded in HSA nanoparticles with covalently attached apolipoprotein B-100
- Loperamide-loaded in unmodified HSA nanoparticles
- Loperamide in solution

The dose of loperamide was 7.0 mg/kg. To prevent any injuries, the test was automatically aborted after 10 seconds. The response time for each animal was tested before and 15, 30, 45, 60, 90, 120, and 180 minutes after dosing.

### 3.2.3 Loading of thalidomide in HSA nanoparticles

<b>Chemicals</b>	<b>Manufacturer/supplier</b>
Dimethylsulfoxide (DMSO)	Sigma, Steinheim
Ethanol	Merck, Darmstadt
Thalidomide	Gruenthal, Stolberg
Triethylamine	Sigma, Steinheim

<b>Instruments</b>	<b>Manufacturer/supplier</b>
Eppendorf Centrifuge 5417	Eppendorf AG, Engelsdorf
Eppendorf thermomixer 5436	Eppendorf AG, Engelsdorf
Magnetic Variomag <sup>®</sup> Multipoint HP15	Dr. Hoiss & Partner, München

<b>Working parameters</b>	
Duration and speed of centrifugation	8 min at 20000 x g
Rate of stirring	500 rpm
Solvent: ethanol-DMSO	8:2
Temperature	25 °C

The HSA nanoparticles were prepared by the earlier established desolvation technique as described in section 3.2.1.

The preparation of thalidomide-loaded HSA nanoparticles (Thal-HSA-NP) was performed by adding 0.1% triethylamine after redispersing of 10 mg HSA nanoparticles in 1 ml of thalidomide solution in a mixture ethanol-DMSO (8:2). The final concentration of thalidomide in the solvent was one mg/ml. The samples were shaken with thermomixer for 24 h. The residues of organic solvents were removed after being washed three times with purified water. Then nanoparticles were characterised for their size, polydispersity, and surface charge as described in section 3.1.3.1.

For the estimation of drug loading the supernatants were collected after each cycle of washing and analysed by UV/VIS HPLC as described below (section 3.2.3.1).

### 3.2.3.1 Determination of thalidomide loading

After each nanoparticle centrifugation, 100  $\mu\text{l}$  of the supernatant were diluted with 900  $\mu\text{l}$  of a mixture ethanol-DMSO (8:2). For preparing standard dilutions, thalidomide was dissolved in the same solvent. These standard dilutions were in 80 - 120% range of the theoretical thalidomide concentration in the nanoparticle formulations. This solution was further diluted to obtain solutions with known concentrations in the range of 10 - 250  $\mu\text{g/ml}$ . The spectra of the samples were recorded and calculated with values from standard solutions.

The drug loading (% of total amount) was calculated by subtracting the free drug amount in the supernatant from the total amount in the vials. The drug concentration was determined with HPLC as described on section 3.2.3.1.1.

The size, polydispersity and the surface charge of the nanoparticles were measured as described in section 3.1.3.1.

#### 3.2.3.1.1 Thalidomide assay by HPLC

##### Chemicals

Milli-Q<sup>®</sup> water  
Acetonitrile

##### Manufacturer/supplier

Millipore, Eschborn  
Merck, Darmstadt

##### Instruments

HPLC column:  
Lichrospher<sup>®</sup>-100 HPLC RP-18

##### Manufacturer/supplier

Merck, Darmstadt

##### HPLC parameters

Detection wavelength  $\lambda = 220 \text{ nm}$   
Flow rate 1.2 ml/min

##### Mobile phase

Water:Acetonitrile 75:25  
Volume of injection 20  $\mu\text{l}$

The assay was performed as described by Gossen *et al.* (Goosen 2002) and using the Hitachi D7000 HPLC system (section 3.1.3.5.1). Under these conditions, the retention time for thalidomide was about 8 min.

### 3.2.3.2 Thalidomide solubility in different solvents and surfactants

#### Chemicals

Glucose

Milli-Q<sup>®</sup> water

poloxamer 188 (Pluronic<sup>®</sup> F68)

Solvents: dimethylsulfoxide, ethanol

Thalidomide

Polysorbate 80

#### Manufacturer/supplier

Sigman, Steinheim

Millipore, Eschborn

Sigma, Steinheim

Sigma, Steinheim

Gruenthal, Stolberg

Fluka, Seelze

#### Instruments

Filtration unit

#### Manufacturer/supplier

Schleicher und Schüll, Dassel

#### Working parameters

Duration of storage

24 h

Rate of stirring

500 rpm

Solvent: ethanol-DMSO

8:2

Temperature

25 °C

The solubility of thalidomide was tested in the mixture of the water-miscible organic solvent (ethanol-Cremophor<sup>®</sup> EL, 49:51). The solubility was also tested in water, 5% glucose as well as 10% aqueous solutions of surfactants, such as poloxamer 188 and PS 80. A known amount of drug (1000 µg/ml) was weighed, dissolved in the above solvents, and stored for 24 h at room temperature. Then these suspensions were filtered through Teflon syringe filters (pore size 0.22 µm) to remove crystals. 100 µl of each suspension was diluted with 900 µl of ethanol-DMSO (8:2), and the concentration of thalidomide was measured by

HPLC. The concentrations of thalidomide in these media were compared with those of thalidomide-loaded HSA nanoparticles.

### **3.2.3.3 Chemotherapy of 101/8 rat glioblastoma using thalidomide formulations**

#### **Animals**

Male Wistar rats (200 - 250 g)

#### **Supplier**

Harlan Winkelmann GmbH, Borcheln

Thalidomide formulations were used for chemotherapy of 101/8 glioblastoma in rats. Thalidomide formulations were injected *i.v.* into the tail caudal vein with the rate of 1 ml/min. The animals were implanted intracranially with the orthotopic model tumour glioblastoma 101/8 (sections 3.1.5.2.1-3). The treatment regimen was  $3 \times 1$  mg/kg as drug (total dose 3 mg/kg) on days 2, 5, and 8 post-tumour implantation.

The animals were divided randomly into 4 groups (n = 10) and the following formulations were used:

- Thalidomide-loaded to HSA nanoparticles (Thal-HSA-NP)
- Thalidomide-loaded to HSA nanoparticles coated with 1% polysorbate 80 (Thal-HSA-NP + PS 80)
- Thalidomide dissolved in corn oil and applied orally with gavage (Thal)
- Untreated animals (control)

### 3.3 Diindolymethane-loaded poly(lactide-co-glycolide) nanoparticles

#### Chemicals

3,3'-Diindolymethane (DIM)  
 Human serum albumin (HSA)  
 Mannitol  
 Milli-Q<sup>®</sup> water (purified water)  
 Poloxamer 188 (Pluronic<sup>®</sup> F68)  
 Polyvinylalcohol (PVA)  
 Resomer<sup>®</sup> RG 502 H  
 (50 lactide:50 glycolide), *i.v.* 0.2 dL/g  
 Solvents: acetonitrile, acetone

#### Manufacturer/supplier

Bioresponse LLC, Boulder  
 Sigma, Steinheim  
 Sigma, Steinheim  
 Millipore, Eschborn  
 Sigma, Steinheim  
 Sigma, Steinheim  
 Boeringher Ingelheim, Germany  
 Merck, Darmstadt

#### Instruments

Lyovac GT 2 Freeze-dryer  
 Magnetic Variomag<sup>®</sup> Multipoint HP15  
 Peristaltic pump  
 Sintered glass filter (G2)

#### Manufacturer/supplier

Leybold AG, Köln  
 Dr. Hoiss & Partner, München  
 Ismatec IPN, Glattbrugg  
 Schott, Mainz

#### Working parameters

Duration of evaporation procedure	4 h
Freeze-drying	24 h at $2 \times 10^{-3}$ mbar
Rate of pumping	1 ml/min
Rate of stirring	600 rpm
Temperature	25 °C

#### 3.3.1 Preparation of DIM-loaded PLGA nanoparticles by nanoprecipitation

The poly(lactide-co-glycolide) nanoparticles (PLGA-NP) were prepared by nanoprecipitation (Bozikir 2005). Polyvinylalcohol (PVA), HSA or poloxamer 188 (Pluronic<sup>®</sup> F68; F68) were used as stabilisers. Briefly, 100 mg of the polymer (Resomer<sup>®</sup>

RG 502, *i.v.* 0.2 dL/g) and 10 mg of 3,3'-diindolylmethane (DIM) were dissolved in 3 ml of acetone. This solution was added under magnetic stirring into a 1% solution of either stabiliser (10 ml) at a rate of 1.0 ml/min using a tubing pump. Stirring was continued in open vials for 4 h to achieve evaporation of the organic solvent and formation of the nanoparticles; then the suspension was filtered through a G2 glass filter to remove the agglomerates, and the final volume was adjusted to the initial quantity by water. The suspension was freeze-dried after the addition of 3% w/v mannitol used as a cryoprotector. Empty PLGA nanoparticles were prepared, as described above, in the absence of the drug.

### 3.3.1.1 Characterisation of the DIM-loaded PLGA nanoparticles

The size, polydispersity and the surface charge of the nanoparticles were measured as described in section 3.1.3.1. The drug content was measured after dissolution of the freeze-dried formulation in acetonitrile. The insoluble material was separated by centrifugation. The samples were then diluted with acetonitrile, and the drug concentrations were analysed by HPLC, as described in the section 3.3.3.1. All of the experiments were performed in triplicate and the result given as the average with standard deviation (mean  $\pm$  SD).

### 3.3.2 Determination of DIM maximum solubility in aqueous media

#### Chemicals

0.01 N Hydrochloric acid

Milli-Q<sup>®</sup> water

Potassium dihydrogen phosphate (KH<sub>2</sub>PO<sub>4</sub>)

#### Manufacturer/supplier

Merck, Darmstadt

Millipore, Eschborn

Sigma, Steinheim

#### Instruments

Polymax 1040 orbital shaker

Syringeless filters; Uniprep<sup>®</sup>

#### Manufacturer/supplier

Heidolph, Schwalbach

Whatman Int. Ltd., Springfield Mill

Determination of maximum solubility of DIM in aqueous media was performed by shake-flask method as described by Lindenberg *et al.* (Lindenberg 2004). The drug was weighed in

## Materials and Methods

excess of its expected solubility in Uniprep<sup>®</sup> vials equipped with a 0.45- $\mu$ m membrane filter. Then 2 ml of either Milli-Q<sup>®</sup> water, 0.01 N HCL (pH 2.0), or phosphate buffer (pH 7.4) (USP) were added into the vial. The vials were incubated at  $37 \pm 0.5$  °C while shaking on a “Polymax 1040” orbital shaker. The samples of the solutions were taken after 4 or 24 h by pressing the Uniprep<sup>®</sup> plunger down, diluted as appropriate, and the concentration of DIM was analysed by HPLC, as described below (section 3.3.3.1). The measurements were done in triplicate (mean  $\pm$  SD).

### 3.3.3 Determination of DIM stability in organic media

Solutions of DIM in acetone and acetonitrile were prepared to test DIM stability in organic media which were used for the preparation of the nanoparticle formulations; the concentration was either 15  $\mu$ g/ml or 25 mg/ml. The samples were stored in clear and brown flasks at room temperature and analysed by HPLC for degradation products. The assay was performed after 4 and 24 h and then after one week.

#### 3.3.3.1 DIM assay by HPLC

##### Chemicals

Acetonitrile

Milli-Q<sup>®</sup> water

Trifluoroacetic acid (TFA)

##### Manufacturer/supplier

Merck, Darmstadt

Millipore, Eschborn

Sigma, Steinheim

##### Instruments

HPLC column:

Lichrospher<sup>®</sup>-100 HPLC RP-18

##### Manufacturer/supplier

Merck, Darmstadt

##### HPLC parameters

Detection wavelength

$\lambda = 280$  nm

Flow rate

1.0 ml/min



## Materials and Methods

### Mobile phases

A (30%) 7 min → B (30%) 13 min

A: 0.2% TFA water

B: 0.2% TFA in acetonitrile

Volume of injection

20  $\mu$ l

Accurately weighed amounts of DIM were dissolved in 5 ml of the acetonitrile and further diluted with the same solvent to obtain solutions with known concentrations in the range of 10 - 250  $\mu$ g/ml. The chromatograms of these solutions and the peak areas were registered. The retention time was about 7 minutes.

## 4 Results

### 4.1 Poly(*butyl cyanoacrylate*) nanoparticles

Doxorubicin-loaded poly(*butyl cyanoacrylate*) nanoparticles coated with polysorbate 80 (Dox-NP + PS 80) have previously exhibited a high antitumour effect against the rat glioblastoma 101/8 (Steiniger 2004). The objective of the present study was to substantiate these findings by extensive histological investigation.

Similarly to the previous protocols used by Steiniger *et al.* (Steiniger 2004) or Petri *et al.* (Petri 2007), the PBCA nanoparticles were prepared by anionic polymerisation carried out by the addition of the monomer (*n*-butyl-2-cyanoacrylate; *n*-BCA) into the polymerisation medium, which consisted of an aqueous acidic solution of 0.01 N HCl and dextran 70,000 used as a stabiliser. The polymerisation was initiated by the OH<sup>-</sup> ions resulting from the dissociation of water (Figure 10). The polymerisation was completed after 2.5 h (Bootz 2004) and the medium was neutralised with 0.01 N sodium hydroxide.

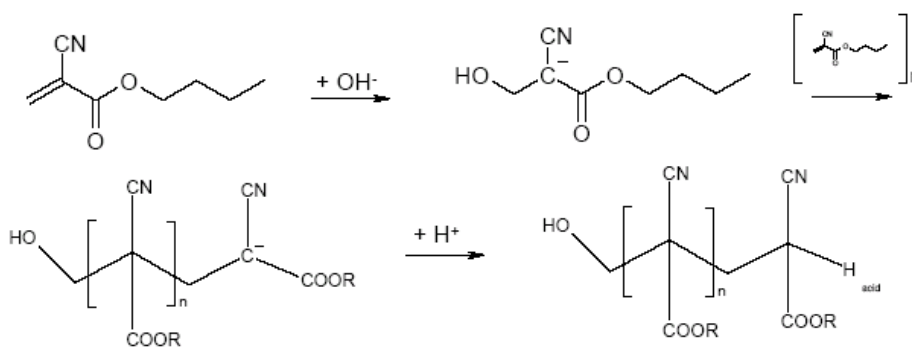


**Figure 10.** Polymerisation mechanism of poly(alkyl cyanoacrylate) (R = alkyl function). Taken from Bootz *et al.* (Bootz 2005).

The doxorubicin (Dox) solution was added into the polymerisation medium 40 minutes after the monomer to prevent the drug interference in the polymerization. The final drug concentration was 0.25%.

#### **4.1.1 Characterisation of doxorubicin poly(butyl cyanoacrylate) nanoparticles**

The physicochemical characterization of the nanoparticles included measurement of the size and polydispersity, surface charge, investigation of the particle morphology by SEM, and evaluation of the drug loading and drug content.

##### **4.1.1.1 Size, polydispersity, and surface charge of the nanoparticles**

The size of the nanoparticles was determined by photon-correlation spectroscopy (PCS). The result showed that the doxorubicin-loaded polysorbate 80-coated nanoparticles had an average diameter of  $260 \pm 5$  nm. The empty nanoparticles prepared in the absence of drug had a slightly smaller size of  $230 \pm 5$  nm. For both empty and drug-loaded nanoparticles, the polydispersity index was 0.02. Coating with surfactant had no influence on the size distribution.

The empty and drug-loaded nanoparticles showed negative zeta potentials in distilled water. The empty nanoparticles had an average surface charge of  $-12 \pm 5$  mV. Coating of dextran-stabilised nanoparticles with polysorbate 80 (PS 80) had slightly reduced the surface charge values. The average surface charge of the Dox-NP + PS 80 was  $-19 \pm 2$  mV.

##### **4.1.1.2 Morphology of the nanoparticles**

The morphology of the nanoparticles was investigated by scanning electron microscopy (SEM) without further purification. Typical micrographs of the empty and drug-loaded nanoparticles are shown in Figure 11. The most prominent property of the particles was their almost perfect spherical shape. The bi-modal size distribution, which is characteristic for dextran stabilised PBCA-NP, were also observable in these figures. The result of SEM measurements was in accordance with the PCS results: it showed a mean average size for empty nanoparticles of about 200 - 230 nm. The loaded nanoparticles had an average size of about 250 - 260 nm.

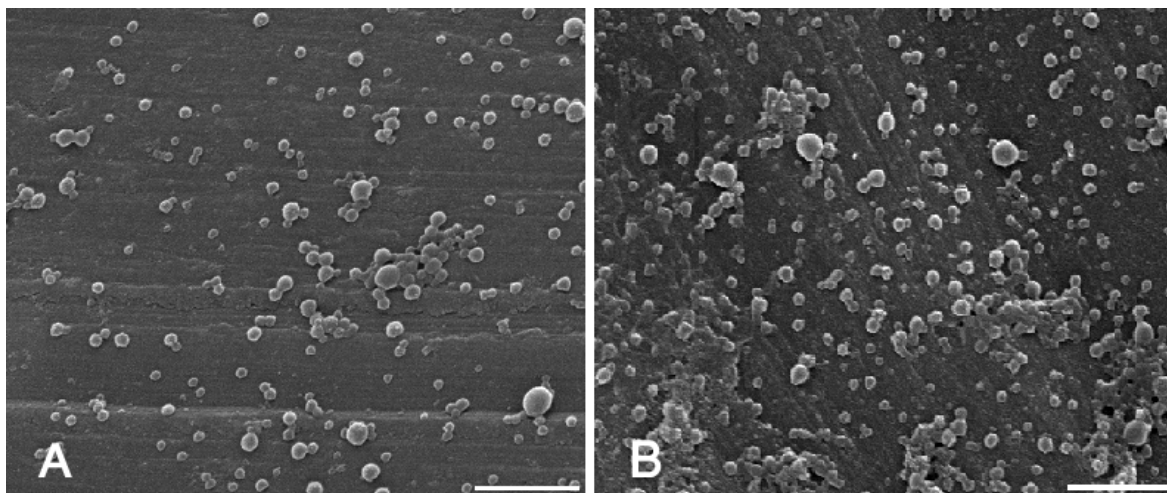


**Figure 11.** Morphology of the PBCA nanoparticles determined by SEM. (A) empty (B) doxorubicin-loaded poly(butylcyanoacrylate) nanoparticles, after freeze-drying. Bimodal distribution is visible in both samples, Bar: 1µm.

#### 4.1.1.3 Drug loading

The percentage of doxorubicin bound to poly(butyl cyanoacrylate) nanoparticles was assessed in the supernatant of the nanoparticles suspension after centrifugation and calculated by subtracting the free drug from the total amount in the vials. It was shown that 70% of the drug in the nanoparticle suspension was associated with the nanoparticles. This result was reported in the previous studies (Steiniger 2004, Petri 2007).

The loading capacity of the nanoparticles calculation (mg DOX/mg PBCA) was possible after assessment of the polymerisation yield and the solubilisation of the nanoparticles in acetonitrile. The polymerisation yield for Dox-NP + PS 80 was  $70 \pm 10\%$  which was higher, as compared to empty nanoparticles ( $65 \pm 1.5\%$ ). The loading capacity of the nanoparticles was 0.154 mg doxorubicin per 1 mg polymer.

#### 4.1.2 Histopathologic and immunocytochemical evaluation of the treatment with different formulations of doxorubicin

The 101/8 glioblastoma is an orthotopic rat model of glioblastoma showing a high cellularity with brisk mitotic activity, necroses, focal microvascular proliferation, and an invasive growth pattern with destruction of parenchymal structures in the host brain satisfying the criteria for the diagnosis of glioblastoma multiforme (Figures 12 and 13).

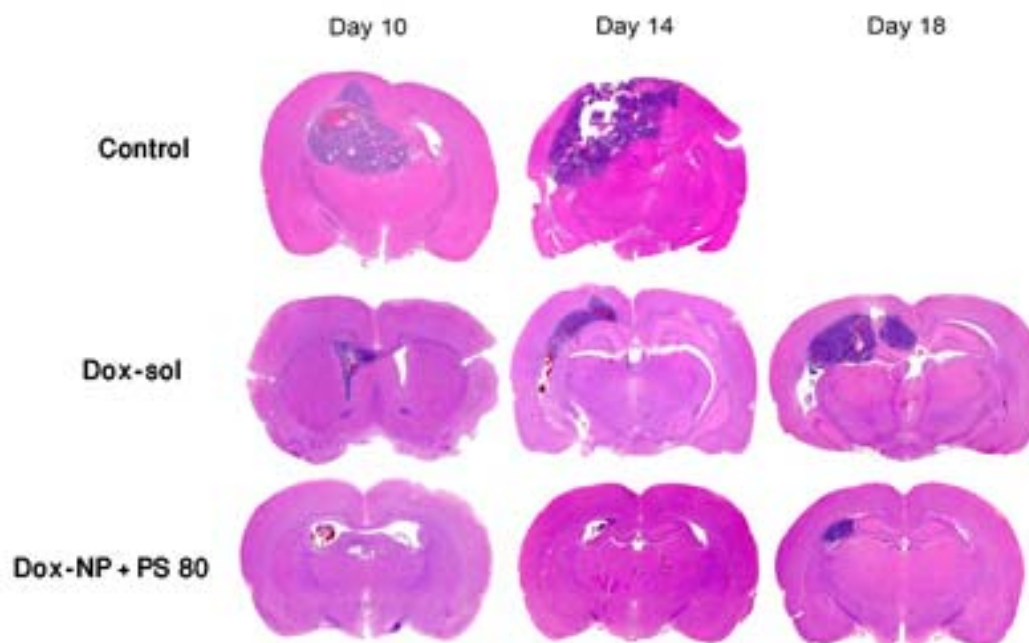


**Figure 12.** Decreased tumour size following treatment with doxorubicin. Rat 101/8 glioblastoma was implanted into the hemisphere of Wistar rats. Untreated animals (Control), animals treated by intravenous injections of doxorubicin in solution (Dox-sol), or doxorubicin bound to polysorbate 80-coated PBCA nanoparticles (Dox-NP + Ps 80), both  $3 \times 1.5$  mg/kg on days 2, 5, and 8 were sacrificed at indicated time points. Hematoxylin-eosin staining of representative brains on day 10, 14, and 18 after tumour implantation is displayed. Note the decreased tumour size in the Dox-sol and especially the Dox-NP + PS 80 group.

The tumour shows generally a reproducible growth pattern leading to death of untreated animals 15 to 17 days after intracerebral implantation. The untreated control animals were sacrificed on days 6, 8, 10, 12, and 14 after implantation (Table 2). The brains were analysed histologically to determine the tumour size, proliferation of the tumour cells, vessel density, and area of necrosis.

**Table 2.** Incidence of 101/8 glioblastoma formation in control animals and animals treated with doxorubicin formulations.

Group	Doxorubicin dose (mg/kg)	Number of rats with tumours / total number of rats					
		Day 6	Day 8	Day 10	Day 12	Day 14	Day 18
Control	-	3/4	4/4	4/4	4/4	4/4	-
Dox-sol	3 x 1.5	-	-	5/6	-	5/6	6/6
Dox-NP + PS 80	3 x 1.5	-	-	4/6	-	3/6	4/6

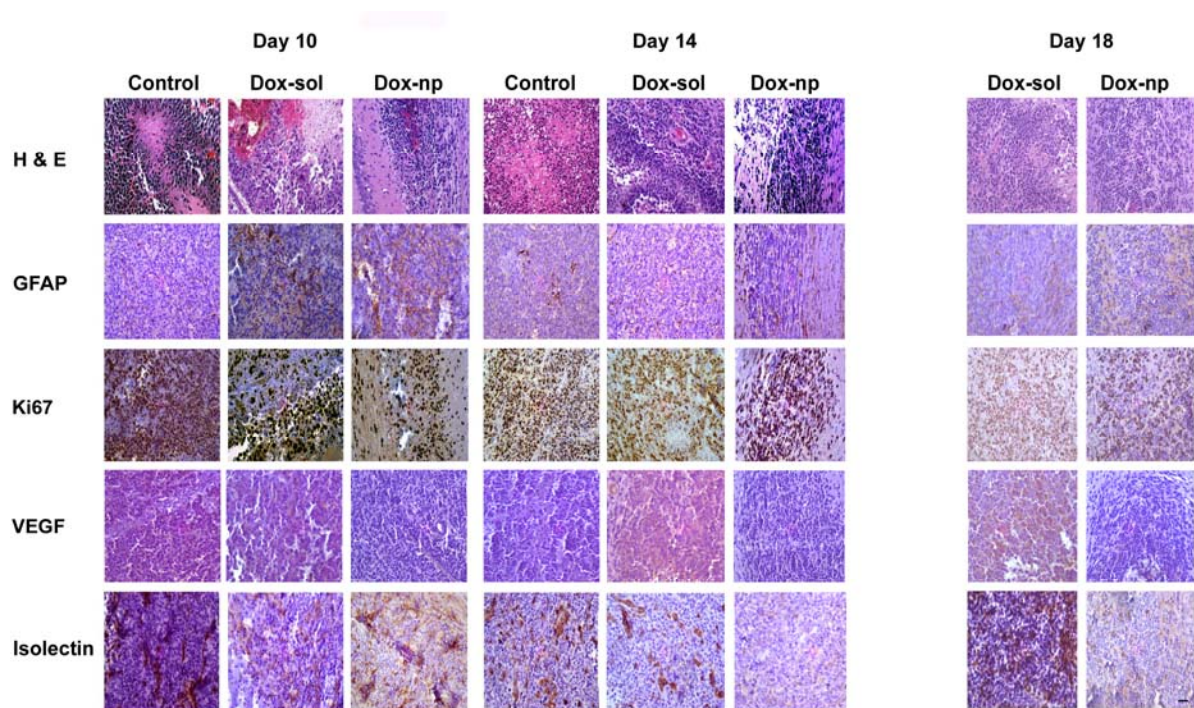


**Figure 13.** Morphological alterations in following treatment with doxorubicin. Hematoxylin-eosin staining and immunohistochemical staining with antibodies against the glial fibrillary acidic protein (GFAP), Ki67, and with Isolectin B4 (Isolectin) in brain sections of untreated control animals (Control), animals treated with intravenous injections of doxorubicin in solution (Dox-sol), or with doxorubicin bound to polysorbate 80-coated PBCA nanoparticles (Dox-NP + PS 80) is displayed. Scale bar = 50  $\mu$ m.

Six days after intracerebral implantation, 3 out of 4 of these animals developed a tumour. After 8, 10, 12, and 14 days all of the controls animals had tumours. The 101/8 glioblastoma showed an increase in size from  $2 \pm 2 \text{ mm}^2$  (maximal cross-sectional area) 6 days after the implantation to  $25 \pm 8 \text{ mm}^2$  14 days after the implantation (Figures 12 - 14a).

The proliferation of tumour cells remained high at all time points ranging from  $78 \pm 7\%$  to  $86 \pm 7\%$  Ki67<sup>+</sup> cells (Figure 14b). The vessel density was negligible 6 days after the implantation but increased significantly reaching a peak of  $11 \pm 2\%$  of the total cross-sectional tumour area 10 days after the implantation (Figure 14c). Furthermore, necroses were absent in the tumours in control animals 6 and 8 days after the implantation while a high degree of necrosis was observed 10, 12, and 14 days after the implantation (Table 3).

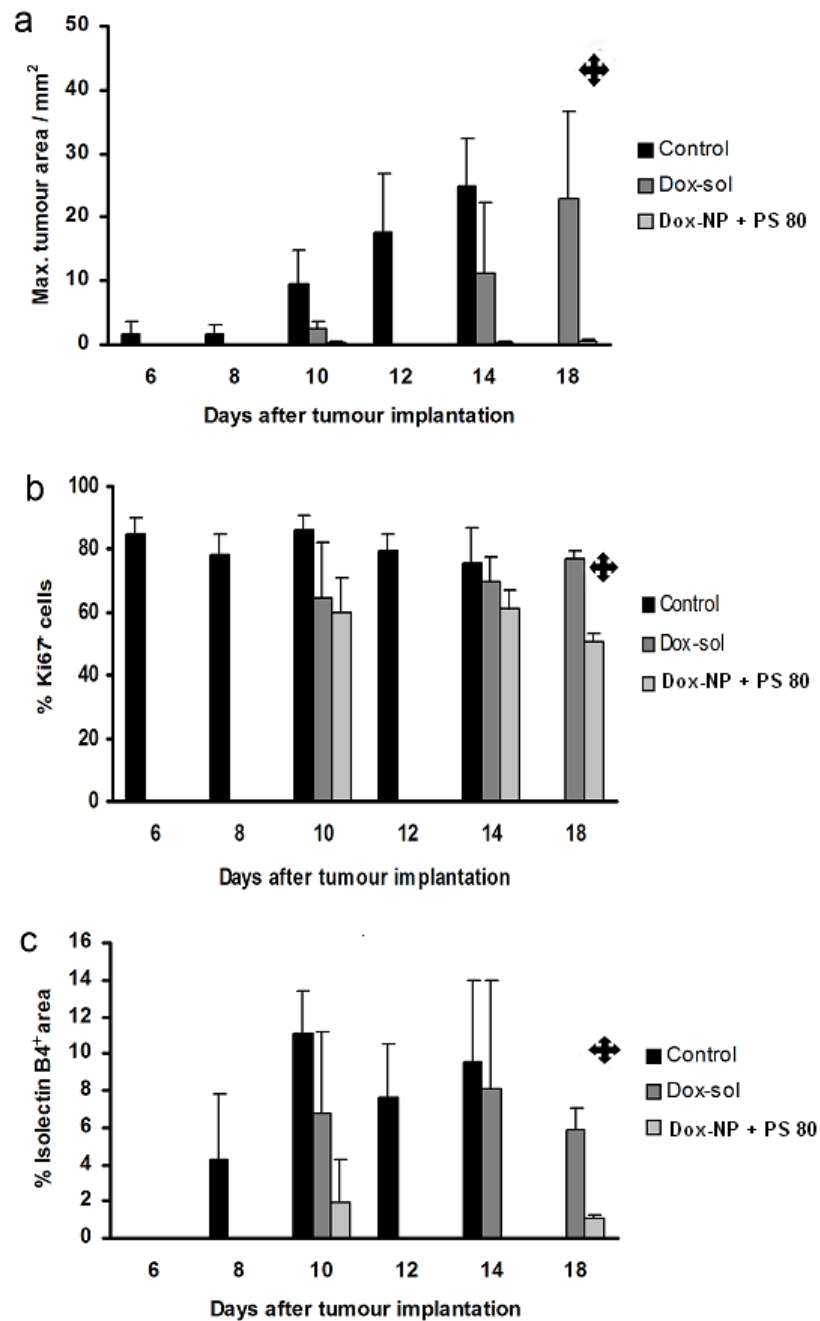


**Figure 14.** Treatment with nanoparticle-coated doxorubicin has antiangiogenic effects. Untreated animals (Control), animals treated with intravenous injections of doxorubicin in solution (Dox-sol) or doxorubicin in solution bound to polysorbate 80-coated PBCA nanoparticles (Dox-NP + PS 80) both,  $3 \times 1.5$  mg/kg on days 2, 5, and 8 were sacrificed at different time points after implantation. Statistical analysis of tumour size (a) estimated by the maximal area occupied by the tumour in serial sections, proliferation (b) determined by analysing the percentage of tumour cells stained with antibodies against Ki67, and vessel density (c) determined by measuring the percentage of the tumour area occupied by cells stained with Isolectin B4 are displayed. On day 14 after tumour implantation, the tumour area occupied by Isolectin B4<sup>+</sup> cells was negligible in the Dox-NP + PS 80 group. On day 18, the columns for the Dox-NP + PS 80 group display the mean values and standard deviations of this group without the outlier. The values for the outlier are marked by the (†) symbol.

**Table 3.** Histological and immunohistochemical evaluation of intracranially implanted 101/8 glioblastoma after treatment with formulations of doxorubicin.

Type of evaluation	Day 6			Day 8			Day 10			Day 12			Day 14			Day 18		
	Control	Dox-sol	Dox-NP + PS 80	Control	Dox-sol	Dox-NP + PS 80	Control	Dox-sol	Dox-NP + PS 80	Control	Dox-sol	Dox-NP + PS 80	Control	Dox-sol	Dox-NP + PS 80	Control	Dox-sol	Dox-NP + PS 80
<b>Necrosis (Score)</b>	0	-	-	0	-	-	3	1	0	3	-	-	3	2	0	-	3	1
<b>GFAP (Score)</b>	1	-	-	2	-	-	1	1	1	1	-	-	2	1	0	-	2	1
<b>Microvascular Proliferation (Score)</b>	0	-	-	1	-	-	1	0	0	1	-	-	2	1	0	-	1	0
<b>VEGF (Score)</b>	1	-	-	2	-	-	2	2	0	2	-	-	1	2	0	-	2	1



Microvascular proliferation was detected from day 8 after implantation. No significant differences were detected in the GFAP expression with a patchy low to moderate expression at all time points. Thus, the 101/8 rat glioblastoma model closely resembled human glioblastomas and showed a reproducible growth pattern allowing its application in the evaluation of potential new therapies for glioblastoma.

The effect of systemic chemotherapy on the temporal development of the 101/8 glioblastoma was evaluated using two different formulations of doxorubicin; doxorubicin bound to PBCA nanoparticles coated with PS 80 (Dox-NP + PS 80), and doxorubicin in solution (Dox-sol), which compared to the untreated controls. The Dox-NP + PS 80 treatment significantly decreased tumour formation. In the control groups, from day 8 to day 14, all animals developed tumours. The tumour incidence at all three comparable time points (day 10, 14 and 18) for the Dox-sol group was 16 out of 18 and for the Dox-NP + PS 80 groups was only 11 out of 18 (Table 2). Tumour size, proliferation of tumour cells, vessel density, and necrosis were compared between the Dox-NP + PS 80, Dox-sol, and control group on day 10 and 14 after the implantation (Figure 14, Table 3). Additionally, the Dox-NP + PS 80 and Dox-sol groups were compared on day 18 after the implantation. Previous experiments demonstrated that only a minor fraction of the animals in the control group survived longer than 16 days (d) after implantation (Steiniger 2004); therefore, day 14 was chosen as the last time point for the tumour assessment in the control group.

### 4.1.2.1 Tumour size

On day 10, there was a significantly decreased tumour size in the Dox-sol ( $p = 0.025$ ) and the Dox-NP + PS 80 ( $p = 0.0003$ ) groups when compared to the control group (Table 4, Figure 14a). The mean areas occupied by the tumours on H&E stained brain sections for the groups of untreated animals, Dox-sol and Dox-NP + PS 80 were  $9.4 \pm 5.2 \text{ mm}^2$ ,  $2.4 \pm 1.2 \text{ mm}^2$  and  $0.3 \pm 0.4 \text{ mm}^2$ , respectively.

On day 14, the mean tumour size in the control group reached  $24.9 \pm 7.6 \text{ mm}^2$ . Dox-NP + PS 80 considerably inhibited the tumour growth: the tumour size in this group was only  $0.4 \pm 0.2 \text{ mm}^2$  (Figure 14a). The tumour growth in Dox-sol was also inhibited and reached  $11.1 \pm 11.3 \text{ mm}^2$ . Statistically significant differences were found between the control and Dox-NP

+ PS 80 group both on day 10 ( $p = 0.0003$ ) and day 14 ( $p = 0.0028$ ) after the implantation. There were also statistical significance differences found between the Dox-sol and Dox-NP + PS 80 groups on day 10 ( $p = 0.025$ ) and on day 14 after the implantation ( $p = 0.04$ ) (Table 4). The considerable increase in efficacy of the tumour growth inhibition enabled by Dox-NP + PS 80 was also visible on day 18 after implantation. The mean tumour size - including one outlier - in this group was  $11.7 \pm 22.4$ , whereas in the Dox-sol group, the size reached  $23.0 \pm 13.5 \text{ mm}^2$ . It is important to note that only one animal (the outlier) in the Dox-NP + PS 80 group developed a considerable tumour of  $45 \text{ mm}^2$ , whereas the tumours of other animals were below  $1 \text{ mm}^2$  (Figure 14a). Without the outlier, the mean tumour area in this group is  $0.48 \pm 0.29 \text{ mm}^2$ , which is significantly lower, as compared to the Dox-sol group ( $p \leq 0.0005$ ) (Table 4). Thus, treatment of 101/8 rat glioblastoma with Dox-NP + PS 80 significantly decreased the incidence of tumours and tumour size when compared to the Dox-sol and the untreated control groups.

### 4.1.2.2 Proliferation

Proliferation was determined by immunohistochemical staining with antibodies against Ki67. Proliferation showed stable levels in all groups (Figure 14b) with an average of  $80 \pm 8\%$  Ki67<sup>+</sup> cells in the control group versus  $71 \pm 11\%$  and  $58 \pm 8\%$  in the Dox-sol and Dox-NP + PS 80 group, respectively. On day 10, the Dox-sol and the Dox-NP + PS 80 groups showed a significantly decreased proliferation after the implantation, when compared to the control;  $p = 0.02$  and  $0.005$  respectively. No statistical significance was observed on day 14 between the groups (Table 4 and Figure 14b). However, a significant decrease of the tumour cells proliferation was observed on day 18 when compared with the Dox-sol group ( $p < 0.0005$ ). Thus, treatment with Dox-NP + PS 80 decreased proliferation of the tumour cells when compared to treatment with Dox-sol and untreated control animals.

### 4.1.2.3 Vessel density

The vessel density in the tumour tissue was determined by measuring the percentage of the tumour area occupied by blood vessels and microvascular proliferation in serial sections

(Figure 14c). On day 10, the tumours in animals treated with Dox-NP + PS 80 showed a decreased vessel density when compared to animals treated with Dox-sol or untreated control animals ( $2 \pm 2\%$ ,  $7 \pm 4\%$ ,  $11 \pm 2\%$ , respectively). A statistical significant difference was found only between the control and the Dox-NP + PS 80 groups ( $p = 0.017$ ) (Table 4). The advantage of Dox-NP + PS 80 became even more pronounced on day 14: the vessel density in this group was negligible, whereas in the group treated with Dox-sol the density was similar to the untreated control ( $8 \pm 6\%$  and  $9 \pm 4\%$ , respectively). On day 18 after the implantation, the vessel density was decreased in the Dox-NP + PS 80 group when compared to the Dox-sol group ( $3 \pm 5\%$  and  $6 \pm 1\%$ , respectively). Again the high standard deviation for the Dox-NP + PS 80 group is due to the single outlier. Without the outlier the mean vessel density in the Dox-NP + PS 80 group is  $0.85 \pm 0.28\%$  which in this case, the difference between the Dox-NP + PS 80 and Dox-sol groups was statistically significant ( $p \leq 0.0005$ ) (Table 4). Thus, vessel density in the tumour tissue was drastically decreased after treatment with Dox-NP + PS 80 when compared to treatment with Dox-sol and untreated control animals.

#### **4.1.2.4 Expression of glial fibrillary acidic protein (GFAP), expression of vascular endothelial growth factor (VEGF), incidence and dimension of necrosis, and microvascular proliferation**

The efficacy of the chemotherapy was further characterized by GFAP expression, VEGF expression, the incidence and dimension of necrosis, and microvascular proliferation (Table 3). While no considerable differences were observed in GFAP expression, the expression of VEGF was decreased in the Dox-NP + PS 80 group when compared to the Dox-sol and the control group at all time points (Figure 13). The incidence of necrosis was decreased in the Dox-sol group when compared to untreated control animals. Necrosis was rarely observed in the Dox-NP + PS 80 group. Microvascular proliferation increased with time in the control group. The Dox-sol group showed decreased microvascular proliferation when compared to the control group, while in the Dox-NP + PS 80 group microvascular proliferation was completely absent. Thus, treatment of rat 101/8 glioblastoma with Dox-sol led to a slight decrease of necrosis and microvascular proliferation, whereas Dox-NP + PS 80 drastically decreased necrosis and led to the complete disappearance of microvascular proliferation.

**Table 4.** Statistical analysis of the anti-tumour effect of doxorubicin formulations in rats bearing intracranial 101/8 glioblastoma tumour.

Type of test	Day of fixation	Groups	p-value	
Tumour size	Day 10	Control vs Dox-sol	0.025*	
		Control vs Dox-NP + PS 80	0.0003*	
		Dox-sol vs Dox-NP + PS 80	0.025*	
	Day 14	Control vs Dox-sol	0.15	
		Control vs Dox-NP + PS 80	0.0028*	
		Dox-sol vs Dox-NP + PS 80	0.04*	
	Day 18**	Dox-sol vs Dox-NP + PS 80	<0.0005*	
	Proliferation	Day 10	Control vs Dox-sol	0.02*
			Control vs Dox-NP + PS 80	0.005*
Dox-sol vs Dox-NP + PS 80			1	
Day 14		Control vs Dox-sol	1	
		Control vs Dox-NP + PS 80	0.16	
		Dox-sol vs Dox-NP + PS 80	0.58	
Day 18**		Dox-sol vs Dox-NP + PS 80	<0.0005*	
Vessel Density		Day 10	Control vs Dox-sol	0.17
			Control vs Dox-NP + PS 80	0.015*
	Dox-sol vs Dox-NP + PS 80		0.2	
	Day 14	Control vs Dox-sol	0.35	
		Control vs Dox-NP + PS 80	<0.0005*	
		Dox-sol vs Dox-NP + PS 80	<0.0005*	
	Day 18**	Dox-sol vs Dox-NP + PS 80	<0.0005*	

\* Statistically significant. The significance level was set at 0.05 ( $p \leq 0.05$ ).

\*\* The comparison between the two groups was performed with the pairwise Student's t-test. The simultaneous comparison between three groups was evaluated with the Kruskal-Wallis model with post-hoc test.

### 4.1.3 Characterisation of drug-loaded PBCA nanoparticles prepared in the presence of organic solvents

The drug-loaded PBCA nanoparticles were produced by anionic polymerisation of n-butyl-2-cyanoacrylate in the presence of a drug. The polymerisation media consisted of a solution of stabilisers/surfactants in a mixture of 0.01 N HCl and an appropriate organic solvent (9:1).

Two substances were chosen; paclitaxel, a widely used antitumour agent and a model drug, loperamide (opiate receptor agonist). The paclitaxel solubility in water is about 1 µg/ml (Liggins 1997); the solubility of loperamide is about 2 µg/ml (Merck ed. 2001). These drugs are sufficiently soluble in organic solvents (Merck 2001, Kim 2004). The drug-to-polymer-ratio was 1:10. The particles were stabilised by commonly used excipients, dextran 70,000 (1%) and poloxamer 188 (0.2%) or, in the case of paclitaxel, also by PEG-PE, a micelle-forming PEGylated phospholipid.

The data on the influence of organic solvents on the physicochemical parameters of the drug-loaded and empty PBCA nanoparticles are presented in Tables 5 - 7 and Figures 15 - 17.

#### 4.1.3.1 Size, polydispersity and surface charge of the nanoparticles

The average particle diameter and polydispersity of the nanoparticles are shown in Table 5. The polymerisation of n-butyl-2-cyanoacrylate in the presence of dextran and poloxamer 188 enabled the preparation of 220 nm nanoparticles with a narrow polydispersity of 0.05, which correlates with the results of other studies (Bootz 2004, Ambrousi 2006).

**Table 5.** Physicochemical parameters of empty PBCA nanoparticles prepared in the presence of organic solvents (a mean value of 3 measurements ± SD).

Organic solvent	Particle size measured by PCS		Charge (mV)	Yield of PBCA (%)
	Mean diameter (nm)	Polydispersity		
None	220 ± 5	0.05 ± 0.02	-17	65 ± 1.61
MeOH	200 ± 11	0.045 ± 0.015	-12	50.50 ± 2.0
EtOH	230 ± 10	0.035 ± 0.02	-10	45.55 ± 6.25
i-PrOH	240 ± 8	0.02 ± 0.01	-10	56.29 ± 2.0
EtOAc	195 ± 7	0.05 ± 0.01	-11	56.70 ± 10.5
CH <sub>2</sub> Cl <sub>2</sub>	185 ± 5	0.025 ± 0.01	-14	65.60 ± 2.6
CH <sub>2</sub> Cl <sub>2</sub> /PEG-PE	320 ± 10	0.3 ± 0.05	-17	55.87 ± 5.11

## Results

The presence of the organic solvents in the polymerisation medium did not considerably influence the physicochemical parameters of the empty nanoparticles.

The surface charges of all samples were negative with values between -10 to -17 mV with similar sizes in the range of 185 - 240 nm and a narrow size distribution of 0.02 to 0.05. The empty nanoparticles produced using 1% PEG-PE were characterised by a larger size of 320 nm with a higher polydispersity of 0.3. The results of the PCS measurements of the particle size were consistent with the data obtained by analytical ultracentrifugation (Figure 15).

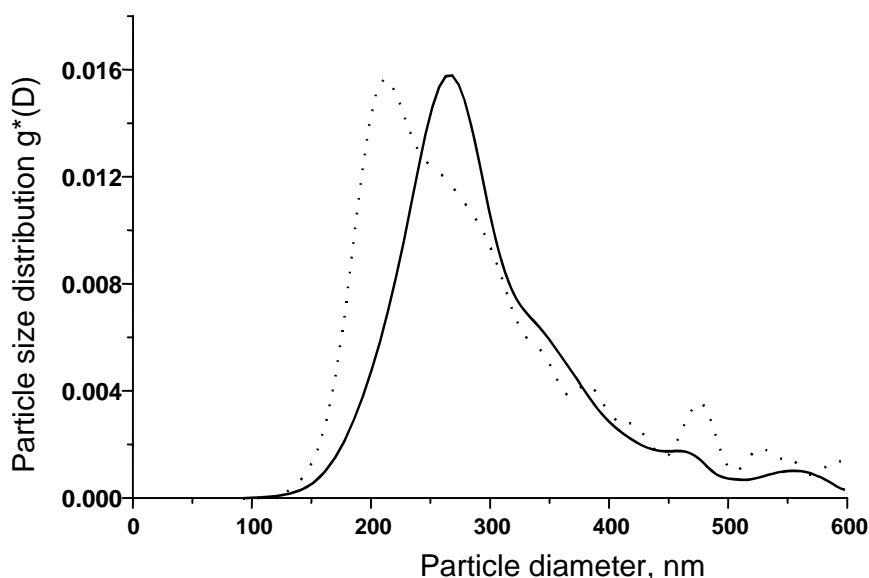


**Figure 15.** Particle size distribution determined by analytical ultracentrifugation (ANUC) of empty (dotted line) and loperamide-loaded (solid line) PBCA nanoparticles prepared in the presence of dichloromethane after freeze-drying.

The empty nanoparticles showed a relatively homogeneous size distribution with a peak at 220 nm. A broad shoulder in the range of ~ 250 nm and a small peak at about 500 nm were obviously caused by the presence of particles of these sizes. These particle populations, however, were not large since they did not produce any significant isolated peaks.

The size and size distribution of loperamide-loaded PBCA nanoparticles determined by PCS and analytical ultracentrifugation did not differ significantly from those of empty nanoparticles (Table 5 - 6, Figure 15).

**Table 6.** Parameters of loperamide-loaded PBCA nanoparticles prepared in the presence of organic solvents (mean values  $\pm$  SD from three replicate samples).

Organic phase	Substance solubility (mg/ml)*	Particle size measured by			Surface charge (mV)	Encapsulation efficiency (%)	Loading capacity ( $\mu$ g bound drug/mg PBCA)	Drug conc. in the nanoparticle suspension (mg/ml)	Yield of PBCA (%)
		PCS		Mean diameter (nm)					
		Mean diameter (nm)	Polydispersity						
MeOH	28.6	225 $\pm$ 5	0.035 $\pm$ 0.02	-5	82.5 $\pm$ 5	157.44	0.825 $\pm$ 0.05	52.4 $\pm$ 10.9	
EtOH	5.37	245 $\pm$ 5	0.030 $\pm$ 0.01	-10	85.5 $\pm$ 5	145.41	0.85.5 $\pm$ 0.05	58.8 $\pm$ 20.5	
CH <sub>2</sub> Cl <sub>2</sub>	35.1	223 $\pm$ 5	0.020 $\pm$ 0.01	-4	80.2 $\pm$ 2	131.60	0.802 $\pm$ 0.02	60.9 $\pm$ 10.1	

\* Data from Merck index, edition 13

The surface charges were less negative, as compared to the empty particles, but remained negative in the range of -5 mV to -10 mV. The encapsulation efficiency of loperamide was as high as 80 - 85%; the capacity of the particles reached 130 - 160  $\mu$ g bound drug/mg PBCA. The yield of PBCA was 50 - 60%, which was similar to that of the empty nanoparticles.

**Table 7.** Parameters of paclitaxel-loaded PBCA nanoparticles prepared in the presence of organic solvents (mean values  $\pm$  SD from three replicate samples).

Organic phase	Substance Solubility*	Particle size measured by			Surface charge (mV)	Encapsulation efficiency (%)	Loading capacity ( $\mu$ g bound drug/mg PBCA)	Drug conc. in the nanoparticle suspension (mg/ml)	Yield of PBCA (%)
		PCS		Mean diameter (nm)					
		Mean diameter (nm)	Polydispersity						
MeOH	Soluble	353.2 $\pm$ 3.3	0.36 $\pm$ 0.02	-15	20 $\pm$ 5	32.0	0.20 $\pm$ 0.05	62.5	
i-PrOH	Soluble	421.3 $\pm$ 42.3	0.38 $\pm$ 0.05	-19	16.5 $\pm$ 2	31.31	0.165 $\pm$ 0.02	52.7	
EtOAc	n/a	365.8 $\pm$ 2.3	0.58 $\pm$ 0.01	-11	20.5 $\pm$ 2	30.73	0.205 $\pm$ 0.02	66.7	
CH <sub>2</sub> Cl <sub>2</sub>	Soluble	307.6 $\pm$ 12	0.24 $\pm$ 0.03	-17	24.2 $\pm$ 5	40.33	0.242 $\pm$ 0.05	60	
CH <sub>2</sub> Cl <sub>2</sub> / PE-PEG	n/a	355.3 $\pm$ 5	0.33 $\pm$ 0.05	-20	45 $\pm$ 5	55.90	0.45 $\pm$ 0.05	80.53	

\* Data from Kim *et al.* (Kim 2004).

The size of paclitaxel-loaded nanoparticles was larger than the empty nanoparticles, with the mean particle diameters ranging from 308 nm to 427 nm depending on the solvent that was used. The polydispersity was also higher – up to 0.3 (Table 7).

The charge of these particles did not considerably differ from that of the empty particles.

#### 4.1.3.2 Morphology of the nanoparticles

The morphology of the PBCA nanoparticles was investigated by scanning electron microscopy (SEM) and atomic force microscopy (AFM). The samples for microscopy were prepared after freeze-drying without further purification. Typical micrographs of empty and loperamide-loaded particles are shown in Figures 16 and 17.

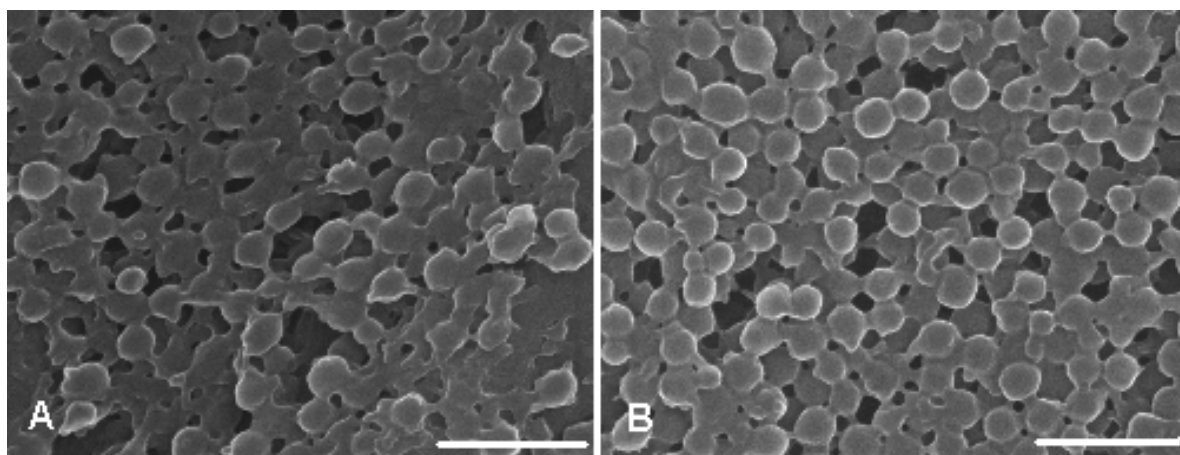


**Figure 16** Scanning electron micrographs (SEM) of the PBCA nanoparticles prepared in the presence of dichloromethane after freeze-drying and redispersion in water: (A) empty and (B) loperamide-loaded nanoparticles. Bar: 800 nm.

It can be seen that both types of particles had a spherical shape. Importantly, the micrographs of loperamide-loaded particles did not exhibit any crystals on the surface of the particles or in the medium, which indicates that all drugs in this formulation were indeed encapsulated and not precipitated in the form of crystals.

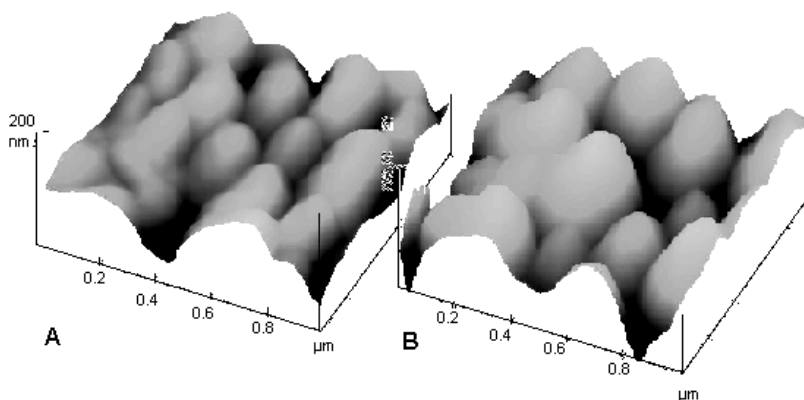


**Figure 17.** AFM surface morphology of the PBCA nanoparticles in the presence of dichloromethane after freeze-drying and redispersion in water: (A) empty and (B) loperamide-loaded nanoparticles. Bar: 200 nm.



#### 4.1.3.3 Particle yield

The yield of PBCA particles were measured with gas chromatography. The particle yield appeared to be lower in the presence of alcohols and ethylacetate, whereas dichloromethane did not affect this parameter. The polymerisation time before adding the organic solvent (30, 40, or 60 min) did not produce any considerable changes in the above parameters of the empty nanoparticles. The presence of the drug appeared to have no major influence on the particle yield. However, the polymerisation yield in the presence of PEG-PE reached about 80%, which was the highest particle yield compared to other excipient (dextran 70,000 (1%) and poloxamer 188 (0.2%)) (Tables 5 - 7).

#### 4.1.3.4 Drug loading

The encapsulation efficiency of paclitaxel in the particles stabilised by dextran and poloxamer 188 was low (16 - 24%); however, in the presence of PEG-PE the loading increased to 45% and the capacity reached 55  $\mu\text{g}/\text{mg}$  PBCA (Table 6). PEG-PE also produced the highest PBCA yield of 80%; whereas for other samples, the yield remained in the range of 50 - 65%.

The concentration of loperamide in the nanoparticle suspensions was  $\sim 0.8$  mg/ml. The measurements of the drug loading performed after freeze-drying demonstrated that the filtrates obtained by ultrafiltration of the nanoparticle suspension contained only trace amounts of free drugs, which suggested that practically all of the drugs in the formulations were incorporated in the nanoparticles. Therefore, the nanoparticles enabled a 400-fold increase in drug content in an aqueous medium (800  $\mu\text{g}/\text{ml}$  versus initial 2  $\mu\text{g}/\text{ml}$ ) (Table 6). Similar results were obtained for paclitaxel: its total concentration in the aqueous medium was increased 200-fold for the dextran/poloxamer-stabilised particles and 450-fold in the case of PEG-PE (Table 6).

#### 4.1.3.5 The content of residual organic solvents

The residual content of the organic solvents in the samples of empty nanoparticle after freeze-drying was analysed by gas chromatography. It was found that the nanoparticles

produced in the presence of ethanol contained the highest residual amount of 1400 ppm organic solvents, whereas the particles produced in the presence of ethylacetate exhibited only trace amounts of 5 ppm. The amounts of residual solvents in the samples prepared in the presence of iso-propanol and dichloromethane were 340 ppm and 50 ppm, respectively.

#### 4.1.3.6 Loperamide-loaded PBCA-based formulations for the tail-flick test

The pharmacological efficacy of the nanoparticulate loperamide was tested using the tail-flick test, as described by Alyautdin *et al.* (Alyautdin 1997). The antinociceptive effects of the formulations measured as percentage of a maximal possible effect (MPE%) are presented in Figure 18.

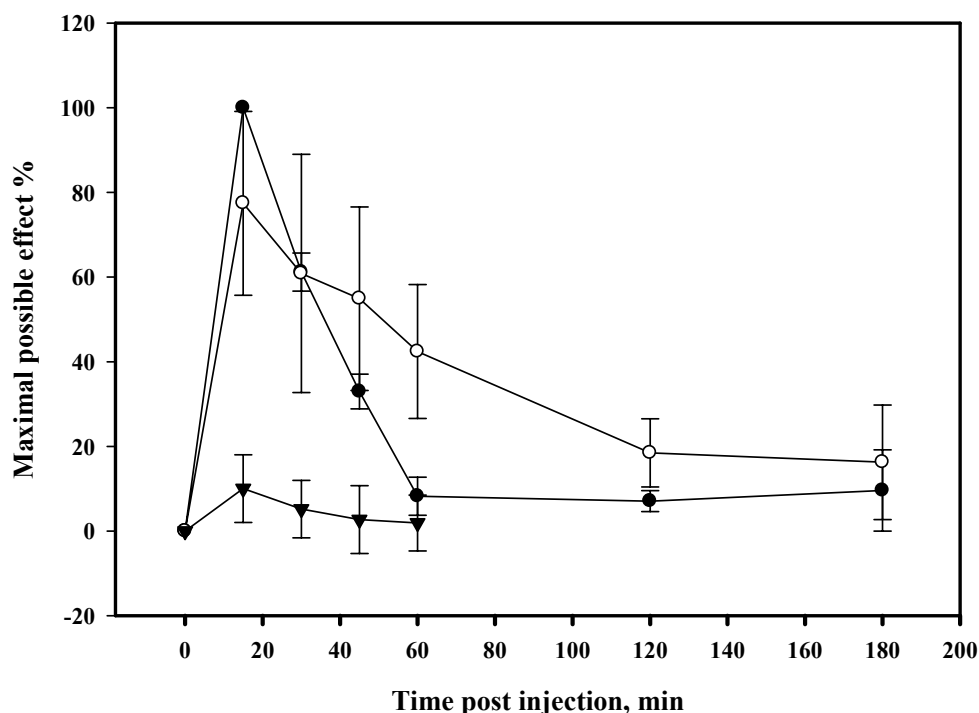


**Figure 18.** Antinociceptive effect of loperamide formulations assessed by a tail-flick test after *i.v.* injection in mice (7.0 mg/kg): ● loperamide bound to non-coated, ○ polysorbate 80-coated PBCA nanoparticles and ▲ loperamide solution (n = 10).

It can be seen that loperamide bound to PBCA nanoparticles coated with polysorbate 80 produced an analgesic effect that reached its maximum of 80% MPE 15 min after injection and was measurable for 120 min. As expected, loperamide in solution was ineffective, and

after 60 minutes the evaluation of this formulation was terminated. These data correlate with the results of Alyautdin *et al.* (Alyautdin 1997). Similarly to the polysorbate 80-coated nanoparticles a considerable analgesia also was produced by the non-coated nanoparticles. The maximal effect of the non-coated nanoparticles formulation (100% MPE) was observed 15 min after injection. However, in this case analgesia lasted only 60 min.

### **4.1.3.7 Treatment of rats bearing intracranial transplanted glioblastoma 101/8 using paclitaxel-loaded nanoparticle formulations**

The antitumour efficacy of paclitaxel in three nanoparticle formulations including paclitaxel bound to PBCA nanoparticles (PXL-NP), PXL-NP coated with polysorbate 80 (PXL-NP + PS 80), and PXL-NP coated with poloxamer 188 (PXL-NP + F68) was tested in glioblastoma-bearing rats. Untreated glioblastoma-bearing rats and the animals treated with the paclitaxel solution (PXL) were used as controls.

The brain tumour model and the treatment regimen for the present study were chosen based on the results of the previous experiments, where this experimental protocol using doxorubicin formulations proved to be effective (Steiniger 2004, Ambrousi 2006, Petri 2007). Therefore, the objective of this experiment was to investigate if this technology could be extended to paclitaxel.

Due to the low loading of paclitaxel to PBCA-NP, administration of a high dose was not possible. Therefore, the chemotherapy of paclitaxel was carried out using the total dose of 4.5 mg/kg ( $3 \times 1.5$  mg/kg). The result of the chemotherapy is presented as numeric values in the form of median and mean survival time (Table 8) and the Kaplan-Meier survival curves (Figure 19).

## Results

**Table 8.** Median and mean survival time of the 101/8 glioblastoma-bearing rats after treatment with different paclitaxel formulations; (PXL-NP), PXL-NP coated with polysorbate 80 (PXL-NP + PS 80) or coated with poloxamer 188 (PXL-NP + F68), and paclitaxel solution (PXL) which compared with untreated animals (Control).

Groups	Survival time, days	
	Median	Mean
Untreated control	11	13
PXL	14	15
PXL-NP	12	13
PXL-NP + PS 80	13	14
PXL-NP + F68	15	14

The median survival time represents the day at which half of the populations with tumour were still alive. As seen from Table 8, the median of survival in the groups treated with PXL and PXL-NP + F68 were 14 and 15 days, respectively, which was slightly higher than in the other groups. The mean survival times measured starting from the day of the tumour implantation were similar in all groups (14 days). None of the groups treated with paclitaxel formulations showed improvement in the mean survival time, as compared to the untreated animals.

As seen from the Kaplan-Meier survival curves, the longest survival time was achieved in the group treated with paclitaxel solution: 25% of the animals (2/8) survived till day 20 post-tumour implantation. However, this effect was not significant. In addition, there were no cases of long-term remission.

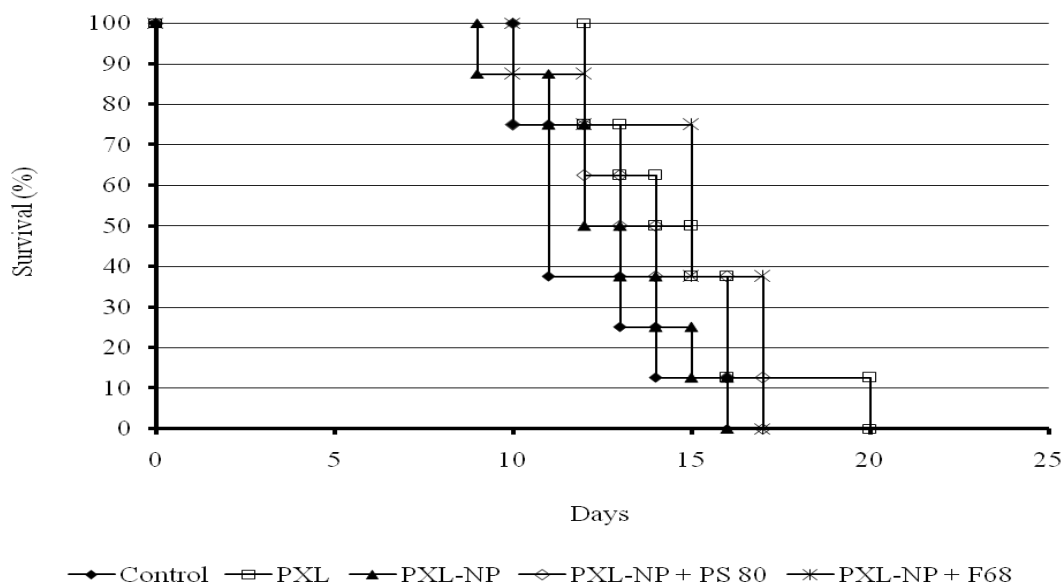


**Figure 19.** Survival (Kaplan-Meier plot) of rats bearing intracranially transplanted 101/8 glioblastoma after *i.v.* administration of paclitaxel-loaded in PBCA nanoparticles formulation; (PXL-NP), PXL-NP coated with polysorbate 80 (PXL-NP + PS 80) or coated with poloxamer 188 (PXL-NP + F68) which compared with paclitaxel solution (PXL), and untreated animals (Control).

All animals were sacrificed after the appearance of the clinical signs of the disease (mostly day 15). The macroscopical observation of the internal organs showed no signs of drug related toxicity.

#### 4.2 Characterisation of human serum albumin nanoparticles

The human serum albumin nanoparticles (HSA-NP) were prepared by desolvation of HSA with ethanol followed by crosslinking with glutaraldehyde (Weber 2000a, Weber 2000b).

The desolvation procedure was performed by the addition of the desolvating agent, ethanol to the protein. The desolvation resulted in the precipitation of the HSA macromolecules. With the help of ethanol the swelling of macromolecules in solution reversed, and the diameter of the macromolecule coil become smaller. After a certain degree of desolvation, the molecules began to aggregate. When sufficient desolvation had occurred, phase separation took place (Kreuter, J. Ed. 1994).

After the desolvation of HSA solution, the nanoparticles were stabilised with glutaraldehyde. The aldehyde amount was corresponding to 100% of the theoretic amount necessary for the

quantitative cross-linking of the 59  $\epsilon$ -amino groups in the HSA molecules of the particle matrix (Langer 2003, Weber 2000a).

The resulting nanoparticles were purified by repetitive washing and the pellets were re-dispersed to the original volume in water.

### 4.2.1 Size, polydispersity and surface charge of the nanoparticles

By using a combination of the pump-controlled system and adjusting of the pH in the presence of sodium chloride, rather homogenous sizes and polydispersities of the nanoparticles were achieved. The size of the empty nanoparticles at pH 8.0 was about  $170 \pm 20$  with the polydispersity of  $0.25 \pm 0.05$ . The purification process removed all particles of diameter below 50 nm, which lead to much more narrow size distributions. The size of nanoparticles after purification was  $200 \pm 25$  nm with a narrow size distribution of  $0.05 \pm 0.01$ .

The surface charge of the empty nanoparticles was  $-50 \pm 6.5$  mV.

### 4.2.2 Characterisation of the HSA nanoparticles modified by apolipoprotein A-I and B-100

The mechanism of the delivery of the drugs across the BBB by nanoparticles still is not fully elucidated. The involvement of different apolipoproteins which enable the interaction of the nanoparticles with the brain endothelial cells and subsequent drug transfer into the brain was demonstrated in different studies (Kreuter 2002, Gessner 2001, Petri 2007).

In the present study, apolipoprotein A-I (Apo A-I) and B-100 (Apo B-100) were covalently coupled to human serum albumin (HSA-NP), and the central analgesic effect of loperamide which was adsorbed to the nanoparticles surface was tested with the tail-flick test.

For the covalent attachment of the apolipoproteins to the nanoparticle, it was necessary to achieve reactive sulfahydryl functions on the surface of the nanoparticles. The nanoparticles were activated using a heterobifunctional PEG-based crosslinker; NHS-PEG3400-MAL.

At pH 8.0, the spacer reacted selectively with primary amine groups which were available on the nanoparticle surface. To achieve complete reaction, the spacer was used in 50-fold molar

## Results

excess. After 2 h, the unreacted spacer was separated with centrifugation from NHS-PEG-MAL activated nanoparticle (Figure 20). The nanoparticles were redispersed in phosphate buffer (pH 8.5).

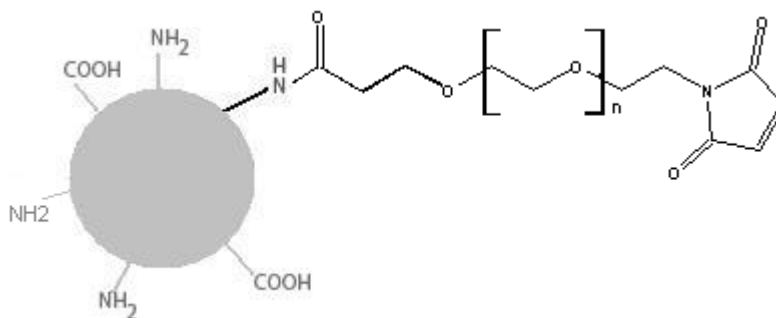


**Figure 20.** Chemical representation of the nanoparticles with the bifunctional NHS-PEG-MAL (mw = 3400).

In a second step, a free sulfhydryl group was introduced on the surface of apolipoproteins by reaction of apolipoprotein amino groups with 2-iminothiolane (Figure 21). 2-iminothiolane (Traut's reagent) is a water soluble reagent and reacts at pH 7 to 10.

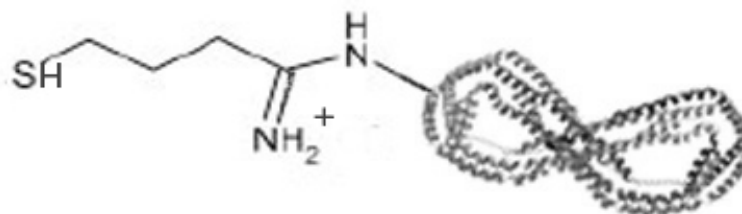


**Figure 21.** Thiolated apolipoprotein.

After thiolation of the apolipoproteins, the nanoparticles were attached *via* a thioether linkage between the sulfhydryl reactive NHS-PEG-maleimide group of the activated nanoparticles and the sulfhydryl groups on the apolipoprotein surface. The apolipoproteins were employed in the highest concentrations (Table 9) that could be attached to the nanoparticles. The Apo A-I concentration was 150  $\mu\text{g/ml}$  nanoparticle suspension which was 3 times higher than that of Apo B-100 (50  $\mu\text{g/ml}$ ).

Loperamide was loaded by the absorption method on the surface of the nanoparticles. The final HSA nanoparticles concentration was 10 mg/ml corresponding to 0.7 mg loperamide. Figure 22 shows the schematic structure of the covalently apolipoprotein modified HSA nanoparticles.

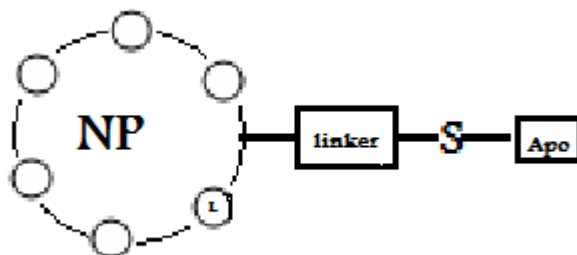


**Figure 22.** Schematic illustration of covalently apolipoprotein-modified HSA-NP. Thiolated apolipoprotein attached *via* thioether linkage to activated nanoparticles. Loperamide loaded to nanoparticle by adsorption method.

#### 4.2.2.1 Size, polydispersity and surface of the nanoparticles

Table 9 shows three preparations based on the HSA nanoparticles which were used in the tail-flick test: loperamide-loaded unmodified nanoparticles (HSA-NP), loperamide-loaded HSA nanoparticles with covalently attached apolipoproteins A-I or B-100 (HSA-NP+ApoA-I, HSA-NP+ApoB-100, respectively).

The nanoparticle preparations were characterised by a similar size, polydispersity index, and zeta potential. The size of the nanoparticles with covalently bound ApoB-100 was about 240 nm which was slightly bigger than that of HSA-NP modified with Apo A-I (225 nm) and the unmodified loperamide-loaded nanoparticles (218 nm). The attachment of apolipoproteins slightly increased the nanoparticles polydispersity from 0.05 (HSA-NP) to 0.3 (HSA-NP + Apo A-I) and 0.6 (HSA-NP + Apo B-100). The surface charges remained negative for all particles. However, the empty nanoparticles showed a slightly more negative charge (-42 mV).



**Table 9.** Physicochemical characteristics of loperamide-loaded HSA nanoparticles (HSA-NP) with apolipoproteins A-I and B-100 (Apo A-I, Apo B-100) covalently attached using the NHS-PEG-Mal 3400 linker.

Preparations	Mean particle size (nm)	Polydispersity	Charge (mV)	Loperamide conc. (mg/ml)	Apolipoprotein conc. (µg/ml)
HSA-NP + Apo A-I	225	0.38	- 35	0.86	150
HSA-NP + Apo B-100	240	0.66	- 37	0.86	50
HSA-NP	218	0.05	- 42	0.86	-

The highest concentrations of the apolipoproteins which could bind to the HSA nanoparticles were differed from each other (Table 9). The highest apolipoprotein A-I concentration was 150 µg/ml of the nanoparticle suspension which was three times higher compared to the nanoparticle preparation with apolipoprotein B-100. However the loperamide loading was similar for all nanoparticle preparations.

#### 4.2.2.2 Tail-flick test with apolipoprotein-modified HSA nanoparticle formulations

The antinociceptive response demonstrating the transport of loperamide across the BBB was measured by the tail-flick test after intravenous injection of the loperamide formulations in mice. A significant antinociceptive response was achieved only in animals treated with loperamide bound to HSA nanoparticles modified by the apolipoproteins A-I and B-100 compared, whereas the effect of empty nanoparticles and the loperamide solution was negligible (Figure 23).

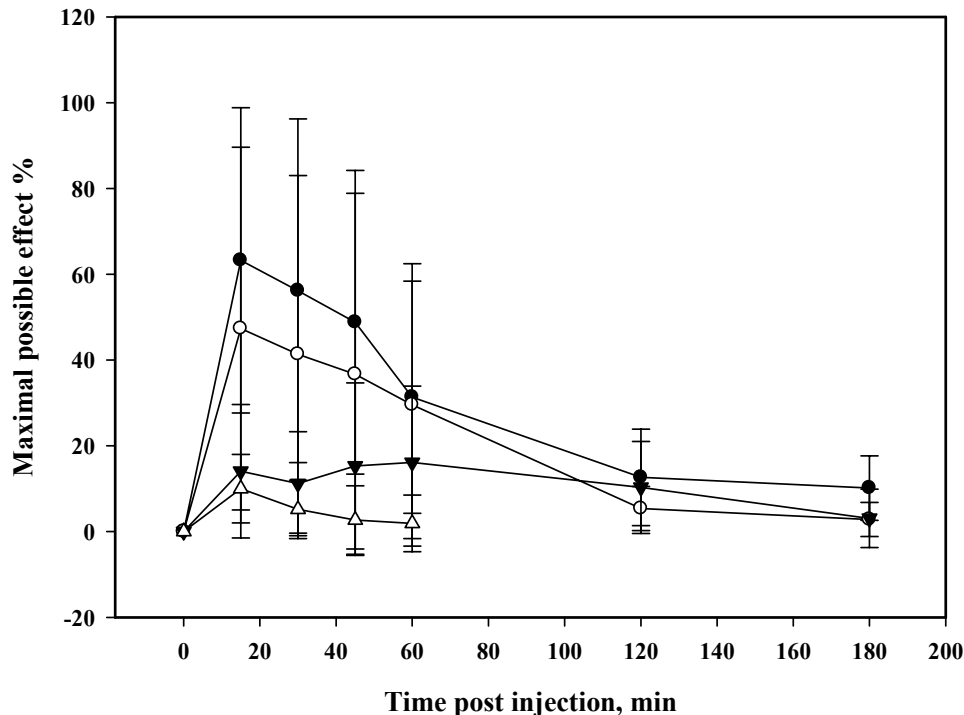


**Figure 23.** Maximal possible effect (MPE) (mean  $\pm$  SD) of the antinociceptive response of male ICR (CD-1) mice after injection of one of the following loperamide formulations into the tail vein in the dose of 7.0 mg/kg ( $n = 10$ ): ● loperamide loaded in HSA nanoparticles with covalently attached apolipoprotein A-I; ○ loperamide loaded in HSA nanoparticles with covalently attached apolipoprotein B-100; ▼ loperamide loaded HSA-NP, and △ loperamide solution.

The antinociceptive effect of the particles modified by apolipoprotein A-I reached 65% after 15 min. The maximal possible effect (MPE) of the particles modified by apolipoprotein B-100 at this time was below 50% but was still statistically different ( $2p < 0.02$ ) from the loperamide solution and the unmodified nanoparticles. The antinociceptive effect of these preparations lasted for over 60 minutes, although at this time, there was no significant difference between two types of the modified nanoparticles. The loperamide-loaded unmodified nanoparticles and loperamide solution produced no considerable effect (MPE below 20%).

These results clearly demonstrated that the binding of apolipoproteins to the surface of the nanoparticles facilitated the transport of this drug across the BBB.

### 4.2.3 Thalidomide bound to human serum albumin nanoparticles

The empty HSA nanoparticles were prepared using the desolvation technique as described in the section 3.1. For thalidomide loading in the HSA-NP, 1 mg of the drug was dissolved in 1 ml of ethanol-DMSO (8:2) mixture. The drug solution then was added to 10 mg of HSA-NP. To destabilise the crystalline structure of thalidomide and to enhance the loading, 10  $\mu$ l triethylamine was added to the suspension, and the mixture was shaken for 24 h.

#### 4.2.3.1 Size, polydispersity, and surface of the nanoparticles

The size of empty nanoparticles produced at pH 8.5 was  $173 \pm 24$  nm with a narrow polydispersity of  $0.05 \pm 0.01$ . The purification process slightly increased the size to  $185 \pm 10$  nm. After thalidomide loading to HSA-NP, the size of the nanoparticles was increased to  $210 \pm 40$  nm (Figure 24). However, the polydispersity was not changed and remained similar to the empty nanoparticles after the purification ( $0.05 \pm 0.01$ ).

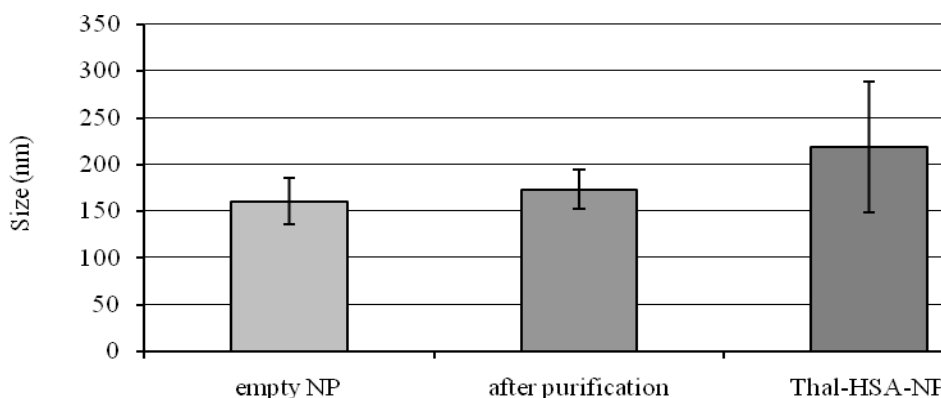


**Figure 24.** Average size of empty HSA nanoparticles (before and after purification with water) and Thalidomide loaded HSA-NP.

The charge of the nanoparticles was  $-50 \pm 6.5$  mV and did not change after the drug loading.

### 4.2.3.2 Drug loading

The loading (%) was calculated as the ratio of the drug bound to the particles to the initial drug concentration. The result showed that the loading of thalidomide to HSA-NP considerably increased after the addition of triethylamine. The solubility of thalidomide in 20 mg/ml HSA-NP suspension reached up to 800 µg of thalidomide (40 µg Thal/mg HSA-NP), whereas the solubility of the free drug (a mixture of enantiomers) in water and 5% glucose solution was only 52 and 70 µg/ml, respectively (Eriksson 2000).

### 4.2.3.3 Solubility of thalidomide

Thalidomide has a poor solubility in water. For this reason, only peroral formulations of this drug are available, although parenteral administration would be desirable in some clinical situations (Eriksson 2000).

The purpose of this set of experiments was to investigate the possibility to increase the solubility of thalidomide by using pharmaceutical excipients. These solvents included 5% glucose solution, 10% polysorbate 80, 10% poloxamer 188, cremophor<sup>®</sup> EL-ethanol (51:49). Thalidomide was used in a form of racemate (a mixture of two enantiomers). The aqueous solubility of thalidomide in water and 5% glucose solution was also tested. The result was compared with the thalidomide concentration in the HSA-NP formulation (400 µg Thal/ml NP suspension).

These formulations were also tested for their stability (storage for 24 h at room temperature). The concentration of thalidomide after 24 h was measured by HPLC and compared with the freshly prepared formulations. The preparations containing more than 5 % of precipitated thalidomide were discarded.

The solubility of thalidomide in 10% solutions of poloxamer 188 or polysorbate 80 was 154.75 and 213.13 µg/ml, respectively. Similar solubility (215 µg/ml) was achieved using the mixture of 51% Cremophor<sup>®</sup> EL and 49% ethanol. These results are summarised in Figure 25.

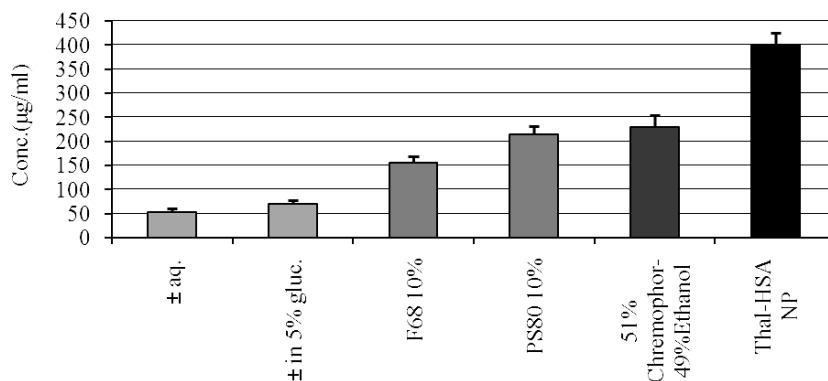


**Figure 25.** Solubility of thalidomide in different organic solvents; water, 5% glucose solution, 10% polysorbate 80, 10% poloxamer 188, 51% cremophor and 49% ethanol and thalidomide-HSA-NP.

The thalidomide solubility in water and in 5% glucose was 50 and 75 µg/ml, respectively, which correlated with the results of Eriksson *et al.* (Eriksson 2000).

In neither of these formulations, solubility of thalidomide could exceed the content of thalidomide in the nanoparticle formulation (400 µg/ml). Furthermore, the solubility of thalidomide in clinically applicable vehicles such as 0.5% solutions of polysorbate 80 or poloxamer 188 was only 75 µg/ml, i.e. the same as in the 5% glucose solution.

#### 4.2.3.4 Treatment of rats bearing intracranial transplanted glioblastoma 101/8 using different thalidomide formulations

The antitumour efficacy of the unmodified thalidomide-loaded HSA-NP (Thal-HSA-NP) and Thal-HSA-NP coated with 1% polysorbate 80 (Thal-HSA-NP + PS 80) were evaluated in the glioblastoma-bearing rats. The effect of these formulations was compared to orally administered thalidomide. Untreated animals were used as control. The nanoparticle formulations were injected intravenously into the tail caudal vein. The treatment regimen was  $3 \times 1$  mg/kg (total dose 3 mg/kg) on days 2, 5, and 8 post-tumour implantation.

Figure 26 shows the Kaplan-Meier survival plot of the rats treated with these formulations. All animals died between day 20 and 25 post-implantation.

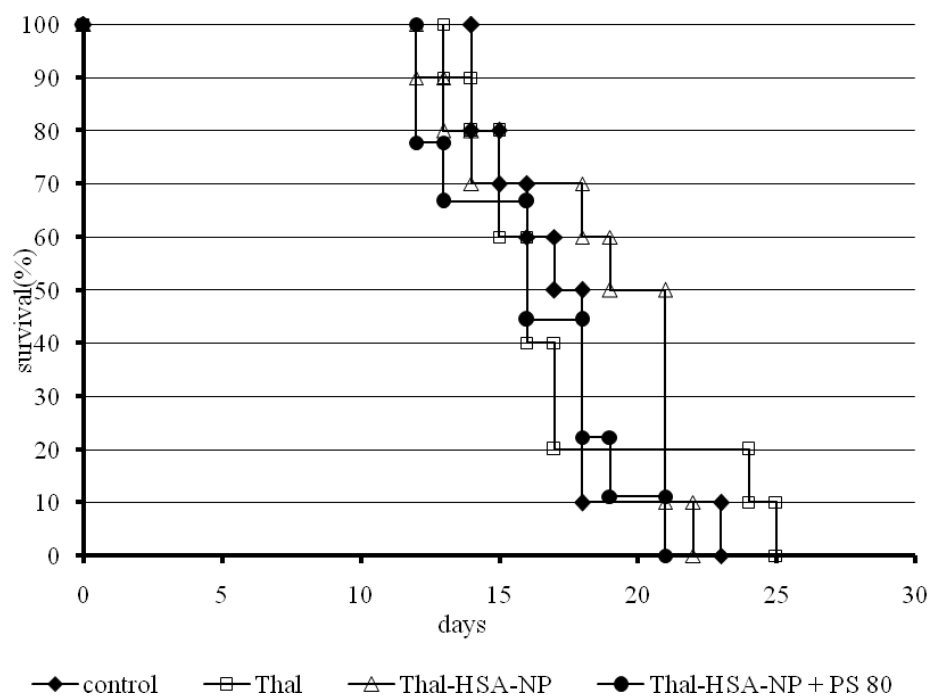


**Figure 26.** Survival (Kaplan-Meier plot) of rats bearing intracranially transplanted 101/8 glioblastoma after *i.v.* administration of thalidomide-loaded in HSA nanoparticles included, the unmodified surface thalidomide HSA-NP (Thal-HSA-NP), coated with 1% polysorbate 80 (Thal-HSA-NP + PS 80).

**Table 10.** Median and mean survival time of the 101/8 glioblastoma-bearing rats after treatment with different thalidomide formulations.

Groups	Survival time, days	
	Median	Mean
Untreated control	17	15
Thalidomide (oral)	16	16
Thal-HSA-NP	19	15
Thal-HSA-NP + PS 80	18	14

As seen in Table 10, the median and mean survival times among the groups were similar. The group treated with thalidomide given orally survived longer than other groups with mean survival of 16 days. The unmodified thalidomide-loaded HSA-NP had the highest median time of the day 19 compared to other groups. However, these differences were not significant.

Thus, thalidomide formulations did not increase survival time of tumour-bearing rats. All the animals were sacrificed after the appearance of the tumour-related illness.

### 4.3 Characterisation of poly(lactide-co-glycolide) nanoparticles

Poly(lactide-co-glycolide) nanoparticles (PLGA-NP) were produced by the precipitation solvent diffusion technique. In this study, polymers were dissolved in an organic solvent miscible with water (acetone) and dispersed in an aqueous phase containing a colloid stabiliser. The stabilisers were polyvinyl alcohol (PVA), human serum albumin (HSA), and poloxamer 188 (F68). The almost instantaneous diffusion of the organic solvent into the aqueous phase resulted in the precipitation of the copolymers as in the form of the nanoparticles. Then the solvent was evaporated.

The hydrophobic drug, 3,3'-diindolylmethane (DIM), was dissolved in acetone and added to the preparation as described above. The drug-to-polymer ratio was 1:10.

For a more homogenous nanoparticles preparation, a pump was used for the addition of the organic phase.

#### 4.3.1 Size, polydispersity, and surface charge of the nanoparticles

The physicochemical parameters of the nanoparticles are shown in Table 11. It can be seen that the size and surface charge of the nanoparticles depended on the type of a stabiliser and were not influenced by the presence of DIM. Among the preparations, the HSA-stabilised nanoparticles had the biggest size of about 330 nm and the lowest negative surface charge (-40 mV). These nanoparticles also had a slightly higher polydispersity of 0.18 - 0.15. Other nanoparticles had similar sizes of 225 - 269 nm and polydispersity of 0.03 - 0.11.

**Table 11.** Physicochemical parameters of empty and DIM-loaded PLGA nanoparticles

Stabiliser (1% w/v)	DIM conc.	Mean diameter (nm)	PD	Surface charge (mV)
	in NP suspension (mg/ml)*			
PVA	-	269.2	0.03	-20.4
	0.65	263.5	0.08	-24.2
HSA	-	333.9	0.18	-38.2
	0.71	334.7	0.15	-42.3
F68	-	225.3	0.08	-34.5
	0.67	234.2	0.11	-38.1

\* Initial DIM concentration in the reaction medium was 1 mg/ml.

### 4.3.2 Morphology of the nanoparticles

Investigation of the nanoparticle morphology was performed by scanning electron microscopy. Figure 27 shows the nanoparticles after freeze-drying which were redispersed in water. The samples were used without further purification.

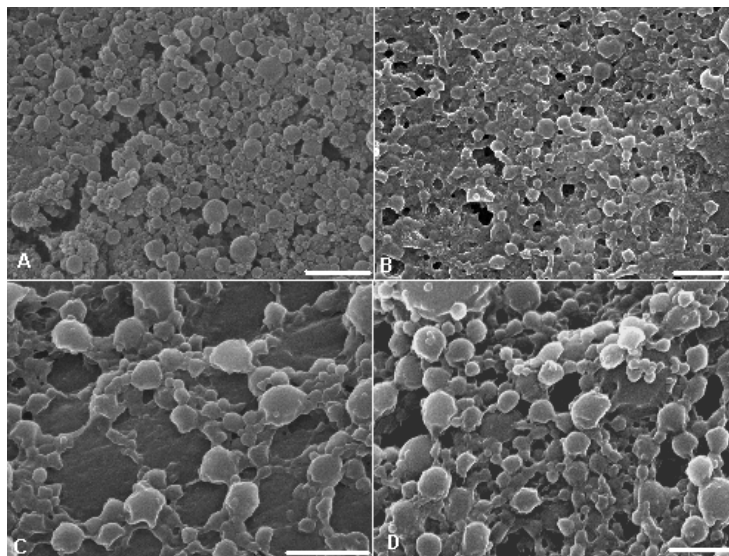


**Figure 27.** Scanning electron micrographs of PLGA nanoparticles after freeze-drying and redispersion in water: (A) empty and (B) DIM-loaded nanoparticles stabilised with PVA, (C) empty and (D) DIM-loaded nanoparticles stabilised with HSA. Bar: 1000 nm.

It can be seen that only particles stabilised with PVA had a round shape. It is obvious from Figure 27 that the preparation method applying a pump system led to the homogenous mean particle size as well as to the narrow particle size distribution. The nanoparticles stabilised with HSA were not spherical and were not always stable after reconstitution in water. No signs of DIM crystallisation were detected in the samples (Figure 27).

### 4.3.3 Drug loading

All types of the nanoparticles enhanced the content of DIM in the aqueous media, which reached 0.65 - 0.71 mg/ml (Table 11). Therefore the DIM solubility was increased 650 - 700-fold, as compared to its solubility in the aqueous solution. The drug might be entrapped and adsorbed on the nanoparticle surface. Interestingly, the nanoparticles stabilised by PVA and HSA also seemed to increase the photostability of DIM.



#### 4.3.4 Determination of maximum solubility in aqueous media

The solubility data obtained using the filter device and the shake-flask method, is displayed in Figure 28. The maximum concentration of DIM in aqueous media used in this study was  $\sim 1 \mu\text{g/ml}$ . The solubility was not influenced by pH and was similar in water, 0.01 N HCl or PBS pH 7.4 (Figure 28). The solubilities after 24 h were similar to the values obtained after 4 h.

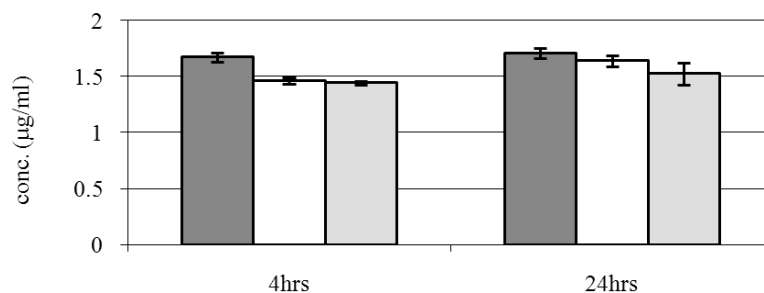


**Figure 28.** Maximum concentration solubility of DIM in water, 0.01 N HCl or phosphate buffer pH 7.4 after 4 and 24 h.

#### 4.3.5 DIM stability in organic media

The HPLC detection limit of DIM in acetone and acetonitrile was  $1.5 \mu\text{g/ml}$ . After 4 h, the solutions in acetone and acetonitrile acquired a red colour indicating the appearance of a degradation product. However, the retention time of DIM and its area under the curve values were not changed as compared to the chromatographs of the freshly prepared solutions. No extra peak was observed at either of  $15 \mu\text{g/ml}$  or  $25 \text{mg/ml}$  concentrations during 4 and 24 h or after one week. The brown flask could not protect the solution from the formation of a red-coloured product.

## 5 Discussion

### *5.1 Doxorubicin-loaded poly(butyl cyanoacrylate) nanoparticles*

The objective of this study was the in-depth evaluation of antitumour effect of doxorubicin bound to PBCA nanoparticles coated with polysorbate 80 (Dox-NP + PS 80) against 101/8 rat glioblastoma. This tumour model is an orthotopic model initially generated by the injection of  $\alpha$ -dimethylbenzanthracene into the cerebellum of Wistar rats followed by a serial transplantation of the tumour tissues into the hemisphere of Wistar rats (Yablonovskaya 1970). Thus, the rat 101/8 glioblastoma differed from other established rat brain tumour models that were generated by an injection of derivatives of nitrosourea or Rous sarcoma virus or by xenografting human glioma cell lines (Barth 1998). The 101/8 glioblastoma is characterised by a reproducible host survival time of sufficient duration to permit therapy and determination of its efficacy. Indeed, this model has been successfully applied in a variety of studies for the evaluation of experimental therapies (Steiniger 2004, Gelperina 2002, Ambruosi 2006).

The morphological evaluation of the 101/8 glioblastoma performed in this study also evidenced that the proliferation of this tumour remained at high levels throughout the host survival time. Moreover, the tumour showed a reproducible growth pattern and temporal development that is comparable to human glioblastomas. The tumours increased in size, vessel density, necrosis, and showed abundant microvascular proliferation. Furthermore, the 101/8 glioblastoma showed an invasive growth pattern with tumour cells diffusely infiltrating surrounding host brain at the edge of the solid tumour mass without signs of encapsulation. Thus the 101/8 rat glioblastoma fulfills most criteria for a valid glioma model (Barth 1998, Peterson 1994, Maggio 1996). It can also be qualified as a reliable brain tumour model for therapeutic studies besides the established models such as the F98 (Barth 1998) and 9L gliosarcoma (Weizsacker 1981), the C6 glioma (Benda 1971), and RG2 glioma (Ko 1980).

According to Professor Glatzel (Institut fuer Neuropathologie, Universtaetsklinikum Hamburg, Eppendorf), the 101/8 rat glioblastoma is the experimental rat glioblastoma that most resembles human glioblastomas (personal communication).

The effects of the therapy of this orthotopic rat glioblastoma model using Dox-NP + PS 80 and Dox-sol was evaluated by morphometric, histochemical and immunohistochemical methods. It was shown that the tumour formation was significantly reduced in the Dox-NP + PS 80 versus the Dox-sol and control groups. These data confirmed the results of the earlier study where more than 20% of the animals treated with Dox-NP + PS 80 showed the long-term remission in the same glioblastoma model (Steiniger 2004). This effect was presumably mediated by the antiangiogenic or cytotoxic effects of doxorubicin. Stan *et al.* (Stan 1999) described a dose-dependent cytotoxic effect of doxorubicin on glioma cell lines *in vitro*. These authors showed that pre-treatment of tumour cells with doxorubicin precluded tumour formation after implantation of tumour cells on the chorioallantoic membrane of embryonated hen eggs.

Moreover, treatment with doxorubicin-loaded nanoparticles showed reduced proliferation and tumour sizes when compared to treatment with doxorubicin in solution and untreated control animals. The antiproliferative effect of doxorubicin was described in organotypic multicellular spheroids of glioma cells *in vitro* (Kaaijk 1996) and also after subcutaneous implantation of rat C6 glioma cells (Van Waarde 2007). However, both are models that do not require passage through the BBB. In our study, doxorubicin in solution produced decreased proliferation of the tumour cells and reduced tumor sizes when compared to untreated controls. However, the excellent result achieved by Dox-NP + PS 80 confirms again that the enhanced transport of doxorubicin through the BBB drastically improves the drug effect against intracranial glioblastoma.

The vessel density, necrosis, and expression of VEGF were decreased and microvascular proliferation was absent in animals treated with doxorubicin-loaded nanoparticles when compared with untreated controls. Treatment with a solution of doxorubicin showed a tendency towards the decreased vessel density that was not statistically significant. At the same time, measurements of vessel density and microvascular proliferation in Dox-NP+PS 80-treated rats demonstrated that the drastic decrease of the vessel density going hand in hand with the virtual absence of microvascular proliferation. These data corroborated the results of the previous studies showing the antiangiogenic effects of doxorubicin (Bocci 2002, Zhou 2002, Straubinger 2004).

## ***5.2 Drug-loaded PBCA nanoparticles prepared in the presence of organic solvents***

The objective of this part of the study was to develop a method for the loading of water-insoluble drugs in the PBCA nanoparticles. The drug-loaded poly(alkyl cyanoacrylate) nanoparticles are generally prepared by anionic polymerization of alkyl cyanoacrylates in an aqueous acidic media in the presence of a drug. Commonly used stabilisers are dextran and/or poloxamer 188 (Vauthier 2003, Couvreur 1979). This method allows efficient loading of hydrophilic or amphiphilic drugs such as ampicillin or doxorubicin (Youssef 1988, Steiniger 2004). However, it is not obviously suitable for the encapsulation of poorly soluble drugs. Attempts to overcome this difficulty included the preparations of the particles in the ethanol-containing media (Alyautdin 1997, Beck 1994) or in the presence of cyclodextrins (Duchene 1999). While the first method is applicable only to the drugs that are soluble in ethanol and is difficult to reproduce, cyclodextrins indeed allowed to considerably increasing the encapsulation efficiency of poorly soluble substances, such as progesterone and testosterone.

In the present study, the method of the preparation was modified so that the drug-loaded PBCA nanoparticles were produced in aqueous media containing 10% (v/v) of the organic solvents. The type of solvent was chosen depending on the drug solubility.

This study shows that the presence of organic solvents did not significantly influence the morphology of the nanoparticles or their physicochemical parameters, such as the surface charge, size and polydispersity, as well as the yield of the polymer. Importantly, the solvents could be efficiently removed from the nanoparticles by evaporation under normal pressure and subsequent lyophilisation. The residual amounts of the solvents in the nanoparticles met the requirements of the European Pharmacopoeia (Eur Pharm. 5<sup>th</sup> eds.).

A high loading of loperamide of about 80% in the nanoparticles was achieved with all tested solvents. The loading capacity of the particles reached 130 - 160 µg bound drug/mg PBCA. In the study of Alyautdin *et al.* (Alyautdin 1997), where the PBCA nanoparticles were manufactured in 50% aqueous ethanol, a considerably lower encapsulation efficiency of loperamide (47%) was obtained.

The encapsulation efficiency of paclitaxel was much lower - about 25%. Therefore, the loading capacity of the particles reached only 30 - 40 µg bound drug/mg PBCA. These

parameters were considerably improved when a PEGylated phospholipid was used as a stabiliser: the encapsulation efficiency increased to 45% and the loading capacity to 55 µg/mg PBCA. This result correlates with the results of Mitra and Lin *et al.* (Mitra and Lin 2003) who also showed that the loading of paclitaxel in PBCA nanoparticles could be increased in the presence of lipids. A higher encapsulation of paclitaxel was achieved in the presence of PEG-PE. It is probably explained by a more efficient solubilisation of paclitaxel within PEG-PE micelles and/or the affinity of these micelles to the growing nanoparticle matrices.

As shown by the determination of the drug loading after freeze-drying, both, loperamide and paclitaxel, were almost fully encapsulated in the nanoparticles. The formulations contained only trace amounts of free drugs. This conclusion is further supported by the absence of the crystals in the micrographs of loperamide-loaded nanoparticles. Remarkably, by means of the nanoparticles, the content of these substances in the aqueous media for a given volume could be increased 200 - 450-fold.

### **5.2.1 Analgesic effect of loperamide-loaded in PBCA nanoparticles (tail-flick test)**

The pharmacological efficacy of the nanoparticulate formulations of loperamide was tested using a tail-flick test. Loperamide is a peripherally acting opioid receptor agonist used for the management of chronic diarrhea. This drug is a substrate of P-glycoprotein (Pgp), its lack of central opioid effects is due to the efflux activity of the Pgp at the blood-brain barrier (Upton 2007). As shown by previous studies, the PBCA nanoparticles coated with polysorbate 80 enabled the delivery of a number of drugs, including loperamide, across the blood-brain barrier. In particular, in the study of Alyautdin *et al.* (Alyautdin 1997) loperamide bound to PBCA nanoparticles coated with polysorbate 80 produced a considerable analgesic effect thus providing evidence of the CNS activity, whereas the free drug was ineffective. Similar results were obtained in the present study. However, in contrast to the study of Alyautdin *et al.* (Alyautdin 1997), loperamide bound to the non-coated nanoparticles also produced a significant analgesia, which was equally pronounced although less prolonged as compared to the polysorbate 80-coated particles (Figure 18).

Obviously, this result suggests that poloxamer 188-coated nanoparticles also enabled the delivery of loperamide across the blood-brain barrier thus inducing the CNS effect. This result correlates with the data obtained in a recent study of Petri *et al.* (Petri 2007), which provided evidence that the coating of PBCA nanoparticles with poloxamer 188 could facilitate drug delivery to the brain.

### **5.2.2 Chemotherapy of 101/8 glioblastoma using paclitaxel-loaded PBCA nanoparticles**

The natural taxan diterpenoid paclitaxel is one of the most important anticancer agents. Although it is known that paclitaxel exhibits activity against malignant glioma and brain metastases (Fellner 2002), its application for the treatment of brain tumours is limited since this drug is a substrate of Pgp and, therefore, its penetration into the CNS is not efficient. The attempts to increase the drug concentrations in the parenchyma by co-administration of the efflux pump inhibitors have been abandoned due to substantial toxicity (Fellner 2002).

As shown by the previous studies, the PBCA-NP coated with polysorbate 80 (PS 80) or poloxamer 188 (F68) could efficiently transport doxorubicin (also a Pgp substrate) across the BBB (Steiniger 2004, Ambruosi 2006, Petri 2007). The uptake of doxorubicin into the brain blood vessels endothelial cells possibly also could be assisted by the circumvention of the Pgp caused by a simultaneous release of doxorubicin and the degradation product of PBCA (polycyanoacrylic acid) at the cell membrane. An ion-pair formed by polycyanoacrylic acid and doxorubicin could enable passage of doxorubicin across the cell membrane without being recognized by P-glycoprotein (Verdiere 1997). Moreover, in the case of brain tumour, the penetration of the nanoparticles into the tumour could be enhanced due to a higher permeability of the BBB at the tumour site (EPR effect).

Therefore, in the present study, it was also assumed that loading of paclitaxel in the surface-modified PBCA-NP would increase the drug therapeutic effect against glioblastoma.

To evaluate paclitaxel delivery to the brain, three paclitaxel-loaded nanoparticle formulations including the unmodified nanoparticles and particles coated with surfactants (polysorbate 80 or poloxamer 188) were tested against 101/8 human glioblastoma implanted in rats. The

effect of the nanoparticulate formulations was compared to that of a paclitaxel solution. Untreated rats were used as control.

The recommended dose of paclitaxel against human glioblastoma is 140 mg/m<sup>2</sup> (Fetell 1997, FDA) which corresponds to the rat dose of about 17.80 mg/kg. However, due to the low loading of paclitaxel to nanoparticles, this dose could not be administered. Therefore, the same dose regimen as doxorubicin was used for the chemotherapy of 101/8 glioblastoma. Thus the treatment regimen was 3 × 1.5 mg/kg on days 2, 5, and 8 post-tumour implantation (total dose was 4.5 mg/kg). None of the formulations containing paclitaxel could improve survival time compared to the control groups. Since the cytotoxic effect of paclitaxel depends on two important factors – the dose and duration of exposure, this lack of efficacy in the present experiment is most probably explained by the low dose and short treatment course. Indeed, in the study performed by Xu *et al.* (Xu 2005) the antitumour effect of the nanoparticle-bound paclitaxel in mice was achieved at a much more intensive treatment regimen of 5 × 20 mg/kg/day. The effect of the paclitaxel conjugate with Angiopep-2 (an aprotinin-derived peptide) against intracerebral U87 MG glioblastoma was also achieved after injection of the dose of 5 × 25 mg/kg (Regina 2008).

### ***5.3 Human serum albumin nanoparticles***

#### **5.3.1 Covalent linkage of Apolipoprotein A-I and B-100 to human serum albumin nanoparticles**

Previously it was believed that apolipoprotein E and to a minor extent apolipoprotein B play a crucial role in the delivery of the drugs to the brain by nanoparticles (Kreuter 2002). Both apolipoproteins bind to lipoprotein receptors including low-density lipoprotein receptor or LDL-R (Knott 1986, De Loof 1986, Kreuter 2004) and lipoprotein receptor-related protein, LRP (Dergunov 2004, Croy 2004). Moreover, the LDL-R is up-regulated on the brain endothelium compared to peripheral vessels (Dehouck 1997, Lucarelli 2002, Vasile 1983, Meresse 1989), and lipoprotein particles appeared to be transported across the BBB by transcytosis (Dehouck 1997). As a consequence, it was hypothesized that the nanoparticles with adsorbed or covalently attached apolipoprotein B or E mimic lipoprotein particles, and

that this represented the exclusive or at least dominating mechanism of the nanoparticle-mediated drug transport across the BBB.

Indeed, the results of the present study corroborate the previous observation. The apolipoproteins B or E attached to the particle surface serve as vectors trafficking nanoparticles to the brain, thus providing the analgesic effect of the otherwise CNS-inactive drug (Kreuter 2002, Michaelis 2006). Furthermore, as evidenced by a pharmacological response, the brain delivery of loperamide also could be mediated by apolipoprotein A-I. However, the mechanism of its interaction with the brain vessel endothelial cells is different and it occurs *via* a different receptor. Apolipoprotein A-I is one of the major components of high density lipoproteins (HDL), whose function is to transfer cholesterol between cells and other lipoproteins. This transfer is facilitated *via* highly specific interaction of HDL with the scavenger receptor class B type I (SR-BI) located at the BBB (Krieger 1999, Petri 2007, Balazs 2004). It is, therefore, possible that drug delivery to the brain by HSA nanoparticles is enabled by the interaction of apolipoprotein A-I attached to these particles with the SR-BI expressed by the brain vessels endothelial cells.

Interestingly, the results of the present study correlate with the study about the interaction of lipid drug conjugate (LDC) nanoparticles with the brain vessels endothelial cells which considerable amounts of apolipoprotein A-I were found to be adsorbed on their surface from the blood (Gessner 2001).

### 5.3.2 Thalidomide bound to HSA nanoparticles

In this part of the study, the therapeutic potential of thalidomide bound to the HSA nanoparticles for the therapy of rats with intracranially implanted glioblastomas was investigated. The accumulation of albumin in solid tumours forms the rationale for developing the albumin-based drug delivery systems for tumour targeting. Albumin accumulates in malignant tissue due to two major reasons: Firstly, albumin is a major energy and nutrition source for the tumour growth (Stehle 1997). Secondly, penetration of albumin into the tumour could be enhanced due to the leaky capillaries feeding the tumour and defective lymphatic drainage system (EPR effect). The tumour uptake of albumin can be



easily visualised by injecting the Evans Blue dye that binds rapidly and tightly to circulating albumin and makes the tumour turn blue within few hours post injection.

Recently, a methotrexate-albumin conjugate, an albumin-bound prodrug of doxorubicin, i.e, the (6-maleimido)caproylhydrazone, and paclitaxel bound to albumin nanoparticles (Abraxane) have been evaluated clinically. Specifically, Abraxane has been approved for treating metastatic breast cancer. Additionally, the biodegradability, lack of toxicity, and immunogenicity of denatured albumin makes it an ideal candidate for drug delivery ([Kratz 2008](#)).

Thalidomide is a known teratogenic agent which induces the inhibition of the blood vessel growth in the development of fetal limb buds. The mechanism of action of thalidomide is complex and it probably includes different molecular targets. The inhibition of angiogenesis by interrupting processes mediated by bFGF and/or vascular endothelial growth factor (VEGF) is one of the prominent thalidomide mechanisms of action ([Eleutherakis-Papaiakovou 2004](#)). The effect of thalidomide on the glioma and glioblastoma as highly vascularised tumours that overexpress angiogenic factors provides the rationale for the evaluation of antiangiogenic effect of thalidomide-loaded nanoparticles. Since antiangiogenic action of doxorubicin loaded nanoparticles was indicated by the histological investigations (section 5.1) the loading of nanoparticles with thalidomide appeared as a rational strategy. However, monotherapy of brain tumours using thalidomide seems to be not effective. As shown by the results of three phase II trials including patients with recurrent glioma, astrocytoma or glioblastoma multiforme thalidomide was generally well tolerated but objective responses were rare ([Papaiakovou 2004](#)). The daily dose was from 100 to 1200 mg.

Similarly, in our study, thalidomide bound to HSA nanoparticles had exerted no effect on the prolongation of the survival times in the rats bearing glioblastoma, as compared to the untreated animals. There was also no improvement in the group treated with polysorbate 80-coated nanoparticles. The treatment regimen in our study was  $3 \times 1$  mg/kg on days 2, 5, and 8 post-tumour implantation (the total dose was 3 mg/kg). The poor results in the thalidomide groups treated orally suggest that the dose level and the dosing regimen were not adequate.

### 5.4 DIM loaded in PLGA nanoparticles

Poly (lactide-co-glycolide) nanoparticles (PLGA-NP) are a biodegradable polymeric system has a good CNS biocompatibility. Kreuter *et al.* (Kreuter 2008) have recently shown that doxorubicin loaded in the PLGA nanoparticles coated with poloxamer 188 have promising effects for the treatment of brain tumours. Treatment of 101/8 glioblastomas with this formulation yielded 40% of long term survivors.

In the present study, a carcinogenesis inhibitor, diindolylmethane (DIM; Figure 29), was loaded to PLGA-NP. DIM is a cruciferous indole which exhibits a potential cancer-protective effect especially in estrogen-related conditions (Chen 1998). The active agent, DIM, is derived from the digestion of indole-3-carbinol, found in Brassica vegetables such as broccoli and cauliflower.

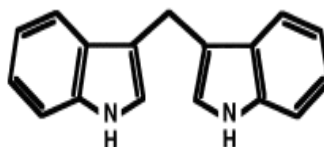


**Figure 29.** Structure of 3-(1H-Indol-3-ylmethyl)-1H-indole, 3,3'-Diindolylmethane (DIM).

Because of its various potent anticancer properties, the National Cancer Institute of the United States has begun clinical trials of DIM as a therapeutic treatment for numerous forms of cancer. It is currently being used as a part of treatment for tumours in the upper respiratory tracts caused by the Human Papilloma Virus. The disadvantage of DIM is its very low solubility in water. Moreover, this substance is sensitive to light and forms highly-coloured degradation products which do not affect the efficacy of the final formulation but they are unfavourable for its appearance.

The nanoparticles were prepared by the nanoprecipitation method. The preparation of the nanoparticles by using a pump for the addition of the organic phase (1 ml/min) yielded relatively homogeneous preparations with reproducible characteristics, whereas manual addition of the organic phase resulted in the variability in size of the nanoparticles for the same preparation procedure. Encapsulation of DIM in PLGA-NP appears to be a suitable formulation approach that enables a >600-fold increase of DIM content in aqueous media and can increase DIM photostability.

## **6 Conclusion**

### ***6.1 Antiangiogenic effects of doxorubicin-loaded poly(butyl cyanoacrylate) nanoparticles***

Immunohistology showed that the rat 101/8 glioblastoma is a valid brain tumour model with morphologic characteristics of human glioblastoma. The intravenous treatment with doxorubicin-loaded polysorbate 80-coated nanoparticles reduced tumour formation, tumour size, and proliferation of tumour cells. Importantly, the intratumoural vessel density and necrosis were drastically reduced and microvascular proliferations were absent pointing to antiangiogenic effects of doxorubicin. This study confirms the promise of nanoparticles in the delivery of compounds to the central nervous system. Furthermore, it indicates that the growth-retarding effect of doxorubicin on gliomas may be attributed to antiangiogenic effects.

### ***6.2 Encapsulation of water-insoluble drugs in poly(butyl cyanoacrylate) nanoparticles***

The preparation of poly(butyl cyanoacrylate) nanoparticles by anionic polymerization in aqueous-organic media appeared to be a suitable method for encapsulation of water-insoluble substances. Among other techniques, this method based on rapidly biodegradable nanoparticles may serve as a formulation approach for “difficult” substances, clinical application of which is hampered by low solubility.

Paclitaxel-loaded poly(butyl cyanoacrylate) nanoparticles showed no improvement in the increasing survival times of glioblastoma implanted rats. Increasing the dose or combining it with other potent anticancer formulations could be beneficial.

### ***6.3 Covalent attachment of apolipoprotein A-I and apolipoprotein B-100 to albumin nanoparticles enables drug transport into the brain***

The present investigation demonstrates that the delivery of drugs to the brain with nanoparticles is at least partly associable with the apolipoprotein E and B pathway. The drug delivery to brain may also be augmented by the interaction of apolipoprotein A-I covalently attached to these nanoparticles with the scavenger receptor SR-BI located at the blood-brain barrier.

Consequently, these results demonstrate the existence of more than one possible interaction mechanism of nanoparticles with the brain endothelium and the followed by delivery of drugs to the CNS.

### ***6.4 Thalidomide bound to human serum albumin nanoparticles***

The thalidomide content in the aqueous phase was increased 8-fold as compared to its aqueous solution due to the drug binding to the nanoparticles. However, the *in vivo* response to thalidomide HSA-NP formulation against *glioblastoma multiforme* of orally administered thalidomide was not improved, as compared to an equal dose. It is known that thalidomide has no immediate antiangiogenic or antiproliferative effect. Higher dosing parallel to early administration of thalidomide in combination with other potent cytostatic agents such as doxorubicin may be a new strategy for the glioblastoma treatment.

### ***6.5 Encapsulation of diindolylmethane in poly(lactide-co-glycolide) nanoparticles***

The preparation of DIM-loaded nanoparticles by precipitation yielded nanoparticles with a narrow size distribution. The encapsulation of DIM in PLGA-NP appears to be a suitable formulation approach that enables a >600-fold increase of DIM content in aqueous media and can prevent DIM from unfavourable colour changing in the formulation.

## **7 Summary**

Many highly active antitumour agents are currently not employable for the systemic chemotherapy of brain tumours since their entrance into the brain is blocked by the BBB. Obviously, the development of a strategy allowing effective delivery of these agents across the BBB would enormously extend the potential of the systemic chemotherapy.

### **Chemotherapy of rat glioblastoma using nanoparticle-bound doxorubicin**

Doxorubicin bound to polysorbate-coated nanoparticles had been previously shown to significantly enhance survival in the orthotopic rat 101/8 glioblastoma model. The objective of this study was to investigate the therapeutic effects of this formulation by morphometric, histological and immunohistological methods.

The 101/8 glioblastoma was implanted intracranially into the male Wistar rats. The animals were randomly divided into 3 groups; one group served as untreated control (n = 20). The second group received doxorubicin in solution (Dox-sol, n = 18), and the third group received doxorubicin bound to PBCA nanoparticles coated with PS 80 (Dox-NP + PS 80, n = 18). The treatment regimen was  $3 \times 1.5$  mg/kg on days 2, 5, and 8 after tumor implantation. The formulations were injected into the tail vein.

The untreated control animals were sacrificed on days 6, 8, 10, 12, and 14 after the implantation. The animals that had received chemotherapy were sacrificed on day 10, 14 and 18 after the implantation. The brains were investigated by morphometrical, histochemical, and immunohistochemical methods such as the measurement of the tumor size, proliferation of tumor cells, vessel density, expression of glial fibrillary acidic protein (GFAP), expression of vascular endothelial growth factor (VEGF), incidence and dimension of necrosis, and microvascular proliferation.

Tumours showed signs of malignancy including invasion to brain tissue and brisk mitotic activity. The tumor proliferation remained stable at high levels throughout the host survival time. Overall, the tumor showed a reproducible growth pattern and temporal development that is comparable to human glioblastoma. Furthermore, the 101/8 glioblastoma had infiltrated diffusely the surrounding host brain at the edge of the solid tumor mass showed no signs of encapsulation. Thus the 101/8 glioblastoma fulfills the most criteria for an adequate glioma model and can be qualified as a reliable model.

Dox-NP + PS 80 produced a pronounced antitumour effect which exhibited as a reduced tumour size, lower proliferation, and a decreased necrotic area compared to Dox-sol and to untreated control groups. This result correlates with the results of the earlier study (Steiniger 2004) where more than 20% of the animals treated with the same nanoparticles showed a long-term remission in the same glioblastoma model. The treatment effect of the nanoparticles was also exhibited as impaired vascular density, decrease in the expression of the VEGF and lack of microvascular proliferation in the 101/8 glioblastoma model when compared to the solution of doxorubicin (Dox-sol) and the untreated animals (control). A drastic effect of Dox-NP + PS 80 on vascularisation was presumably mediated by antiangiogenic or cytotoxic effects of doxorubicin.

### **Encapsulation of water-insoluble drugs in poly(butyl cyanoacrylate) nanoparticles**

Development of the parenteral formulations of the poorly water soluble drugs is considered to be a challenging task. These drugs can be solubilized in non-aqueous solutions composed entirely of organic solvent(s), which are usually but not always diluted prior to administration (Strickley 2004). Many of these currently used excipients are not inert vehicles and could exert a range of intrinsic adverse effects and have the potential to cause clinically significant drug interactions.

The nanoparticle technology represents a promising approach to enhance the content of these drugs in the aqueous media and may optimize their in-vivo performance.

In this study, the effectiveness of this approach was investigated using poly(butyl cyanoacrylate) nanoparticles and two hydrophobic drugs, loperamide and paclitaxel. For this purpose, the standard method of the preparation of these particles was modified so that the drug-loaded PBCA nanoparticles were produced in aqueous media containing 10% (v/v) of the organic solvents. The type of solvent was chosen depending on the drug solubility.

The nanoparticles were produced by anionic polymerization of n-butyl-2-cyanoacrylate in aqueous-organic media in the presence of a drug. The particles were stabilized by dextran 70,000 and poloxamer 188 or by 1,2-dioleoyl-sn-glycero-3-phosphoethanolamine-N-[methoxy(polyethylene glycol)-5000] sodium salt. The polymerization media consisted of a solution of stabilizers/surfactants in a mixture of 0.01 N HCl and an appropriate organic solvent (1 : 9). The presence of the organic solvents in the polymerization medium did not

considerably influence the physicochemical parameters of the empty nanoparticles. It was shown that in the presence of dichloromethane, methanol, or ethanol the encapsulation efficiency of loperamide in the nanoparticles reached 80%. The loperamide-loaded nanoparticles were coated additionally with 1% polysorbate 80. The analgesic effect of these formulations (with or without PS 80 coating) was measured in vivo using the tail-flick test, as described in the paper of Alyautdin *et al.* (Alyautdin 1997). The loperamide solution was chosen as a control formulation. Loperamide is a substrate of P-glycoprotein (Pgp), its lack of central opioid effects is due to the efflux activity of the Pgp at the blood-brain barrier (Upton 2007).

As expected, the loperamide solution was ineffective of exerting the central analgesic effect, whereas the polysorbate 80-coated nanoparticles as well as the non-coated nanoparticles produced considerable analgesia, providing the evidence of the CNS activity. However, the central analgesic effect of the nanoparticles without coating did not last as long as with the coated nanoparticles. Similar results were obtained in the study of Alyautdin *et al.* (Alyautdin 1997) and Petri *et al.* (Petri 2007). Obviously, this result suggests that the presence of poloxamer 188 in nanoparticles also enabled the drug delivery of across the blood-brain barrier thus inducing the CNS effect of loperamide.

The paclitaxel loading in the PBCA-NP in the presence of dextran/poloxamer 188 as a mixture of stabilizers, was low (~ 25%). The maximum loading was achieved in the presence of the lipid (~ 45%) which lead to an encapsulation efficacy of 55 µg/mg PBCA. This result correlated with the results of Mitra and Lin *et al.* (Mitra and Lin 2003) and is due to more efficient solubilisation of paclitaxel within PEG-PE micelles and/or the affinity of these micelles to the growing nanoparticle matrices.

Paclitaxel also is a substrate of Pgp and, therefore, its penetration into the CNS after systemic administration is not efficient. The objective of this study was to investigate if the PBCA-NP coated with polysorbate 80 (PS 80) or poloxamer 188 (F68) were able to deliver paclitaxel across the BBB. As shown by the previous studies, these NP could efficiently transport doxorubicin (also a Pgp substrate) across the BBB (Steiniger 2004, Ambruosi 2006, Petri 2007). Moreover, in the case of brain tumour, the penetration of the nanoparticles into the tumour could be enhanced due to a higher permeability of the BBB at the tumour site.

Therefore, the antitumour efficacy of three formulations of paclitaxel including: paclitaxel bound to PBCA nanoparticles (PXL-NP), PXL-NP coated with polysorbate 80 (PXL-NP + PS 80) and PXL-NP coated with poloxamer 188 (PXL-NP + F68) was tested in glioblastoma 101/8-bearing rats. Untreated glioblastoma-bearing rats and the animals treated with the paclitaxel solution (PXL) were used as controls.

Due to the low loading of paclitaxel in the nanoparticles, the recommended dose of paclitaxel against glioblastoma, which is 17.80 mg/kg (Fetell 1997, FDA), could not be administered. Therefore, the paclitaxel formulations were administered in the same dose regimen as doxorubicin: 3 x 1.5 mg/kg on days 2, 5, and 8 post tumour implantation. None of the formulations containing paclitaxel could improve the survival time compared to the control groups. This lack of efficiency is thought to be due to the low drug dosage and the short duration of the treatment course.

### **Covalent attachment of apolipoprotein A-I and apolipoprotein B-100 to albumin nanoparticles enabled drug transport into the brain**

Apolipoproteins A-I and B-100 were covalently attached to the HSA nanoparticles *via* the NHS-PEG-Mal 3400 linker. Loperamide as a model drug was bound to these nanoparticles, and the antinociceptive reaction of these preparations was recorded after intravenous injection in mice by the tail-flick test. After 15 min, both nanoparticle preparations with the coupled apolipoproteins A-I and B-100 yielded considerable antinociceptive effects which lasted over 1 h. The maximally possible effects (MPE) of these preparations reached 65% and 50%, respectively, and were statistically different from the controls (loperamide loaded to unmodified nanoparticles and loperamide solution). The loperamide solution achieved no effect. This result demonstrates that more than one mechanism is involved in the interaction of nanoparticles with the brain endothelial cells and the resulting delivery of drugs to the central nervous system: while Apo B can transport the drug across the BBB via binding to the lipoprotein receptor expressed at the BBB, Apo A-I enables this transport via the scavenger receptor SR-BI also located at the BBB.



### **Thalidomide bound to human serum albumin nanoparticles**

Thalidomide, an antiangiogenic drug, has poor solubility in water and, so far, is administered only orally, although parenteral administration would be desirable in certain clinical situations such as impaired intestinal absorption or chemotherapy-induced nausea hampering drug intake.

The objective of the present study was to develop an injectable formulation of thalidomide based on the HSA nanoparticles (HSA-NP). As previously reported, the solubility of the free drug (a mixture of enantiomers) in water and 5% glucose solution was only 52 and 70 µg/ml, respectively (Eriksson 2000). It was shown that binding of thalidomide to these nanoparticles enabled a 8-fold increase of the drug content in the water phase which reached 400 µg Thal/ml NP suspension.

In this study, the influence of water soluble organic solvents/surfactants on the solubility of thalidomide also has been studied. The solvents included 5% glucose solution, 10% polysorbate 80, 10% poloxamer 188, Cremophor<sup>®</sup> EL - ethanol (51:49). Thalidomide was used in a form of racemate (a mixture of two enantiomers). In neither of the above mentioned solvents, the solubility of thalidomide could exceed the content of thalidomide in the nanoparticle formulation.

The antitumour efficacy of the unmodified thalidomide-loaded HSA-NP (Thal-HSA-NP) and Thal-HSA-NP coated with 1% polysorbate 80 (Thal-HSA-NP + PS 80) was evaluated in the glioblastoma 101/8-bearing rats. The effect of these formulations was compared to orally administered thalidomide. Untreated animals were used as control. The nanoparticle formulations were injected into the tail caudal vein. Thalidomide bound to HSA nanoparticles exerted no effect on the prolongation of the survival times in the rats bearing the glioblastoma, as compared to the untreated animals. There was also no improvement in the group treated with the polysorbate 80-coated nanoparticles. The poor results in the thalidomide groups treated orally suggest that the dose level and the dosing regimen were not adequate.

### **Encapsulation of diindolylmethane in poly(lactide-co-glycolide) nanoparticles**

3,3'-Diindolylmethane (DIM) is a cruciferous indole which exhibits a potential cancerprotective effect especially in estrogen-related conditions (Chen 1998). The

## Summary

disadvantage of DIM is its very low solubility in water. Moreover, this substance is sensitive to light and forms highly coloured degradation products that, however, do not affect the efficacy of the final formulation but are unfavorable for the appearance. The objective of the present study was to investigate the feasibility of increasing DIM contents in the aqueous phase as well as its photostability by encapsulation in poly(lactide-co-glycolide) nanoparticles (PLGA-NP).

Encapsulation of DIM in PLGA-NP appeared to be a suitable formulation approach that enabled a > 600 fold increase of the DIM content in aqueous media and could prevent DIM from unfavorable color changing in the formulation.

## 8 References

- Abbott NJ, Romero A. Transporting therapeutics across the blood-brain barrier. *Mol Med Tod.* 2, 106 - 113 (1996).
- Alyautdin R, Gothier D, Petrov V, Kharkevich D, Kreuter J. Analgesic activity of the hexapeptide dalargin adsorbed on the surface of polysorbate 80-coated poly(butylcyanoacrylate) nanoparticles. *Eur J Pharm Biopharm.* 41, 44 - 48 (1995).
- Alyautdin R, Petrov VE, Langer K, Berthold A, Kharkevich DA, Kreuter J. Delivery of loperamide across the blood-brain barrier with polysorbate 80-coated polybutylcyanoacrylate nanoparticles, *Pharm. Res.* 14, 325 - 328 (1997).
- Alyautdin RN, Tezikov EB, Ramege P, Kharkevich DA, Begley DJ, Kreuter J. Significant entry of tubocurarine into the brain of rats by absorption to polysorbate 80-coated polybutyl-cyanoacrylate nanoparticles: an in situ brain perfusion study, *J. Microencapsul.* 15, 67 - 74 (1998).
- Alyautdin R, Reichel A, Loebenberg R, Ramege P, Kreuter J, Begley D. Interaction of poly(butylcyanoacrylate) nanoparticles with the blood-brain barrier in vivo and in vitro. *J Drug Targeting.* 9, 209 - 221 (2001).
- Ambruosi A, Yamamoto H, Kreuter J. Body distribution of polysorbate-80 and doxorubicin-loaded [14C] poly(butyl cyanoacrylate) nanoparticles after *i.v.* administration in rats, *J Drug Target.* 13, 535 - 42 (2005).
- Ambruosi A, Gelperina S, Khalansky A, Tanski S, Theisen A, Kreuter J. Influence of surfactants, polymer and doxorubicin loading on the anti-tumour effect of poly(butyl cyanoacrylate) nanoparticles in a rat glioma model. *J Microencapsul.* 23,582 - 92 (2006a).
- Ambruosi A, Khalansky AS, Yamamoto H, Gelperina SE, Begley DJ, Kreuter J. Biodistribution of polysorbate 80-coated doxorubicin-loaded [14C]-poly(butyl cyanoacrylate) nanoparticles after intravenous administration to glioblastoma-bearing rats. *J Drug Target.* 14, 97 - 105 (2006b).
- Araujo L, Löbenberg R, Kreuter J. Influence of the surfactant concentration on the body distribution of nanoparticles, *J Drug Target* 5, 373 - 385 (1999).

## References

- Balazs Z, Panzenboeck U, Hammer A, Sovic A, Quehenberger O, Malle E, Sattler W. Uptake and transport of high-density lipoprotein (HDL) and HDL-associated alpha-tocopherol by an *in vitro* blood-brain barrier model, J Neurochem. 89, 939 - 950 (2004).
- Barraud L, Merle P, Soma E, Lefrancois L, Guerret S, Chevallier M, Dubernet C, Couvreur P, Trepo C, Vitvitski L. Increase of doxorubicin sensitivity by doxorubicin-loading into nanoparticles for hepatocellular carcinoma cells *in vitro* and *in vivo*. J Hepatol. 42, 736 - 743 (2005).
- Barth RF. Rat brain tumour models in experimental neuro-oncology: The 9L, C6, T9, F98, RG2 (D74), RT-2 and CNS-1 gliomas. J Neurooncology. 36, 91 - 102 (1998).
- Bart J, Groen HJ, Hendriks NH, van der Graaf WT, Wallburg W, de Vries EG. The blood-brain barrier and oncology: new insights into function and modulation. Cancer Treat Rev. 26, 449-62 (2000).
- Batrakova EV, Li S, Alakhov VY, Miller DW, Kabanov AV. Optimal structure requirements for pluronic block copolymers in modifying P-glycoprotein drug efflux transporter activity in bovine brain microvessel endothelial cells. Pharm Res. 20, 1581 - 90 (2003).
- Batrakova EV, Li S, Vinogradov SV, Alakhov VY, Miller DW, Kabanov AV. Mechanism of pluronic effect on P-glycoprotein efflux system in blood- brain barrier: contributions of energy depletion and membrane fluidization. J Pharmacol Exp Ther. 299, 483–493 (2001).
- Beck PH, Kreuter J, Müller W.E.G, Schatton W. Improved Peroral Delivery of Avarol with Polybutylcyanoacrylate Nanoparticles, Eur J Pharm Biopharm. 40, 134 - 137 (1994).
- Begely DJ. The blood-brain barrier: principles for targeting peptides and drugs to the central nervous system. J Pharm Pharmacol. 48, 136 – 146 (1996).
- Begley DJ, Bradbury MW, Kreuter J. The blood-brain barrier and drug delivery to the CNS. M. Dekker, New York, 205 - 223 (2000).
- Begley DJ. Understanding and circumventing the blood-brain barrier. Acta Paediatr Suppl. 92, 83 - 91(2003a).

## References

- Begley DJ, Brightman MW. Structural and functional aspects of the blood-brain barrier. Review, *Prog Drug Res.* 61, 39 - 78 (2003b).
- Begley DJ. Delivery of therapeutic agents to the central nervous system: the problems and the possibilities, *Pharmacol Ther.* 104, 29 - 45 (2004).
- Benda P, Someda K, Messer J, Sweet WH. Morphological and immunochemical studies of rat glial tumours and clonal strains propagated in culture. *J Neurosurg.* 34, 310 - 323 (1971).
- Bocci G, Nicolaou KC, Kerbel RS. Protracted low-dose effects on human endothelial cell proliferation and survival in vitro reveal a selective antiangiogenic window for various chemotherapeutic drugs. *Cancer Res.* 62, 6938 - 6943 (2002).
- Bonstelle CT, Kori SH, Rekaite H. Intracarotid chemotherapy of glioblastoma after induced blood-brain barrier disruption. *AJNR Am J Neuroradiol.* 4, 810 - 2 (1983).
- Bootz A, Vogel V, Schubert D, Kreuter J. Comparison of scanning electron microscopy, dynamic light scattering and analytical ultracentrifugation for the sizing of poly(butyl cyanoacrylate) nanoparticles, *Eur. J. Pharm. Biopharm.* 57, 369 - 375 (2004).
- Bootz A, Russ T, Gores F, Karas M, Kreuter J. Molecular weights of poly(butyl cyanoacrylate) nanoparticles determined by mass spectrometry and size exclusion chromatography, *Eur J Pharm Biopharm.* 60,391 - 9 (2005).
- Borchard G, Audus KL, Shi F, Kreuter J. Uptake of surfactant-coated poly(methyl methacrylate)-nanoparticles by bovine brain microvessel endothelial cell monolayers. *Int J Pharm.* 110, 29 - 35 (1994).
- Bozikir A, Saka OM. Formulation and investigation of 5-FU nanoparticles with factorial design-based studies. *Il Farmaco.* 60, 840 - 846 (2005).
- Brandes AA, Pasetto LM, Monfardini S. New drugs in recurrent high grade gliomas. *Anticancer Res.* 20, 1913 - 20 (2000).
- Brigger I, Morizet J, Aubert G, Chacun H, Terrier-Lacombe M-J, Couvreur P, Vassal G. Poly(ethylene glycol)-coated hexadecylcyanoacrylate nanospheres display a combined effect for brain tumour targeting. *J Pharmacol Exp Ther.* 303, 928 - 936 (2002).

## References

- Brightman MW, and Reese TS. Junctions between intimately apposed cell membranes in the vertebrate brain. *J. Cell Biol.* 40, 648 - 677 (1969).
- Brown VI, Greene MI. Molecular and cellular mechanisms of receptor-mediated endocytosis. *DNA Cell Biol.* 10, 399 - 409 (1991).
- Bullock k, Blackwell K. Clinical efficacy of taxane-trastuzumab combination regimens for HER-2-positive metastatic breast cancer. *Oncol.* 13, 515 - 525 (2008).
- Calvo P, Gouritin B, Chacun H, Desmaele D, D'Angelo J, Noel J-P, Georgin D, Fattal E, Andreux JP, Couvreur P. Long-circulating PEGylated polycyanoacrylate nanoparticles as new drug carrier for brain delivery. *Pharm Res.* 18, 1157 - 1166 (2001).
- Chen DB, Yang TZ, Lu WL, Zhang Q. In vitro and in vivo study of two types of long-circulating solid lipid nanoparticles containing paclitaxel. *Chem Pharm Bull.* 49, 1444 - 1447 (2001).
- Chen H, Gaul F, Guo D, Maycock A. Determination of loperamide in rat plasma and bovine serum albumin by LC, *J. Pharm. Biomed. Anal.* 22, 555 - 561 (2000).
- Chen I, McDougal, Wang F, Safe S. Aryl hydrocarbonreceptor-mediated antiestrogenic and antitumorigenic activity of diindolylmethane. *Carcinogenesis.* 19, 1631-1639 (1998).
- Cordon-Cardo C, O'Brien JP, Casals D, Rittman-Grauer L, Biedler JL, Melamed MR, Bertino JR. Multidrug-resistance gene (P-glycoprotein) is expressed by endothelial cells at blood-brain barrier sites. *Proc Natl Acad Sci.* 86, 695 - 8 (1989).
- Couvreur P, Kante B, Roland M, Guiot P, Bauduin P, Speiser P. Polycyanoacrylate nanocapsules as potential lysosomotropic carriers: preparation, morphological and sorptive properties, *J. Pharm. Pharmacol.* 31, 331 - 332 (1979).
- Couvreur P, Kante B, Grislain L, Roland M, Speiser P. Toxicity of polyalkylcyanoacrylate nanoparticles II: Doxorubicin-loaded nanoparticles. *J Pharm Sci,* 71, 790 - 792 (1982).
- Couvreur P, Grislain L, Lenaerts V, Brasseur F, Guiot P, Biernacki A. Biodegradable polymeric nanoparticles as drug carrier for antitumour agents. In: *Polymeric Nanoparticles and Microspheres*, Guiot P, Couvreur P (Eds), CRC Press, Boca Raton, 27 - 93 (1986).

## References

- Croy J. E, Brandon T, Komives E. A. Two apolipoprotein E mimetic peptides, ApoE (130 - 149) and ApoE (141 - 155)<sub>2</sub>, bind to LRP1, *Biochemistry*. 43, 7328 - 7335 (2004).
- Cucullo L, Aumayr B, Rapp E, Damir J. Drug delivery and in vitro models of the blood-brain barrier, *Curr Opin Drug Discov Devel*. 8, 89 - 99 (2005).
- Damascelli B, Cantu G, Mattavelli F, Tamplenizza P, Bidoli P, Leo E, Dosio F, Cerrotta AM, Di Tolla G, Frigerio LF, Garbagnati F, Lanocita R, Marchiano A, Patelli G, Spreafico C, Ticha V, Vespro V, Zunino F. Intraarterial chemotherapy with polyoxyethylated castor oil free paclitaxel, incorporated in albumin nanoparticles (ABI-007): Phase II study of patients with squamous cell carcinoma of the head and neck and anal canal: preliminary evidence of clinical activity. *Cancer*. 92, 2592 - 2602 (2001).
- Damascelli B, Patelli GL, Lanocita R, Di Tolla G, Frigerio LF, Marchiano A, Garbagnati F, Spreafico C, Ticha V, Gladin CR, Palazzi M, Crippa F, Oldini C, Calo S, Bonaccorsi A, Mattavelli F, Costa L, Mariani L, Cantu G. A novel intraarterial chemotherapy using paclitaxel in albumin nanoparticles to treat advanced squamous cell carcinoma of the tongue: preliminary findings. *AJR Am J Roentgenol*. 181, 253 - 260 (2003).
- Davis SS, Illum L. Colloidal delivery systems. Opportunities and challenges. In Tomlinson, E and Davis S S Eds. Site -Specific Drug delivery, Wiley, 93 - 110 (1986).
- De Angelis LM. Brain tumours. *N Engl J Med*. 344, 114 - 23 (2001).
- De Loof H, Rosseneu M, Brasseur R, Ruyschaert JM. Use of hydrophobicity profiles to predict receptor binding domains on apolipoprotein E and the low density lipoprotein apolipoprotein B-E receptor, *Proc. Natl. Acad. Sci*. 83, 2295 - 2299 (1986).
- Dehouck B, Fenart L, Dehouck M.P, Pierce A, Torpier G, Cecchelli R. A new function for the LDL receptor: Transcytosis of LDL across the blood-brain barrier, *J. Cell Biol*. 138, 877 - 889 (1997).

## References

- Dergunov AD. Apolipoprotein E structure and substrate and receptor-binding activities of triglyceride-rich human plasma lipoproteins in normo- and hypertriglyceridemia. *Biochemistry*. 69, 720 - 737(2004).
- Donelli MG, Zucchetti M, D'Incalci M. Do anticancer agents reach the tumor target in the human brain? *Cancer Chemother Pharmacol*. 30, 251 - 60 (1992).
- Dreis S, Rothweiler F, Michaelis M, Cinatl J Jr, Kreuter J, Langer K. Preparation, characterisation and maintenance of drug efficacy of doxorubicin-loaded human serum albumin (HSA) nanoparticles. *Int J Pharm*. 341, 207 - 14 (2007).
- Duchene D, Ponchel G, Wouessidjewe D. Cyclodextrins in targeting. Application to nanoparticles. *Adv. Drug Deliv. Rev*. 36, 29 - 40 (1999).
- Duncan R, Dimitrijevic S, Evagorou EG. The role of polymer conjugated in the diagnosis and treatment of cancer, *STP Pharma Sci*. 6, 237 - 263 (1996).
- Eleutherakis-Papaiakovou V, Bamias A, Dimopoulos MA. Thalidomide in cancer medicine, *Annals of Oncology*. 15, 1151 - 1160 (2004).
- Eriksson T , Bjoerkman S, Roth B, Hoeglund P. Intravenous Formulations of the Enantiomers of thalidomide: Pharmacokinetic and Initial Pharmacodynamic Characterization in Man. *J. Pharm. Pharmacol*. 52, 807 - 817 (2000).
- European Pharmacopoeia. 5<sup>th</sup> Edition, Chapter 5.4. Residual Solvents, 507 - 510 (2005).
- Fellner S, Bauer B, Miller DS, Schaffrik M, Fankhanel M, Spruss T, Bernhardt G, Graeff C, Farber L, Gschaidmeier H, Busschauer A, Fricker G. Transport of paclitaxel (Taxol) across the blood-brain barrier in vitro and in vivo, *J Clin Invest*. 110, 1309 - 1318 (2002).
- Fenart L, Casanova A, Dehouck B, Duhem C, Slupek S, Cecchelli R, Betbeder D. Evaluation of effect of charge and lipid coating on ability of 60-nm nanoparticles to cross an in vitro model of the blood-brain barrier. *J Pharmacol Exp Ther*. 291, 1017 - 22 (1999).
- Fetell MR, Grossman SA, Fisher JD, Erlanger B, Rowinsky, Stockel J, Piantadosi S. Preirradiation paclitaxel in glioblastoma multiforme: efficacy, pharmacology, and drug interactions. *New Approaches to Brain Tumour Therapy Central Nervous System Consortium. J.Clin.Oncol*. 15, 3121 - 3128 (1997).



## References

- Friese A, Seiler E, Quack G, Lorenz B, Kreuter J. Enhancement of the duration of the anticonvulsive activity of a novel NMDA receptor antagonist using poly(butylcyanoacrylate) nanoparticles as a parenteral controlled release delivery system, *Eur. J. Pharm. Biopharm.* 49, 103 - 109 (2000b).
- Friese A. Kleinpartikuläre Trägersysteme (Nanopartikel) als ein parenterales Arzneistofftransportsystem zur Verbesserung der Bioverfügbarkeit ZNS-aktiver Substanzen dargestellt am Beispiel der NMDA-Rezeptor-antagonisten MRZ 2/576 und MRZ 2/596. PhD. Thesis, J.W.G Universität Frankfurt, (2000a).
- Fundaro A, Cavalli R, Bargoni A, Vighetto D, Zara GP, Gasco MR. Non-stealth and stealth solid lipid nanoparticles carrying doxorubicin: pharmacokinetics and tissue distribution after *i.v.* administration to rats. *Pharm Res.* 42, 337 - 343 (2000).
- Garber K. Improved paclitaxel formulation: hints at new chemotherapy approach. *J Natl Cancer Inst.* 96, 91 - 92 (2004).
- Gelperina SE, Khalansky AS, Skidan IN, Smirnova ZS, Bobruskin AI, Severin SE, Turowski B, Zanella FE, Kreuter J. Toxicological studies of doxorubicin bound to polysorbate 80-coated poly(butyl cyanoacrylate) nanoparticles in healthy rats and rats with intracranial glioblastoma. *Toxicol Letters.* 126, 131 - 141 (2002).
- Gessner A, Olbrich C, Schroeder W, Kayser O, Müller RH. The role of plasma proteins in brain targeting: species dependent protein adsorption patterns on brain-specific lipid drug conjugate (LDC) nanoparticles. *Int J Pharm.* 214, 87 - 91 (2001).
- Goossen C, Laing T.J, Plessis J, Goosen TC, Rao TB, Flynn GL. Chemical stabilities and biological activities of thalidomide and its N-alkyl analogs. *Pharm res.* 19, 1232 - 1235 (2002).
- Gref R, Luck M, Quellec P, Marchand M, Dellacherie E, Harnisch S, Blunk T, Müller RH. 'Stealth' corona-core nanoparticles surface modified by polyethylene glycol (PEG): influences of the corona (PEG chain length and surface density) and of the core composition on phagocytic uptake and plasma protein adsorption. *Colloids Surf B Biointerfaces.* 18, 301 - 313 (2000).
- Gulyaev AE, Gelperina SE, Skidan IN, Antropov AS, Kivman GYa, Kreuter J. Significant transport of doxorubicin into the brain with polysorbate 80-coated nanoparticles, *Pharm. Res.* 16, 1564 - 1569 (1999).

## References

- Hamann Pr, Berger MS. Mylotarg: the first antibody-targeted chemotherapy agent. In: Page M (eds.) Tumour targeting in cancer therapy, Totowa: Humana Press, 239 - 254 (2002).
- Hobbs SK, Monsky WL, Yuan F, Roberts WG, Griffith L, Torchilin VP, Jain RK. Regulation of transport pathways in tumour vessels: Role of tumour type and microenvironment. *Proc Natl Acad Sci.* 95, 4607 - 4612 (1998).
- Hu YP, Jarillon S, Dubernet C, Couvreur P, Robert J. On the mechanism of action of doxorubicin encapsulation in nanospheres for the reversal of multidrug resistance. *Cancer Chemother Pharmacol.* 37, 556 - 650 (1996).
- Huncharek M, Muscat J, Geschwind JF. Multi-drug versus single agent chemotherapy for high grade astrocytoma: results of a metaanalysis. *Anticancer Res.* 18, 4693 - 7 (1998).
- Ibrahim NK, Desai N, Legha S, Soon-Shiong P, Theriault RL, Rivera E, Esmaeli B, Ring SE, Bedikian A, Hortobagyi GN, Ellerhorst JA. Phase I and pharmacokinetic study of ABI-007, a Cremophor-free, protein-stabilised, nanoparticle formulation of paclitaxel. *Clin Cancer Res.* 8, 1038 - 1044 (2002).
- Kaaijk P, Troost D, de Boer OJ, Van Amstel P, Bakker PJ, Leenstra S, Bosch DA. Daunorubicin and doxorubicin but not BCNU have deleterious effects on organotypic multicellular spheroids of gliomas. *Br J Cancer.* 74, 187 - 193 (1996).
- Kattan J, Droz JP, Couvreur P, Marino JP, Boutan-Laroze A, Rougier P, Brault P, Vranckx H, Grognet JM, Morge X, Sancho-Garnier H. Phase I clinical trial and pharmacokinetic evaluation of doxorubicin carried by polyisohexylcyanoacrylate nanoparticles. *Invest New Drugs.* 10, 191 - 199 (1992).
- Kim JH, Pre-purification of paclitaxel by micelle and precipitation, *Process Biochem.* 39, 1567 - 1571 (2004).
- Kniesel U, Wolburg H. Tight junctions of the blood-brain barrier, Review. *Cell Mol Neurobiol.* 20, 57 - 76 (2000).
- Knott TJ, Pease PJ, Powell LM, Wallis SC, Rall Jr. SC, Innerarity TL, Blackhart B, Taylor WH, Marcel Y, Milnes R, Johnson D, Fuller M, Lusic AJ, McCarty BJ, Mahley RW, Levy-Wilson B, Scott J. Complete protein sequence and identification of structural domains of human apolipoprotein B, *Nature.* 323, 734 - 738 (1986).

## References

- Ko L, Koestner A, Wechsler W. Morphological characterisation of nitrosourea-induced glioma cell lines and clones. *Acta Neuropathol.* 51, 23 - 31 (1980).
- Kornblith PL, Walker M. Chemotherapy for malignant gliomas. *J Neurosurg.* 68, 1 - 17 (1988).
- Koziara JM, Lockman PR, Allen DD, Mumper RJ. In situ blood-brain barrier transport of nanoparticles. *Pharm Res.* 20, 1772 - 1778 (2003).
- Kratze F. Albumin as a drug carrier: Design of prodrugs, drug conjugates and nanoparticles. *J Control Release* (2008).
- Kreuter J. Factors influencing the body distribution of polyacrylic nanoparticles. *Drug Targ.* P. Buri and A. Gumma. Amsterdam, Elsevier Science Publishers BV, (1985).
- Kreuter J. Nanoparticles. Swarbrick J, Boylan Jc (eds.) encyclopedia of pharmaceutical technology. 10 Marcel Dekker: New York, pp.165 (1994).
- Kreuter J, Alyautdin RN, Kharkevich DA, Ivanov AA. Passage of peptides through the blood-brain barrier with colloidal polymer particles (nanoparticles), *Brain Res.* 674, 171 - 174 (1995).
- Kreuter J, Petrov VE, Kharkevich DA, Alyautdin RN. Influence of the type of surfactant on the analgesic effects induced by the peptide dalargin after its delivery across the blood-brain barrier using surfactant-coated nanoparticles. *J Control Release.* 49, 81 - 87 (1997).
- Kreuter J. Nanoparticulate systems for brain delivery of drugs, *Adv Drug Deliv Rev.* 47, 65 - 81 (2001).
- Kreuter J, Shamenkov D, Petrov V, Ränge P, Cychutek K, Koch-Brandt C, Alyautdin R. Apolipoprotein-mediated transport of nanoparticle-bound drugs across the blood-brain barrier, *J Drug Target.* 10, 317 - 325 (2002a).
- Kreuter J. Transport of drugs across the blood-brain barrier by nanoparticles, *Curr Med Chem Central Nervous Syst Agents.* 2, 241 - 249 (2002b).
- Kreuter J. Nanoparticles as drug delivery systems, *Encyclopedia of nanoscience and nanotechnology*, edited by Nalawa HS., 7, 161 - 180 (2004).
- Kreuter J. Nanoparticulate carriers for drug delivery to the brain. In: *Nanoparticles as Drug Carriers*, Torchilin VP (Ed), Imperial College Press, London, 527 - 547 (2006).

## References

- Kreuter J, Gelperina S. Use of nanoparticles for cerebral cancer. *Tumori*. 94, 271-277 (2008).
- Krieger M. Charting the fate of the “good cholesterol”: identification and characterisation of the high-density lipoprotein receptor SR-BI, *Annu. Rev. Biochem.* 68, 523 - 558 (1999).
- Krishnadas A, Rubinstein I, Onyuksel H. Sterically stabilised phospholipid mixed micelles: in vitro evaluation as a novel carrier for water-insoluble drugs, *Pharm. Res.* 20, 297 - 302 (2003).
- Langer K, Seegmüller E, Zimmer A, Kreuter J. Characterisation of polybutylcyanoacrylate nanoparticles: I. Quantification of PBCA polymer and dextrans, *Int. J. Pharm.* 110, 21 - 27 (1994).
- Langer K, Balthasar S, Vogel V, Dinauer N, Von Briesen H, Schubert D. Optimization of the preparation process for human serum albumin (HSA) nanoparticles, *Int. J. Pharm.* 257, 169 - 180 (2003).
- Lehne G. P-glycoprotein as a drug target in the treatment of multidrug resistant cancer. *Curr Drug Targets*.1, 85 - 99 (2000).
- Liggins R.T, Hunter W. L, Burt H.M. Solid-state characterisation of paclitaxel, *J. Pharm. Sci.* 86, 1458 - 1463 (1997).
- Lindenberg M, Kopp S, Dressman JB. Classification of orally administered drugs on the World Health Organization Model list of Essential Medicines according to the biopharmaceutics classification system, *EurJ Pharm Biopharm.* 58, 265 - 78 (2004).
- Liu S. Lipoproteins as Pharmaceutical Carriers, in: *Nanoparticulates as drug carriers* editor, Vladimir P. Torchilin. 173 - 211 (2006).
- Lockman PR, Koziara J, Roder KE, Paulson J, Abbruscato TJ, Mumper RJ, Allen DD. In vivo and in vitro assessment of baseline blood-brain barrier parameters in the presence of novel nanoparticles. *Pharm Res.* 20, 705 - 13 (2003).
- Lucarelli M, Borelli V, Fiori A, Cucina A, Granata F, Potenza R. L, Scarpa S, Cavallaro A, Strom R, The expression of native and oxidised LDL receptors in brain microvessels is specifically enhanced by astrocytes-derived soluble factor(s), *FEBS Letters.* 522, 19 - 23 (2002).

## References

- Lück M. Plasmaproteinadsorption als möglicher Schlüsselfaktor für eine kontrollierte Arzneistoffapplikation mit partikulären Trägern. PhD Thesis, Freie Universität Berlin, 14 - 24, 137 - 154, (1997).
- Maggio WW. Rodent glioma models. In: Perez-Polo JR (eds) *Methods in neurosciences*, Vol. 30, San Diego; *Paradigms of neural injury*, Academic Press Inc. 81 - 96 (1996).
- Mavroudis D, Kouroussis Ch, Kakolyris S, Agelaki S, Kalbakis K, Androulakis N, Souglakos J, Samonis G, Georgoulas V. Phase I study of paclitaxel (taxol) and pegylated liposomal doxorubicin (caelyx) administered every 2 weeks in patients with advanced solid tumours. *Oncology*. 62, 216 - 22 (2002).
- Merck Index, 13th Edition, Loperamide, 5592 (2001).
- Meresse S, Delbart C, Fruchart J. C, Cecchelli R. Low-density lipoprotein receptor on endothelium of brain capillaries, *J. Neurochem*. 53, 340 - 345 (1989).
- Michaelis K, Hoffmann M. M, Dreis S, Herbert E, Alyautdin R. N, Michaelis M, Kreuter J, Langer K. Covalent linkage of apolipoprotein E to albumin-nanoparticles strongly enhances drug transport into the brain, *J. Pharmacol. Exp. Ther*. 317, 1246 - 1253 (2006).
- Misra A, Ganesh S, Shahiwala A, Shah S. Drug delivery to the central nervous system: a review. *J Pharm Pharmaceut Sci*. 6, 252 - 273 (2003).
- Mitra A, Lin S. Effect of surfactant on fabrication and characterisation of paclitaxel-loaded polybutylcyanoacrylate nanoparticulate delivery systems, *J. Pharm. Pharmacol*. 55, 895 - 902 (2003).
- Mizushima Y, Shiokawa Y, Kashiwazaki S, Ichikawa Y, Hashimoto H, Sakuma A. A multicenter double-blind controlled study of lipo-PGE1 incorporated in lipid microspheres, in peripheral vascular disease secondary to connective tissue disorders. *J Rheumatol*. 14, 97 - 101 (1987).
- Moghimi SM, Hunter AC, Umrray JC. Long-circulating and target-specific nanoparticles: theory to practice, *Pharmacol Rev*. 53, 283 - 318 (2001).
- Moghimi SM, Szebeni J. Stealth liposomes and long circulating nanoparticles: critical issues in pharmacokinetics, opsonization and protein-binding properties. *Prog Lipid Res*. 42, 463 - 78 (2003).

## References

- Nelson DF, Nelson JS, Davis DR, Chang CH, Griffin TW, Pajak TF. Survival and prognosis of patients with astrocytoma with atypical or anaplastic features. *J Neurooncol.* 3, 99 - 103 (1985).
- Nerurkar MW, Burto PS, Borchardt. The use of surfactants to enhance the permeability of peptides through Caco-2 cells by inhibition of an apically polarised efflux system. *Pharm Res.* 13, 528 - 534 (1996).
- Nomura T, Inamura T, Black KL. Intracarotid infusion of bradykinin selectively increases blood-tumour permeability in 9L and C6 brain tumours. *Brain Res.* 659, 62 - 6 (1994).
- Oldendorf WH, Cornford ME, Brown WJ. The large apparent work capability of the blood-brain barrier: a study of the mitochondrial content of capillary endothelial cells in brain and other tissues of the rat. *Ann Neurol.* 1, 409 - 17 (1977).
- Olivier JC, Fenart L, Chauvet R, Pariat C, Cecchelli R, Couet W. Indirect evidence that drug brain targeting using PS 80-coated polybutylcyanoacrylate nanoparticles is related to toxicity. *Pharm Res.* 16, 1836 - 1842 (1999).
- Owens DE 3rd, Peppas NA. Opsonization, biodistribution, and pharmacokinetics of polymeric nanoparticles. Review, *Int J Pharm.* 307, 93 - 102 (2006).
- Panzenboeck U, Balazs Z, Sovic A, Hrzenjak A, Levak-Frank S, Wintersperger A, Malle E, Sattler W. ABCA1 and scavenger receptor class B, type I, are modulators of reverse sterol transport at an in vitro blood-brain barrier constituted of porcine brain capillary endothelial cells, *J. Biol.Chem.* 277, 42781 - 42789 (2002).
- Pardridge WM. Non-invasive drug delivery to the human brain using endogenous blood-brain barrier systems. *Pharm Sci Technolo Today.* 2, 49 - 59 (1999).
- Peracchia MT, Vauthier C, Passirani C, Couvreur P, Labarre D. Complement consumption by poly(ethylene glycol) in different conformations chemically coupled to poly(isobutyl 2-cyanoacrylate) nanoparticles. *Life Sci.* 61, 749 - 761 (1997).
- Pereverzeva E, Treschalin I, Bodyagin D, Maksimenko O, Langer K, Dreis S, Asmussen B, Kreuter J, and Gelperina S. Influence of the formulation on the tolerance profile of nanoparticle-bound doxorubicin in healthy rats: Focus on cardio- and testicular toxicity. *Int. J. Pharm.* 337, 346 - 356 (2007).

## References

- Pereverzeva E, Treschalin I, Bodyagin D, Maksimenko O, Kreuter J, Gelperina S. Intravenous tolerance of a nanoparticle-based formulation of doxorubicin in healthy rats. *Toxicol Letters*, (2008).
- Peterson DL, Sheridan PJ, Brown WE. Animal models for brain tumours: historical perspectives and future directions. *J Neurosurg*. 80, 865 - 876 (1994).
- Petri B, Bootz A, Khalansky A, Hekmatara T, Muller R, Uhl R, Kreuter J, Gelperina S. Chemotherapy of brain tumour using doxorubicin bound to surfactant-coated poly(butyl cyanoacrylate) nanoparticles: revisiting the role of surfactants. *J Control Release*. 117, 51 - 58 (2007).
- Pluen A, Boucher Y, Ramanujan S, McKee TD, Gohongi T, di Tomaso E, Brown EB, Izumi Y, Campbell RB, Berk DA, Jain RK. Role of tumour-host interactions in interstitial diffusion of macromolecules: cranial vs. subcutaneous tumours. *Proc Natl Acad Sci*. 98, 4628 - 4633 (2001).
- Poste GR, Kirsh R. et al. The challenge of liposome targeting in vivo. *Liposome technology Vol III: targeted drug delivery and biological interactions*. G Gregoriadis. Boca Rton, FL, CRC Press: 1 - 28 (1984).
- Range P, Kreuter J, Lemmer B. Circadian phase-dependent antinociceptive reaction in mice after intravenous injection of dalargin-loaded nanoparticles determined by the hot-plate test and the tail-flick test. *Chronobiol Int*. 17, 767 - 777 (1999).
- Range P, Unger RE, Oltrogge JB, Zenker D, Begley D, Kreuter J, von Briesen H. PS 80-coating enhances uptake of polybutylcyanoacrylate (PBCA) nanoparticles by human, bovine and murine primary brain capillary endothelial cells. *Eur J Neurosci*. 12, 1931 - 1940 (2000).
- Reese TS and Kamovsky MJ. Fine structural localization of a blood-brain barrier to exogenous peroxidase. *J. Cell Biol*. 34, 207 - 217 (1967).
- Regina A et al., Antitumour activity of ANG1005, a conjugate between paclitaxel and the new brain delivery vector Angiopep. *Br J Pharmacol*, (2008).
- Roberts HC, Roberts TP, Bollen AW, Ley S, Brasch RC, Dillon WP. Correlation of microvascular permeability derived from dynamic contrast-enhanced MR imaging with histologic grade and tumour labeling index: a study in human brain tumours. *Acad Radiol*. 8, 384 - 91 (2001).

## References

- Roullin VG, Deverre JR, Lemaire L, Hindre F, Venier-Julienne MC, Vienet R, Benoit JP. Anit-cancer drug diffusion within living rat brain tissue: An experimental study using [(3)H](6)-5-fluorouracil-loaded PLGA microsphere. *Eur J Pharm Biopharm* 53, 293 - 299 (2002).
- Sanchez de Juan B, von Briesen H, Gelperina SE, Kreuter J. Cytotoxicity of doxorubicin bound to poly(butyl cyanoacrylate) nanoparticles in rat glioma cell lines using different assays. *J Drug Target* 14, 614 - 622 (2006).
- Schaller B. Usefulness of positron emission tomography in diagnosis and treatment follow-up of brain tumours. *Neurobiol Dis* 15, 119 - 124 (2004).
- Schlageter KE, Molnar P, Lapin GD, Groothuis DR. Microvessel organization and structure in experimental brain tumours: microvessel populations with distinctive structural and functional properties. *Microvasc Res.* 58, 312 - 328 (1999).
- Schoch G, Seeger H, Bogousslavsky J, Tolnay M, Janzer RC, Aguzzi A, Glatzel M. Analysis of prion strains by PrPSc profiling in sporadic Creutzfeldt-Jakob disease. *Plos Med.* 3, e14 (2006).
- Schroeder U, Sabel BA. Nanoparticles, a drug carrier system to pass the blood-brain barrier, permit central analgesic effects of intravenous dalargin injections. *Brain Res.* 710, 121 - 124 (1996).
- Schroeder U, Sommerfeld P, Ulrich S, Sabel BA. Nanoparticles technology for delivery of drugs across the blood-brain barrier, *J Pharm Sci.* 87, 1305 - 1307 (1998).
- Schuck P, Rossmannith P. Determination of the sedimentation coefficient distribution by least-squares boundary modeling, *Biopolymers*, 54, 328 - 341 (2000).
- Sharma US, Sharma A, Chau RI, Straubinger RM. Liposome-mediated therapy of intracranial brain tumours in a rat model. *Pharm Res.* 14, 992 - 998 (1997).
- Soma CE, Dubernet C, Bentolila D, Benita S, Couvreur P. Reversion of multidrug resistance by co-encapsulation of doxorubicin and cyclosporin A in polyalkylcyanoacrylate nanoparticles. *Biomaterials.* 21, 1 - 7 (2000).
- Sparreboom A, Scripture CD, Trieu V, Williams PJ, De T, Yang A, Beals B, Figg WD, Hawkins M, Desai N. Comparative preclinical and clinical pharmacokinetics of a cremophor-free, nanoparticle albumin-bound paclitaxel (ABI-007) and paclitaxel formulated in Cremophor (Taxol). *Clin Cancer Res.* 11, 4136 - 4143 (2005).



## References

- Stan AC, Casares S, Radu D, Walter G.F, Brumeanu T.D. Doxorubicin-induced cell death in highly invasive human gliomas, *Anticancer Res.* 19, 941 - 950 (1999).
- Steiniger S, Zenker D, von Briesen H, Begley D, Kreuter J. The influence of PS 80-coated nanoparticles on bovine brain capillary endothelial cells in vitro. *Proc Int Symp Control Release Bioact Mater.* 26, 789 - 790 (2000).
- Steiniger SC, Kreuter J, Khalansky AS, Skidan IN, Bobruskin AI, Smirnova ZS, Severin SE, Uhl R, Kock M, Geiger KD, Gelperina SE. Chemotherapy of glioblastoma in rats using doxorubicin-loaded nanoparticles, *Int. J. Cancer.* 109, 759 - 767 (2004).
- Stehle G, Sinn H, Wunder A, Schrenk H.H, Stewart JC, Stewart G, Hartung W, Maier-Borst D, Heene L. Plasma protein (albumin) catabolism by the tumour itself implications for tumour metabolism and the genesis of cachexia. *Crti.Rev.Oncol.* 26, 77 - 100 (1997).
- Straubinger RM, Arnold RD, Zhou R, Mazurchuk R, Slack JE. Antivascular and antitumour activities of liposome-associated drugs. *Anticancer Res;* 24, 397 - 404 (2004).
- Strickley RG. Solubilising Excipients in Oral and Injectable Formulations. *Pharm. Res.* 21(2), 201 - 230 (2004).
- Sun W, Xie C, Wang H, Hu Y. Specific role of PS 80 coating on the targeting of nanoparticles to the brain. *Biomaterials.* 25, 3065 - 3071 (2004).
- Tamai I, Tsuji A. Transport-mediated permeation of drug across the blood-brain barrier, *J pharm Sci.* 89, 1371 - 1388 (2000).
- Tröster SD, Müller U, Kreuter J. Modification of the body distribution of poly(methyl methacrylate) nanoparticles in rats by coating with surfactants, *Int J pharm.* 61,85 - 100 (1990).
- Tröster SD, Kreuter J. Influence of the surface properties of low contact angle surfactants on the body distribution of <sup>14</sup>C-poly(methyl methacrylate) nanoparticles, *J Microencapsulation.* 9, 19 - 28 (1992).
- Upton R.N. Cerebral uptake of drugs in humans, *Clin. Exp. Pharmacol. Physiol.* 34, 695 - 701 (2007).

## References

- Uriely B, Jeffers S, Isacson R, Kutsch K, Wei-Tsao D, Yehoshua Z, Libson E, Muggia FM, Gabizon S. Liposomal doxorubicin: antitumour activity and unique toxicities during two complementary phase I studies. *J Clin Oncol.* 13, 1777 - 1785 (1995).
- Vajkoczy P, Menger MD. Vascular microenvironment in gliomas. *Cancer Treat Res.* 117, 249 - 62 (2004).
- Van Waarde A, Shiba K, de Jong JR, Ishiwata K, Dierckx RA, Elsinga PH. Rapid reduction of sigma1-receptor binding and 18F-FDG uptake in rat gliomas after in vivo treatment with doxorubicin. *J Nucl Med.* 48, 1320 - 1326 (2007).
- Vasile E, Simionescu M, Simionescu N. Visualization of the binding, endocytosis, and transcytosis of low-density lipoprotein in the arterial endothelium in situ, *J. Cell Biol.* 96, 1677 - 1689 (1983).
- Vauthier C, Dubernet C, Chauvierre C, Brigger I, Couvreur P. Drug delivery to resistant tumours: the potential of poly(alkyl cyanoacrylate) nanoparticles. *J Control Release.* 93, 151 - 160 (2003a).
- Vauthier C, Dubernet C, Fattal E, Pinto-Alphandary H, Couvreur P. Poly(alkylcyanoacrylates) as biodegradable materials for biomedical applications. *Adv Drug Delivery Rev.* 55, 519 - 548 (2003b).
- Venne A, Li S, Mandeville R, Kabanov A, Alakhov V. Hypersensitizing effect of pluronic L61 on cytotoxic activity, transport, and subcellular distribution of doxorubicin in multiple drug-resistant cells. 56, 3626-9 (1996).
- Verdiere AC, Dubernet C, Nemati F, Soma E, Appel M, Ferte J, Bernard S, Puisieux F, Couvreur P. Reversion of multidrug resistance with polyalkylcyanoacrylate nanoparticles: towards a mechanism of action, *Br. J. Cancer.* 76, 198 - 205 (1997).
- Vinogradov SV, Bronich TK, Kabanov AV. Nanosized cationic gels for drug delivery: preparation, properties and interactions with cells. *Adv Drug Delivery Rev.* 54, 135 - 147 (2002). Vinogradov SV, Batrakova EV, Kabanov AV. Nanogels for oligonucleotide delivery to the brain. *Bioconjugate Chem.* 15, 50 - 60 (2004).
- Vogel V, Langer K, Balthasar S, Schuck P, Mächtle W, Haase W, Van den Broek J.A, Tziatios C, Schubert D. Characterisation of serum albumin nanoparticles by

- sedimentation velocity analysis and electron microscopy, *Progr. Colloid Polym. Sci.* 119, 31 - 36 (2002).
- von Holst H, Knochenhauer E, Blomgren H, Collins V.P, Ehn L, Lindquist M, Noren G, Peterson C. Uptake of adriamycin in tumour and surrounding brain tissue in patients with malignant gliomas, *Acta Neurochir*, 104, 13 - 6 (1990).
  - Vorbrodth AW, Lossinsky AS, Dobrogowska DH, Wisniewski HM. Cellular mechanisms of the blood-brain barrier (BBB) opening to albumin-gold complex. *Histol Histopathol.* 8, 51 - 61 (1993).
  - Walter KA, Tamargo RJ, Olivi A, Burger PC, Brem H. Intratumoural chemotherapy, *Neurosurgery.* 37, 1128 - 45 (1995).
  - Weber C, Coester C, Kreuter J, Langer K. Desolvation process and surface characterisation of protein nanoparticles, *Int. J. Pharm.* 194, 91 - 102 (2000a).
  - Weber C, Kreuter J, Langer K. Desolvation process and surface characteristics of HSA-nanoparticles, *Int. J. Pharm.* 196, 197 - 200 (2000a).
  - Weizsacker M, Deen DF, Rosenblum ML, Hoshino T, Gutin PH, Barker M. The 9L rat brain tumour: description and application of an animal model. *J Neurol.* 224, 183 - 192 (1981).
  - Widder KJ, Senyei AE, Ranney DF. Magnetically responsive microspheres and other carriers for the biophysical targeting of antitumour agents. In S Garattini, A Goldin, F Howking, IJ Kopin and RJ Schnitzer (Eds). *Adv. Pharmacol. Chemother.* Academic Press, New York. 16, 213 - 271 (1979).
  - Woodcock DM, Jefferson S, Linsenmeyer ME, Crowther PJ, Chojnowski GM, Williams B, Bertoncetto I. Reversal of multidrug resistance phenotype with Cremophor EL, a common vehicle for water-insoluble vitamins and drugs, *Cancer Res.* 50,4199 - 4230 (1990).
  - Woodcock DM, Linsenmeyer ME, Chojnowski GM, Kriegler AB, Nink V, Webster LD, Sawyer WH. Reversal of multidrug resistance by surfactants, *Br J Cancer.* 66, 62 - 68 (1992).
  - Xu Z et al. In vitro and in vivo evaluation of actively targetable nanoparticles for paclitaxel delivery, *Int J Pharm* 288, 361 - 368 (2005).

## References

- Yablonovskaya L, Spryshkova NA. Morphologic and biologic characteristics of experimental tumours of the cerebellum in rats. *Arkh Patol.* 33, 50 - 53 (1970).
- Yokoyama M. Drug targeting with nano-sized carrier system, *J Artif Organs.* 8, 77 - 84 (2005).
- Youssef M, Fattal E, Alonso M.J, Roblot-Treupel LSauzieres, J, Tancrede C, Omnes A, Couvreur P, Andremont A. Effectiveness of nanoparticle-bound ampicillin in the treatment of *Listeria monocytogenes* infection in athymic nude mice, *Antimicrob. Agents Chemother.* 32, 1204 - 1207 (1988).
- Zagzag D, Nomura M, Freidiander DR, Blanco CY, Gagner JP, Nomura N, Newcomb EW. Geldanamycin inhibits migration of glioma cells in vitro: A potential role for hypoxia inducible factor (HIF-1 $\alpha$ ) in glioma cell invasion. *J Cell Physiol* 196, 394 - 402 (2003).
- Zara GP, Cavalli R, Bargoni A, Fundaro A, Vighetto D, Gasco MR. Intravenous administration to rabbits of non-stealth and stealth doxorubicin-loaded solid lipid nanoparticles at increasing concentrations of stealth agent: pharmacokinetics and distribution of doxorubicin in brain and other tissues. *J Drug Target.* 10, 327 - 335 (2002).
- Zhou R, Mazurchuk R, Straubinger RM. Antivasculature effects of doxorubicin-containing liposomes in an intracranial rat brain tumour model. *Cancer Res.* 62, 2561 - 2566 (2002).
- Zlokovic BV. The blood-brain barrier in health and chronic neurodegenerative disorders. 57, 178 - 201 (2008).
- Zordan-Nudo, Linge V, Liv ZL, Geroges E. Effects of nonionic detergents on P-glycoprotein drug binding and reversal of multidrug resistance. *Cancer Res.* 55, 5994 - 6000 (1993).
- [www.fda.gov/cder/cancer/animalframe.htm](http://www.fda.gov/cder/cancer/animalframe.htm)

## 9 Curriculum Vitae



### Personal

Date of Birth: 21/09/1977  
Place of Birth : Tehran

### Education

11/2004-

Ph.D. student in Pharmaceutical Technology Department,  
University of Frankfurt, Germany  
Dissertation: Nanoparticle formulations for new cytostatic agents  
against glioblastoma  
Advisor: Prof. Dr. Jörg Kreuter

09/1995-07/2000

Master of Pharmacy. Faculty of Pharmacy, University of Szeged,  
Hungary  
English Curriculum  
Thesis: Active ingredients of Hypericum Perforatum and their  
variations  
Advisor: Prof. Imre Máthé D.Sc.

1990-1995

Aboureihan High school, Tehran, Iran  
Diploma in Natural Science

### Research Experience

*Doctoral Research:*  
Institute of Pharmaceutical Technology, University of Frankfurt  
Nanosystem LTD, Moscow, Russia  
Institute of Neuropathology, Hamburg-Eppendorf-University  
Development of nanoparticles for the lipophilic  
chemotherapeutics against glioblastoma

Study of active drug transport across the blood brain barrier and  
the receptor-drug interaction

Immunohistochemistry study of glioblastoma in Rats

12/2003-1/2004	<p><i>Research:</i>  Department of Pharmaceutical Technology, University of Szeged  Microparticle formulation of chitosan  Adviser: Prof. Dr. Hódi Klara</p>
09/2000-03/2002	<p><i>Research:</i>  Department of Drug and Food Control, Tehran University, Iran  Measuring of selenium plasma concentration differences between age related macular degeneration patients by differential pulse cathodic stripping voltammetry  Adviser: Asst. Prof. Dr. M. R. Oveisi</p>
<b>Professional Training</b>	<p>Institute of Pharmaceutical Technology, University of Frankfurt  Teaching assistant in Good Manufacturing Practices (GMP)</p>
12/2003-11/2004	<p>Department of Pharmaceutical Technology, University of Szeged  Teaching assistant in preparation of dispensary dosage form-laboratory practice  Parenteral dosage form-laboratory practice</p>
<b>Working Experience</b>	<p>Receptura Pharmaproduktion, Frankfurt am Main  Consultant and manager analytical quality control  Preparation of HRT-formulations under GMP regulation</p>
06/2006-	
03/2002-11/2003	<p>Clinical pharmacy department, Pars Hospital, Tehran  Pharmacist</p>
<b>Membership</b>	<p>Hungarian Pharmacist Society (licensed)  Iranian Pharmacist Society (licensed)  Controlled Release Society (CRS)  Arbeitsgemeinschaft für Pharmazeutische Verfahrenstechnik (APV)  Deutsche Pharmazeutische Gesellschaft (DPHG)</p>
<b>Certification</b>	<p>Frankfurt Innovation Zentrum (FIZ)- Frankfurt  ZAFES-Curriculum on Drug Research and Development for Postgraduates and Graduates</p>
03/2006-03/2007	
<b>Extracurricular Activities</b>	<p>Member of EPSU (English Program Students Union), Szeged University, Hungary</p>
1998-2000	
<b>Language Skills</b>	<p>English: excellent in writing and speaking  German: very good in writing and speaking  Hungarian: certified by University of Szeged  Farsi: mother tongue</p>

## 10 Patent and Publications

<b>Patent</b>	LTS LOHMANN THERAPIE-SYSTEME AG, University of Frankfurt Agent enriched nanoparticles based on hydrophilic proteins, (WO/2007/104422)
<b>Publications &amp; Presentations</b>	
accepted	<i>Article:</i> Efficient systemic therapy of rat glioblastoma by nanoparticle-bound doxorubicin is due to antiangiogenic effects First author, Neuropathology
09/2008	<i>Article:</i> Transferrin- and transferrin-receptor-antibody-modified nanoparticles enable drug delivery across the blood-brain barrier (BBB); co-author. Eur J Pharm Biopharm.
accepted 2008	<i>Article:</i> Encapsulation of water-insoluble drugs in poly(butyl cyanoacrylate) nanoparticles- first author, Journal of Nanoscience and Nanotechnology
03/2007	<i>Article:</i> Covalent attachment of Apolipoprotein A-I and Apolipoprotein B-100 to albumin-nanoparticles enables drug transport into the brain; co-author. J Controlled Release
01/2007	<i>Article:</i> Chemotherapy of brain tumour using doxorubicin bound to surfactant-coated poly(butyl cyanoacrylate) nanoparticles: Revising the role of surfactants; co-author. J Controlled Release
06/2008	<i>Poster:</i> Nanoparticle-based formulation approach for the poorly soluble drug substances; co-author IC-CCPCM 2008, Moscow Russia
04/2008	<i>Poster:</i> Encapsulation of diinodolylmethane (DIM) in poly(DL-Lactide-Co-Glycolide) nanoparticles PBP 6 <sup>th</sup> world meeting, Barcelona, Spain
09/2006	<i>Poster:</i> Development of a paclitaxel formulation based on poly(butyl cyanoacrylate) nanoparticles; DPHG, Nürnberg
07/ 2006	<i>Poster:</i> Thalidomide bound to human serum albumin nanoparticles; Controlled Release Society, Vienna, Austria
03/ 2006	<i>Poster:</i> Doxorubicin-loaded poly(butyl cyanoacrylate) nanoparticles: Influence of stabilizer and drug-to-polymer ratio on size, polymerization yield, and drug loading; co-author <i>Poster:</i> Chemotherapy of brain tumour using doxorubicin loaded in surfactant-coated poly(butyl cyanoacrylate) nanoparticles: Towards mechanism of action; co-author PBP 5 <sup>th</sup> world meeting, Geneva, Switzerland

## **Acknowledgment**

I have worked with a great number of people whose contribution in assorted ways to the research and the making this thesis possible and an enjoyable experience for me. It is a pleasure to convey my gratitude to them all in my humble acknowledgment.

In the first place I would like to express my deepest gratitude to Professor Dr. Jörg Kreuter, for accepting me as a PhD student and also for his supervision, advices, and guidance whole through my work. He made the way possible and I will always be thankful to him.

I am also thankful to Dr. Svetlana Gelperina for her supervision from the very early stage of this study. I also thank Dr. Alexander Khalansky for his professional work for the in vivo experiments. It was a pleasant time working with him.

I am also indebted to Professor Dr. Jennifer Dressman for the opportunity to work in the Institute of Pharmaceutical Technology at Goethe University. I had a chance to join in her GMP laboratory team which became a precious experience for me.

I am thankful to PD Dr. Klaus Langer who was abundantly helpful and offered important scientific support and guidance through my research.

I also benefited by outstanding works from Professor Dr. Markus Glatzel and his supportive team, specially Dr. Christian Bernreuther at Institute of Neuropathology, University Medical Center Hamburg-Eppendorf.

I acknowledge the financial support by the LTS Lohmann Therapie-Systeme for providing the financial means and laboratory facilities.

I would like to thank the Goethe University Frankfurt am Main for permitting this thesis in the first instance, doing the necessary research work and benefiting from all the university facilities such as the workshops and the libraries.

My sincere appreciation goes to Professor Dr. Mihály Kata and Professor Dr. Klára Pintye-Hodi at Univeristy of Szeged in Hungary who with their support my PhD study was enormously facilitated.

My thanks go in particular to the following people; Dr. Vitali Vogel (Institute of Biophysics, Goethe University), Dr. Ekarat Jantratid, Elisabeth Herbert, Sylvia Niederdorf, Birgit Johann (Institute of Pharmaceutical Technology, Goethe University), Dr. Shang-Ray Yang (Institute



## Acknowledgment

of Inorganic and Analytical Chemistry, Goethe University), Manfred Ruppel (Botanical Institute, Goethe University), Dr. Alf Theisen (Zentrale Forschungseinrichtung, Klinikum Goethe-University), Dr. Weissenberger (Neuro Science Center, Exp. Neurochirurgie Goethe University) and Dr. M. Zelig (Bioscience, USA) and Dr. Irwin Jacobs (St. Louis, USA). Their presence and generous support was the best thing that could happen to me and my thesis.

I am grateful to the all members of the Pharmaceutical Technology Institute at Goethe University for their support and their comradeship; especially to Karsten Ulbrich, Jürgen Kufleitner, Sonja Arnold, Melisander Holzer, Stefanie Wohlfart, Anja Zensi, Mathias Wacker, Thomas Knobloch, Karim Sempf for sharing the literature and great assistance. My thanks go as well to my former colleagues Dr. Hiro Yamamoto, Dr. Alessandra Ambrousi, Dr. Berta Sanchez de Jaun, Dr. Alexander Bootz and Dr. Sebastian Dreis who guided this work and helped whenever I was in need.

I am grateful in every possible way to my friends Desiree Argott, Efthimia Athanasia dou, Isabella Béke Sandorné, Laura Rangel-Ordóñez, Marion Weisser, Hedieh Arab, Dr. Hooman Arab, Dr. Parya Reisi-Nassab, Marziyeh Maoussavi, Dr. Rana Al Kurdi, Dr. Heidrun Wartlick, Emil Magyar and Sarolta Papai for their endless emotional support and being always there for me.

I would like to express my eternal gratitude to my parent Dr. Mohammad Hossein Hekmatara and Manijeh Rabbani for their everlasting love and indescribable support. I am thankful to my sisters Dr. Anali Hekmatara and Dr. Nazli Hekmatara for their constant support and understanding. I thank Dr. Hamed Batani, Marlies Wagner, Hans Wagner and Baran Batani.

Finally, I would like to deeply thank my soul-mate Dr. Maik Wagner for his endless love and constant motivation whole through this work.